RECUEIL DES ACTIVITES 2018 DU THEME "ARCHIVES & TRACEURS"

Sommaire

Avant-propos

2018 = année du rapprochement entre les équipes avec l'emménagement dans le bâtiment 714
Et l'année de l'évaluation HCERES, avec un retour positif sur les activités du thème et leur valorisation, des recommandations

LISTE DES PUBLICATIONS 2018

Publications dans des revues de rang A

- Publication donnant lieu à une fiche ci-après

- Alexandre A., **Landais** A., Vallet-Coulomb C., Piel C., Devidal S., Pauchet S., Sonzogni C., Couapel M., Pasturel M., Cornuault P., Xin J., Mazur J.-C., **Prié** F., Bentaleb I., Webb E., Chalié F., Roy J. (2018) The triple oxygen isotope composition of phytoliths as a proxy of continental atmospheric humidity: insights from climate chamber and climate transect calibrations. *Biogeosciences* 15, 3223-3241- doi: 10.5194/bg-15-3223-2018

Bai XM, Dawson RJ, Urge-Vorsatz D, Delgado GC, Barau AS, Dhakal S, Dodman D, Leonardsen L, **Masson-Delmotte** V, Roberts D, Schultz S (2018) Six research priorities for cities and climate change. *Nature* 555, 23-25 doi:

- Balesdent J., Basile-Doelsch I., Chadoeuf J., Cornu S., Derrien D., Fekiacova Z., **Hatté** C. (2018) Atmosphere-soil carbon transfer as a function of soil depth. *Nature* 559, 599-602 - doi:10.1038/s41586-018-0328-3

Balkanski Y., Menut L., Garnier E., Wang R., Evangeliou N., Jourdain S., **Eschstruth** C., Vrac M., Yiou P. (2018) Mortality induced by PM2.5 exposure following the 1783 Laki eruption using reconstructed meteorological fields. Scientific Reports 8, 15896 – doi: 10.1038/s41598-018-34228-7

Bertler N. A. N., Conway H., Dahl-Jensen D., Emanuelsson D. B., Winstrup M., Vallelonga P. T., Lee J. E., Brook E. J., Severinghaus J. P., Fudge T. J., Keller E. D., Troy Baisden W., Hindmarsh R. C. A., Neff P. D., Blunier T., Edwards R., Mayewski P. A., Kipfstuhl S., Buizert C., Canessa S., Dadic R., Kjær H. A., Kurbatov A., Zhang D., Waddington E. D., Baccolo G., Beers T., Brightley H. J., Carter L., Clemens-Sewall D., Ciobanu V. G., Delmonte B., Eling L., Ellis A., Ganesh S., Golledge N. R., Haines S., Handley M., Hawley R. L., Hogan C. M., Johnson K. M., Korotkikh E., Lowry D. P., Mandeno D., McKay R. M., Menking J. A., Naish T. R., Noerling C., Ollive A., **Orsi** A., Proemse B. C., Pyne A. R., Pyne R. L., Renwick J., Scherer R. P., Semper S., Simonsen M., Sneed S. B., Steig E. J., Tuohy A., Ulayottil Venugopal A., Valero-Delgado F., Venkatesh J., Wang F., Wang S., Winski D. A., Holly W., Whiteford A., Xiao C., Yang J., Zhang, X. (2018) The Ross Sea Dipole-temperature, snow accumulation and sea ice variability in the Ross Sea region, Antarctica, over the past 2700 years. *Climate of the Past* 14, 193-214- doi: 10.5194/cp-14-193-2018

- Bisse S.B., Ekomane E., Takem Eyong J., Ollivier V., **Douville** E., Maffo Nganne M.J., Bitom L.D (2018) Sedimentological and geochemical study of the Bongongo and Ngol travertines located at the Cameroon Volcanic Line. *Journal of African Earth Sciences* 143, 201-214. doi:

Bonfardeci A., Caruso A., Bartolini A., **Bassinot** F., Blanc-Valleron M. M. (2018) Distribution and ecology of the Globigerinoides ruber — Globigerinoides elongatus morphotypes in the Azores region during the late Pleistocene-Holocene. *Palaeogeography, Palaeoclimatology, Palaeoecology* 491, 92-111 - doi: 10.1016/j.palaeo.2017.11.052

Bonfardeci A., Caruso A., Bartolini A., **Bassinot** F., Blanc-Valleron M.M. (2018) Climatic and oceanographic changes in the Azores region during the last 74.7 ka. *Alpine and Mediterranean Quaternary* 31, 105-108.

- Bonneau L., Colin C., **Pons-Branchu** E., Mienis F., **Tisnérat-Laborde** N., **Blamart** D., Elliot M., Collart T., Frank N., Foliot L., **Douville** E. (2018) Imprint of Holocene climate variability on cold-water coral reef growth at the SW Rockall Trough margin, NE Atlantic. *Geochemistry, Geophysics, Geosystems* - doi: 10.1029/2018gc007502.

Brigolin D., **Rabouille** C., **Bombled** B., Colla S., Vizzini S., Pastres R., Pranovi F. (2018) Modelling biogeochemical processes in sediments from the north-western Adriatic Sea: Response to enhanced particulate organic carbon fluxes. *Biogeosciences* 15, 1347-1366 - doi: 10.5194/bg-15-1347-2018

Burgos M., Ortega T., Bohórquez J., Corzo A., **Rabouille** C., Forja J. M. (2018) Seasonal variation of early diagenesis and greenhouse gas production in coastal sediments of Cadiz Bay: Influence of anthropogenic activities. *Estuarine, Coastal and Shelf Science* 200, 99-115 - doi: 10.1016/j.ecss.2017.10.016

Caley, T., **Extier**, T., Collins, J.A., Schefuss, E., Dupont, L., Malaize, B., Rossignol, L., Souron, A., McClymont, E.L., Jimenez-Espejo, F.J., Garcia-Comas, C., Eynaud, F., Martinez, P., Roche, D.M., Jorry, S.J., Charlier, K., Wary, M., Gourves, P.-Y., Billy, I. and Giraudeau, J. (2018) A two-million-year-long hydroclimatic context for hominin evolution in southeastern Africa. Nature 560, 76-79 – doi:10.1038/s41586-018-0309-6..

Canavesio R., **Pons-Branchu** E., Chancerelle Y. (2018) Limitations to U/Th dating of reef-platform carbonate boulders produced by high-energy marine inundations in the Tuamotu Archipelago (French Polynesia). *Coral Reefs* 37, 1139-1155.

- **Casado** M., **Landais** A., Picard G., Münch T., Laepple T., Stenni B., Dreossi G., Ekaykin A., Arnaud L., Genthon C., **Touzeau** A., **Masson-Delmotte** V., **Jouzel** J. (2018) Archival processes of the water stable isotope signal in East Antarctic ice cores. *The* Cryosphere 12(5), 1745-1766 - doi: 10.5194/tc-12-1745-2018

Chetverikov Y.O., Aruev N.N., Bulat S.A., Gruzdov K.A., Ezhov V.F., **Jean-Baptiste** P., Kamenskii I.L., Lipenkov V.Y., Prasolov E.M., Solovei V.A., Tyukal'tsev R.V., Fedichkin I.L. (2018) Content and isotope ratios of noble gases in congelation ice of Lake Vostok. Technical Physics 63, 738-746.

Collart T., Verreydt W., Hernández-Molina F. J., Llave E., León R., Gómez-Ballesteros M., **Pons-Branchu** E., Stewart H., Van Rooij D. (2018) Sedimentary processes and cold-water coral mini-mounds at the Ferrol canyon head, NW Iberian margin. *Progress in Oceanography* 169, 48-65 - doi: 10.1016/j.pocean.2018.02.027

Cornuault M., Tachikawa K., Vidal L., Guihou A., Siani G., Deschamps P., **Bassinot** F., Revel M. (2018) Circulations changes in the Eastern Mediterranean Sea over the past 23,000 years inferred from authigenic Nd isotopic ratios *Paleoceanography and Paleoclimatology* 33, 264-280 - doi: 10.1002/2017PA003227

Crosta X., Crespin J., Swingedouw D., Marti O., **Masson-Delmotte** V., Etourneau J., Goosse H., Braconnot P., Yam R., Brailovski I., Shemesh A. (2018) Ocean as the main driver of Antarctic ice sheet retreat during the Holocene. Global and Planetary Change 166, 62-74 – doi: 10.1016/j.gloplacha.2018.04.007.

Dang H., Jian Z., Wang T., **Bassinot** F., **Kissel** C., Wu, J. (2018) The calcification depth and Mg/Ca thermometry of Pulleniatina obliquiloculata in the tropical Indo-Pacific: a core-top study, Marine Micropaleontology, 145, 28-40, DOI: doi.org/10.1016/j.marmicro.2018.11.001.

Dassié E., **Genty** D., Noret A., Mangenot X., Massault M., Lebas N., Duhamel M., Bonifacie M., Gasparrini M., **Minster** B., Michelot J.L (2018) A newly designed analytical line to examine fluid inclusion isotopic compositions in a range of carbonate samples. *Geochemistry, Geophysics, Geosystems* doi: 10.1002/2017GC007289

- **Daux** V., Michelot A., Lavergne A., Breda N., Damesin C. (2018) Comparison of the performance of $\delta^{13}C$ and $\delta^{18}O$ in oak, beech and pine in the record of past climate variations. *Journal of Geophysical Research Biogeosciences* doi: 10.1002/2017JG004203

de Montety V., Aquilina L., Labasque T., Chatton E., Fovet O., Ruiz L., **Fourré** E., de Dreuzy J. R. (2018) Recharge processes and vertical transfer investigated through long-term monitoring of dissolved gases in shallow groundwater. *Journal of Hydrology* 560, 275-288 - doi: 10.1016/j.jhydrol.2018.02.077

Degeai J. P., Villa V., Chaussé C., **Pereira** A., **Nomade** S., Aureli D., Pagli M., Nicoud E. (2018) Chemical weathering of palaeosols from the Lower Palaeolithic site of Valle Giumentina, central Italy. *Quaternary Science Reviews* 183, 88-109 - doi: 10.1016/j.quascirev.2018.01.014

Delhasse A., Fettweis X., Kittel C., Amory C., **Agosta** C. (2018) Brief communication: Impact of the recent atmospheric circulation change in summer on the future surface mass balance of the Greenland Ice Sheet. The Cryosphere 12, 3409-3418.

Dogan-Kulahci G. D., Temel A., Gourgaud A., Varol E., **Guillou** H., Deniel C. (2018) Contemporaneous alkaline and calc-alkaline series in Central Anatolia (Turkey): Spatio-temporal evolution of a post-collisional Quaternary basaltic volcanism. *Journal of Volcanology and Geothermal Research* 356, 56-74 - doi: 10.1016/j.jvolgeores.2018.02.012

Duchamp-Alphonse S., Siani G., **Michel** E., Beaufort L., Gally Y., Jaccard S. (2018) Enhanced ocean-atmosphere carbon partitioning via the carbonate counter pump during the last deglacial. *Nature Communications* 9, 2396 - doi: 10.1038/s41467-018-04625-7

Dumoulin J.P., **Pozzato** L., **Rassman** J., **Toussaint** F., **Fontugne** M., **Tisnérat-Laborde** N., **Rabouille** C. (2018) Isotopic signature ($\delta^{13}C$, $\Delta^{14}C$) of DIC in porewaters: an example from the Rhone River Delta. Radiocarbon 60(5), 1465-1481 - doi: 10.1017/RDC.2018.111

- **Extier** T., **Landais** A., **Bréant** C., **Prié** F., **Bazin** L., Dreyfus G., Roche D. M., Leuenberger M. (2018) On the use of $\delta^{18}O_{atm}$ for ice core dating. *Quaternary Science Reviews* 185 244-257 - doi: 10.1016/j.quascirev.2018.02.008

Fan W., Jian Z., Chu Z., Dang H., Wang Y., **Bassinot** F., Han X., Bian Y. (2018) Variability of the Indonesian Throughflow in the Makassar Strait over the last 30 ka. *Scientific Reports* 8, 5678. doi:10.1038/s41598-018-24055-1

Fegyveresi J. M., Alley R. B., Muto A., **Orsi** A. J., Spencer M. K. (2018) Surface formation, preservation, and history of low-porosity crusts at the WAIS Divide site, West Antarctica. *Cryosphere* 12, 325-341 - doi: 10.5194/tc-12-325-2018

Fischer H., Meissner K.J., Mix A.C., Abram N.J., Austermann J., Brovkin V., Capron E., Colombaroli D., Daniau A.-L., Dyez K.A., Felis T., Finkelstein S.A., Jaccard S.L., McClymont E.L., Rovere A., Sutter J., Wolff E.W., Affolter S., Bakker P., Ballesteros-Canovas J.A., Barbante C., Caley T., Carlson A.E., Churakova O., Cortese G., Cumming B.F., Davis B.A.S., de Vernal A., Emile-Geay J., Fritz S.C., Gierz P., Gottschalk J., Holloway M.D., Joos F., Kucera M., Loutre M.-F., Lunt D.J., Marcisz K., Marlon J.R., Martinez P., **Masson-Delmotte** V., Nehrbass-Ahles C., Otto-Bliesner B.L., Raible C.C., Risebrobakken B., Goni M.F.S., Arrigo J.S., Sarnthein M., Sjolte J., Stocker T.F., Alvarez P.A.V., Tinner W., Valdes P.J.,

Vogel H., Wanner H., Yan Q., Yu Z., Ziegler M., Zhou, L. (2018) Palaeoclimate constraints on the impact of 2 degrees C anthropogenic warming and beyond. *Nature Geoscience* 11, 474-485 – doi: 10.1038/s41516-018-0146-0.

- **Fourré** E., **Landais** A., **Cauquoin** A., **Jean-Baptiste** P., Lipenkov V., Petit J. R. (2018) Tritium Records to Trace Stratospheric Moisture Inputs in Antarctica. *Journal of Geophysical Research: Atmospheres* - doi: 10.1002/2018JD028304

Franchi F., Bergamasco A., Da Lio C., Donnici S., Mazzoli C., **Montagna** P., Taviani M., Tosi L., Zecchin M. (2018) Petrographic and geochemical characterization of the early formative stages of Northern Adriatic shelf rocky buildups. *Marine and Petroleum Geology* 91, 321-337 - doi: 10.1016/j.marpetgeo.2018.01.012

Gao J., He Y., **Masson-Delmotte** V., Yao T. (2018) ENSO effects on annual variations of summer precipitation stable isotopes in Lhasa, southern Tibetan Plateau. *Journal of Climate* 31, 1173-1182 - doi: 10.1175/JCLI-D-16-0868.1

Gdaniec S., **Roy-Barman** M., **Foliot** L., **Thil** F., **Dapoigny** A., Burckel P., Garcia-Orellana J., Masque P., Morth C. M., Andersson P. S. (2018) Thorium and protactinium isotopes as tracers of marine particle fluxes and deep water circulation in the Mediterranean Sea. *Marine Chemistry* 199, 12-23 - doi: 10.1016/j.marchem.2017.12.002

- Gottschalk J., Szidat S., **Michel** E., **Mazaud** A., Salazar G., Battaglia M., Lippold J., Jaccard S. L. (2018) Radiocarbon measurements of small-size foraminifer samples with the accelerator mass spectrometer (AMS) MIni-CArbon DAting System (MICADAS) at the University of Bern: implications for paleoclimate reconstructions. *Radiocarbon* 60(2), 469-491 - doi: 10.1017/RDC.2018.3

Goursaud S., **Masson-Delmotte** V., Favier V., **Orsi** A., Werner M. (2018) Water stable isotope spatio-temporal variability in Antarctica in 1960-2013: observations and simulations from the ECHAM5-wiso atmospheric general circulation model. *Climate of the Past* 14, 923-946 – doi: 10.5194/cp-14-923-2018

Gudlaugsdottir H., Steen-Larsen H.C., Sjolte J., **Masson-Delmotte** V., Werner M., Sveinbjornsdottir A.E. (2018) The influence of volcanic eruptions on weather regimes over the North Atlantic simulated by ECHAM5/MPI-OM ensemble runs from 800 to 2000 CE. *Atmospheric Research* 213, 211-223.

Guenet B., Camino-Serrano M., Ciais P., **Tifafi** M., Maignan F., Soong J.L., Janssens I.A. (2018) Impact of priming on global soil carbon stocks. *Global Change Biology* 24, 1873-1883.

- **Guillou** H., **Scao** V., **Nomade** S. (2018) $^{40}Ar/^{39}Ar$ age of cryptochron C2r.2r-1 as recorded in a lava sequence within the Ko'olau volcano (Hawaii, USA). *Quaternary Geochronology* 43, 91-101 - doi: 10.1016/j.quageo.2017.10.005

Guolaugsdottir H., Steen-Larsen H.C., Sjolte J., **Masson-Delmotte** V., Werner M., Sveinbjornsdottir A.E. (2018). The influence of volcanic eruptions on weather regimes over the North Atlantic simulated by ECHAM5/MPI-OM ensemble runs from 800 to 2000 CE. *Atmospheric Research* 213, 211-223

Gutierrez J. M., Maraun D., Widmann M., Huth R., Hertig E., Benestad R., Roessler O., Wibig J., Wilcke R., Kotlarski S., San Martín D., Herrera S., Bedia J., Casanueva A., Manzanas R., Iturbide M., Vrac M., Dubrovsky M., Ribalaygua J., Pórtoles J., Räty O., Räisänen J., Hingray B., Raynaud D., **Casado** M. J., Ramos P., Zerenner T., Turco M., Bosshard T., Stepánek, P., Bartholy J., Pongracz R., Keller D. E., Fischer A. M., Cardoso R. M., Soares P. M. M., Czernecki B., Page C. (2018) An intercomparison of a large ensemble of statistical downscaling methods over Europe: Results from the VALUE perfect predictor cross-validation experiment International. Journal of Climatology 39(9) - doi: 10.1002/joc.5462

Haddam N.A., Siani G., **Michel** E., Kaiser J., Lamy F., Duchamp-Alphonse S., Hefter J., Braconnot P., **Dewilde** F., **Isguder** G., **Tisnérat-Laborde** N., **Thil** F., Durand N., **Kissel** C. (2018) Changes in latitudinal sea surface temperature gradients along the Southern Chilean margin since the last glacial. *Quaternary Science Reviews* 194, 62-76.

- Hershkovitz I., Weber G. W., Quam R., Duval M., Grun R., Kinsley L., Ayalon A., Bar-Matthews M., **Valladas** H., Mercier N., Arsuaga J. L., Martinón-Torres M., De Castro J. M. B., Fornai C., Martín-Frances L., Sarig R., May H., Krenn V. A., Slon V., Rodríguez L., García R., Lorenzo C., Carretero J. M., Frumkin A., Shahack-Gross R., Mayer D. E. B. Y., Cui Y., Wu X., Peled N., Groman-Yaroslavski I., Weissbrod L., Yeshurun R., Tsatskin A., Zaidner Y., Weinstein-Evron M. (2018) The earliest modern humans outside Africa. *Science* 359, 456-459 - doi: 10.1126/science.aap8369

Ingicco, T., van den Bergh, G.D., Jago-on, C., Bahain J.J., Chacon, G., Amano, N., Forestier, H., King, C., Manalo, K., **Nomade**, S., **Pereira**, A., Reyes, M., Sémah, A.M., Shao, Q., Voinchet, P., Falguères, C., Celiberti, V., Albers, P., Lising, M., Lyras, G., Yurnaldi, D., Bautista, A., de Vos, J. 2017. Earliest known hominin activity in The Philippines by 709 kyr. *Nature* 557, 233–237 - doi:10.1038/s41586-018-0072-8.

- **Jean-Baptiste** P., **Fontugne** M., **Fourré** E., Marang L., Antonelli C., Charmasson S., Siclet F. (2018) Tritium and radiocarbon levels in the Rhône river delta and along the French Mediterranean coastline. *Journal of Environmental Radioactivity* 187, 53-64 - doi: 10.1016/j.jenvrad.2018.01.031

- **Jean-Baptiste** P., **Fourré** E., Cassette P. (2018) New determination of the He-3 mixing ratio in the Earth's lower atmosphere from an international tritium intercomparison exercise. Applied Geochemistry 98, 17-21.
- **Jean-Baptiste** P., **Fourré** E., Petit J.R., Lipenkov V., Chetverikov Y., Bulat S., Raynaud D. (2018) Helium and neon in the accreted ice of the subglacial Antarctic Lake Vostok. *Geophysical Research Letters* 45(10) - doi: 10.1029/2018GL078068.
- Jomelli V., Schimmelpfennig I., Favier V., Mokadem F., **Landais** A., Rinterknecht V., Brunstein D., Verfaillie D., Legentil C., Aumaitre G., Bourles D. L., Keddadouche K. (2018) Glacier extent in sub-Antarctic Kerguelen archipelago from MIS 3 period: Evidence from ^{36}Cl dating. *Quaternary Science Reviews* 183, 110-123 - doi: 10.1016/j.quascirev.2018.01.008
- **Jreich** R., **Hatté C.**, Balesdent J., Parent E. (2018) Bayesian selection of mixed covariates in the latent layer: application to hierachical model on soil carbon dynamics. Journal de la Société Française de Statistique. 159(2), 128-155
- **Juillet-Leclerc** A., Rollion-Bard C., Reynaud S., Ferrier-Pages C. (2018) A new paradigm for δ^{18}O in coral skeleton oxygen isotope fractionation response to biological kinetic effects. *Chemical Geology* 483, 131-140 - doi: 10.1016/j.chemgeo.2018.02.035

Kassi S., Stoltmann T., **Casado** M., **Daeron** M., Campargue A. (2018) Lamb dip CRDS of highly saturated transitions of water near 1.4 µm. Journal of Chemical Physics 148, 054201 - doi: 10.1063/1.5010957

Khalil K., Laverman A. M., Raimonet M., **Rabouille** C. (2018) Importance of nitrate reduction in benthic carbon mineralization in two eutrophic estuaries: Modeling, observations and laboratory experiments. *Marine Chemistry* 199, 24-36 - doi: 10.1016/j.marchem.2018.01.004

- **Kissel** C., Sarnthein M., Laj C., Wang P.X., **Wandres** C., Egli R. (2018) Magnetic fingerprints of modern sediments in the South China Sea resulting from source-to-sink processes. *Geochemistry, Geophysics, Geosystems* 19(7) - doi: 10.1029/1018GC007571

Kittel C., Amory C., **Agosta** C., Delhasse A., Doutreloup S., Huot P.V., Wyard C., Fichefet T., Fettweis X. (2018) Sensitivity of the current Antarctic surface mass balance to sea surface conditions using MAR. The Cryosphere 12, 3827-3839.

Konn C., Donval J.P., Guyader V., Roussel E., **Fourré** E., **Jean-Baptiste** P., Pelleter E., Charlou J.L., Fouquet Y. (2018) Organic, gas and element geochemistry of hydrothermal fluids of the newly discovered extensive hydrothermal area in the Wallis and Futuna region (SW Pacific). *Geofluids* 7692839 - doi: 10.1155/2018/7692839

- Labuhn I., Hammarlund D., Chapron E., Czymzik M., Dumoulin J.-P., Nilsson A., **Régnier** É., Rodbyg J., **von Grafenstein** U. (2018) Holocene Hydroclimate Variability in Central Scandinavia Inferred from Flood Layers in Contourite Drift Deposits in Lake Storsjön. *Quaternary* 1, 45323 - doi: 10.3390/quat1010002
- Laepple T., Munch T., **Casado** M., Hoerhold M., **Landais** A., Kipfstuhl S. (2018) On the similarity and apparent cycles of isotopic variations in East Antarctic snow pits. *Cryosphere* 12, 169-187 - doi: 10.5194/tc-12-169-2018
- **Landais** A., Capron E., **Masson-Delmotte** V., Toucanne S., Rhodes R., Popp T., Vinther B., **Minster** B., **Prié** F. (2018) Ice core evidence for decoupling between midlatitude atmospheric water cycle and Greenland temperature during the last deglaciation. *Climate of the Past* 14, 1405-1415.
- **Lavergne** A., **Daux** V., **Pierre** M., **Stievenard** M., Srur A. M., Villalba R. (2018) Past Summer Temperatures Inferred From Dendrochronological Records of Fitzroya cupressoides on the Eastern Slope of the Northern Patagonian Andes. *Journal of Geophysical Research: Biogeosciences* 123(1), 32-45 - doi: 10.1002/2017JG003989

Lécuyer C., Atrops F., Amiot R., Angst D., **Daux** V., Flandrois J.-P., Fourel F., Rey K., Royer A., Seris M., Touzeau A., Rousseau, D.-D. (2018) Tsunami sedimentary of Crete records climate during the Minoan warming period (≈3,350 years BP). *The Holocene* 28(6), 914-929 - doi: 10.1177/0959683617752840

Lessin G., Artioli Y., Almroth-Rosell E., Blackford J. C., Dale A. W., Glud R. N., Middelburg J. J., Pastres R., Queirós A. M., **Rabouille** C., Regnier P., Soetaert K., Solidoro C., Stephens N., Yakushev E. (2018) Modelling marine sediment biogeochemistry: Current knowledge gaps, challenges, and some methodological advice for advancement. *Frontiers in Marine Science* 5 - doi: 10.3389/fmars.2018.00019

Lopez T., Aguilera F., Tassi F., de Moor M., Bobrowski N., Aiuppa A., Cardellini C., Tamburello G., Rizzo A., Luizzo M., Vivieros F., Cardellini C., Silva C., Fischer T., **Jean-Baptiste** P., Kazahaya R., Hidalgo S., Malowany K., Lucic G., Bagnato E.M., Bergsson B., Reath K., Liotta M., Carn S., Chiodini G. (2018) New insights into the magmatic-hydrothermal system and volatile budget of Lastarria Volcano, Chile: Integrated results from the 2014 IAVCEI CCVG 12th Volcanic Gas Workshop. *Geosphere* 14(3): 983-1007 - doi: 1130/GES01495.1

Lougheed B.C., Metcalfe B., Ninnemann U.S., Wacker L. (2018) Moving beyond the age-depth model paradigm in deep-sea palaeoclimate archives: dual radiocarbon and stable isotope analysis on single foraminifera. *Climate of the Past* 14, 515-526.

Mannella G., Giaccio B., Zanchetta G., Regattieri E., Leicher N., Scheidt S., Grelle T., Lehne C., Rolf C., Wonik T., **Nomade** S., **Pereira** A., Niespolo E., Renne P., Leng M., Dean J., Thomas C., Ariztegui D., Gaeta M., Florindo F., Cavinato G.P., Provenzale A., Wagner B. Fucino palaeo-lake: towards the palaeoenvironmental history of the last 430 ka. *Alpine and Mediterranean Quaternary* 31, 141-145.

Marchitto T. M., Bryan S. P., Doss W., McCulloch M. T., **Montagna** P. (2018) A simple biomineralization model to explain Li, Mg, and Sr incorporation into aragonitic foraminifera and corals. *Earth and Planetary Science Letters* 481, 20-29 - doi: 10.1016/j.epsl.2017.10.022

Marino M., **Bassinot** F., Bertini A., Gallicchio S., Girone A., Herbert T., Maiorano P., Nomade S., Petrosino P., Quivelli O., Rodrigues T., Toti F., Ciaranfi N. The climate variability during Marine Isotope Stage 19: Evidences from a west-east Mediterranean transect. *Alpine and Mediterranean Quaternary* 31, 151-154.

- Marra F., **Nomade** S., **Pereira** A., Petronio C., Salari L., Sottili G., Bahain J. J., Boschian G., Di Stefano G., Falgueres C., Florindo F., Gaeta M., Giaccio B., Masotta M. (2018) A review of the geologic sections and the faunal assemblages of Aurelian Mammal Age of Latium (Italy) in the light of a new chronostratigraphic framework *Quaternary Science Reviews* 181, 173-199 - doi: 10.1016/j.quascirev.2017.12.007
- **Missiaen** L., Pichat S., **Waelbroeck** C., **Douville** É., Bordier L.,. **Dapoigny** A., **Thil** F., **Foliot** L., Wacker L. (2018) Downcore variations of sedimentary detrital ($^{238}U/^{232}Th$) ratio: implications on the use of $^{230}Th_{xs}$ and $^{231}Pa_{xs}$ to reconstruct sediment flux and ocean circulation. *Geochemistry, Geophysics, Geosystems* 19(8) - doi: 10.1029/2018gc007502

Moncel M-E., **Landais** A., Lebreton V., Combourieu-Nebout N., **Nomade** S., **Bazin** L. (2018) Linking environmental changes with human occupations between 900 and 400 ka in Western Europe. *Quaternary International* 480, 78-94 - doi: 10.1016/j.quaint.2016.09.065

Mucci A., Levasseur M., Gratton Y., Martias C., Scarratt M., Gilbert D., Tremblay J.E., Ferreyra G., **Lansard** B. (2018) Tidally induced variations of pH at the head of the Laurentian Channel. *Can. J. Fish. Aquat. Sci.* 75, 1128-1141.

Obrochta S.P., Yokoyama Y., Yoshimoto M., Yamamoto S., Miyairi Y., Nagano G., Nakamura A., Tsunematsu K., Lamair L., Hubert-Ferrari A., **Lougheed** B.C., Hokanishi A., Yasuda A., Heyvaert V.M.A., De Batist M., Fujiwara O., the QuakeRecNankai team (2018) Mt. Fuji Holocene eruption history reconstructed from proximal lake sediments and high-density radiocarbon dating. *Quat. Sci. Rev.* 200, 395-405.

- Ollivier V., **Fontugne** M., Hamon C., Decaix A., **Hatté C.**, Jalabadze M. (2018) Neolithic water management and flooding in the Lesser Caucasus (Georgia). Quaternary Science Reviews, 197, 267-287. doi: 10.1016/j.quascirev.2018.08.016

Pastor L., **Rabouille** C., Metzger E., Thibault de Chanvalon A., Viollier E., Deflandre B. (2018) Transient early diagenetic processes in Rhône prodelta sediments revealed in contrasting flood events. *Cont. Shelf Res.* 166, 65-76.

- **Paterne** M., Feuillet N., Cabioch G., **Cortijo** E., **Blamart** B., Weill-Accardo J., Bonneau L. Colin C., **Douville** É., **Pons-Branchu** E (2018) Reservoir ages in the western tropical north Atlantic from one coral off Martinique island (lesser Antilles). *Radiocarbon* 60, 639–652 - doi: 10.1017/RDC.2017.118

Pedoja K., Husson L., Bezos A., Pastier AM, Imran A, Arias Ruiz C, Sarr AC, Elliot M, **Pons-Branchu** E, Nexer M., Regard V., Hafidz A., Robert X., Benoit L, Delcaillau B., Authemayou C., Dumoulin C., Choblet G. (2018) On the long-lasting sequences of coral reef terraces from SE Sulawesi (Indonesia): distribution, formation, and global significance. *Quaternary Science Reviews* 188, 37-57 - doi: 10.1016/j.quascirev.2018.03.033

Péral M., **Daeron** M., **Blamart** D., **Bassinot** F., **Dewilde** F., **Smialkowski** N., **Isguder** G., Bonnin J., Jorissen F., **Kissel** C., **Michel** E., **Riveiros** N.V., **Waelbroeck**, C. (2018) Updated calibration of the clumped isotope thermometer in planktonic and benthic foraminifera. *Geochimica Et Cosmochimica Acta* 239, 1-16.

Pereira A., **Nomade** S., Moncel M. H., Voinchet P., Bahain J. J., Biddittu I., Falgueres C., Giaccio B., Manzi G., Parenti F., Scardia G., **Scao** V., Sottili G., Vietti A. (2018) Integrated geochronology of Acheulian sites from the southern Latium (central Italy): Insights on human-environment interaction and the technological innovations during the MIS 11-MIS 10 period. *Quaternary Science Reviews* 187, 112-129 - doi: 10.1016/j.quascirev.2018.03.021

- Péron O., **Fourré** E., Pastor L., Gegout C., Reeves B., Lethi H. H., Rousseau G., Baglan N., Landesman C., Siclet F., Montavon G. (2018) Towards speciation of organically bound tritium and deuterium: Quantification of non-exchangeable forms in carbohydrate molecules. *Chemosphere* 196, 120-128 - doi: 10.1016/j.chemosphere.2017.12.136
- Petersen J. O., Deschamps P., Hamelin B., **Fourré** E., Gonçalves J., Zouari K., Guendouz A., Michelot J. L., Massault M., **Dapoigny** A., Team A. (2018) Groundwater flowpaths and residence times inferred by ^{14}C, ^{36}Cl and ^{4}He isotopes in the Continental Intercalaire aquifer (North-Western Africa). *Journal of Hydrology*, 560, 11-23 - doi: 10.1016/j.jhydrol.2018.03.003

- Piret L., Bertrand S., **Kissel** C., De Pol-Holz R., Tamayo Hernando A., Van Daele M. (2018) First evidence of a mid-Holocene earthquake-triggered megaturbidite south of the Chile Triple Junction. *Sedimentary Geology* 375, 120-133 - doi: 10.1016/j.sedgeo.2018.01.002
- **Pons-Branchu** E. , Bergonzini L., **Tisnérat-Laborde** N., Branchu P., Dumont E., Massault M., Bultez G., Malnar D., **Kaltnecker** E., Dumoulin J.P., Noret A., Pelletier N., Roy-Barman M. (2018) ^{14}C in urban speleothem-like deposits: a new tool for environmental study. *Radiocarbon* 60(4), 1269-1281 - doi: 10.1017/RDC.2018.25

Pozzato L., **Rassmann** J., **Lansard** B., Dumoulin J.-P., van Breugel P., **Rabouille** C. (2018) Origin of remineralized organic matter in sediments from the Rhone River prodelta (NW Mediterranean) traced by Delta C-14 and delta C-13 signatures of pore water DIC. Progress in Oceanography 163, 112-122.

- Prud'homme C., Lécuyer C., Antoine P., **Hatté** C., Moine O., Fourel F., Amiot R., Martineau F., Rousseau, D. D. (2018) $\delta^{13}C$ signal of earthworm calcite granules: A new proxy for palaeoprecipitation reconstructions during the Last Glacial in western Europe. *Quaternary Science Reviews* 179, 158-166 - doi: 10.1016/j.quascirev.2017.11.017

Rabouille C., Olu K., Baudin F., Khripounoff A., Dennielou B., Arnaud-Haond S., Babonneau N., Bayle C., Beckler J., Bessette S., **Bombled** B., Bourgeois S., Brandily C., Caprais J.C., Cathalot C., Charlier K., Corvaisier R., Croguennec C., Cruaud P., Decker C., Droz L., Gayet N., Godfroy A., Hourdez S., Le Bruchec J., Saout J., Le Saout M., Lesongeur F., Martinez P., Mejanelle L., Michalopoulos P., Mouchel O., Noel P., Pastor L., Picot M., Pignet P., Pozzato L., Pruski A.M., Rabiller M., Raimonet M., Ragueneau O., Reyss J.L., Rodier P., Ruesch B., Ruffine L., Savignac F., Senyarich C., Schnyder J., Sen A., Stetten E., Sun M.Y., Taillefert M., Teixeira S., Tisnérat-Laborde N., Toffin L., Tourolle J., Toussaint F., Vétion G., Jouanneau J.M., Bez M. (2018) The Congolobe project, a multidisciplinary study of Congo deep-sea fan lobe complex: Overview of methods, strategies, observations and sampling. *Deep-Sea Res. II* 142, 7-24.

Raimonet M., Thieu V., Silvestre M., Oudin L., **Rabouille** C., Vautard R., Garnier J. (2018) Landward perspective of coastal eutrophication potential under future climate change: The Seine river case (France). *Front. Mar. Sci.* 5, 136

- Raji O., Dezileau L., Tessier B., Niazi S., Snoussi M., **von Grafenstein** U., Poujol A. (2018) Climate and tectonic-driven sedimentary infill of a lagoon as revealed by T high resolution seismic and core data (the Nador lagoon, NE Morocco). *Marine Geology* 398, 99-111 - doi: 10.1016/j.margeo.2018.01.010
- Rapuc W., Sabatier P., Andrič M., Crouzet C., Arnaud F., Chapron E., Smuc A., Develle A. L., Wilhelm B., Demory F., Reyss J. L., **Régnier** É., Daut G., **von Grafenstein** U. (2018) 6600 years of earthquake record in the Julian Alps (Lake Bohinj, Slovenia). *Sedimentology* 65(5) - doi: 10.1111/sed.12446

Rassmann J., **Lansard** B., Gazeau F., Guidi-Guilvard L., Pozzato L., Allouiane S., Grenz C., **Rabouille** C. (2018) Impact of ocean acidification on the biogeochemistry and meiofaunal assemblage of carbonate-riche sediments: Results from core incubations (Bay of Villefranche, NW Mediterranean Sea). *Marine Chemistry* 203, 102-119 - doi: 10.1016/j.marchem.2018.05.006

Richard M., Falguères C., **Pons-Branchu** E., Foliot L., Guillem M., Martínez-Valle R., Eixea A., Villaverde V. (2018) ESR/U-series chronology of early Neanderthal occupations at Cova Negra (Valence, Spain). *Quaternary Geochronology* 49, 283-290 - doi: 10.1016/j.quageo.2018.05.004

Rintoul S.R., Chown S.L., DeConto R.M., England M.H., Fricker H.A., **Masson-Delmotte** V., Naish T.R., Siegert M.J., Xavier J.C. (2018) Choosing the future of Antarctica. Nature 558, 233-241.

- Roche D.M., **Waelbroeck** C., Metcalfe B., Caley T. (2018) FAME (v1.0): a simple module to simulate the effect of planktonic foraminifer species-specific habitat on their oxygen isotopic content. *Geoscientific Model Development* 11, 3587-3603.

Sarthou G., Lherminier P., Achterberg E.P., Alonso-Perez F., Bucciarelli E., Boutorh J., Bouvier V., Boyle E.A., Branellec P., Carracedo L.I., Casacuberta N., Castrillejo M., Cheize M., Contreira Pereira L., Cossa D., Daniault N., De Saint-Léger E., Dehairs F., Deng F., Desprez de Gésincourt F., Devesa J., Foliot L., Fonseca-Batista D., Gallinari M., Garcia-Ibanez M.I., Gourain A., Grossteffan E., Hamon M., Heimburger L.E., Henderson G.M., Jeandel C., Kermabon C., Lacan F., Le Bot P., Le Goff M., Le Roy E., Lefebvre A., Leizour S., Lemaitre N., Masqué P., Ménage O., Menzel Barraqueta J.L., Mercier H., Perault F., Perez F.F., Planquette H.F., Planchon F., Roukaerts A., Sanial V., Sauzède R., Schmechtig C., Shelley R.U., Stewart G., Sutton J.N., Tang Y., **Tisnérat-Laborde** N., Tonnard M., Tréguer P., Van Beek P., Zurbrick C.M., Zunino P. (2018) Introduction to the French GEOTRACES North Atlantic Transect (GA01): GEOVIDE cruise. *Biogeosciences* 15, 7097-7109.

Schiebel R., Smart S.M., Jentzen A., Jonkers L., Morard R., Meilland J., **Michel** E., Coxall H.K., Hull P.M., De Garidel-Thoron T., Aze T., Quillévéré F., Ren H., Sigman D.M., Vonhof H.B., Martinez-Garcia A., Kucera M., Bijman J., Spero H.J., Haug G.H. (2018) Advances in planktonic foraminifer research: New perspectives for paleoceanography. *Rev. Micropal.* 61, 113-138.

Shi C., **Daux** V., Li Z., Wu X., Fan T., Ma Q., Wu X., Tian H., Carré M., Ji D., Wang W., Rinke A., Liu Y., Chen Y., **Masson-Delmotte** V. (2018) The response of relative humidity to centennial-scale warming over the southeastern Tibetan Plateau inferred from tree-ring width chronologies. *Climate Dynamics* 51(9-10), 3735-3746 - doi: 10.1007/s00382-018-4107-5

Simon Q., Bourles D. L., Thouveny N., Horng C. S., Valet J. P., **Bassinot** F., Choy S. (2018) Cosmogenic signature of geomagnetic reversals and excursions from the Réunion event to the Matuyama–Brunhes transition (0.7–2.14 Ma interval). *Earth and Planetary Science Letters* 482, 510-524 - doi: 10.1016/j.epsl.2017.11.021

Simon Q., Thouveny N., Bourles D. L., **Bassinot** F., Savranskaia T., Valet J. P., ASTER Team (2018) Increased production of cosmogenic 10Be recorded in oceanic sediment sequences: Information on the age, duration, and amplitude of the geomagnetic dipole moment minimum over the Matuyama–Brunhes transition. *Earth and Planetary Science Letters* 489, 191-202 - doi: 10.1016/j.epsl.2018.02.036

Stetten L., Mangeret A., Brest J., Seder-Colomina M., Le Pape P., Ikogou M., Zeyen N., Thouvenot A., Julien A., Alcalde G., Reyss J. L., **Bombled** B., **Rabouille** C., Olivi L., Proux O., Cazala C., Morin G. (2018) Geochemical control on the reduction of U(VI) to mononuclear U(IV) species in lacustrine sediments. *Geochimica et Cosmochimica Acta* 222, 171-186 - doi: 10.1016/j.gca.2017.10.026

- Studer A., Sigman D., Martinez-Garcia A., Thöle L.M., **Michel** E., Jaccard S.L., Lippold J.A., **Mazaud** A., Wang X.T., Robinson L., Adkins J.F., Haug G.H. (2018) Increased nutrient supply to the Southern Ocean during the Holocene and its implication for the pre-industrial atmosphéric CO_2 rise. *Nature Geoscience*, 11, 756-760.

Tifafi M., Camino-Serrano M., **Hatté C.**, Morras H., Moretti L., Barbaro S., Cornu S., Guenet B. (2018) The use of radiocarbon ^{14}C to constrain carbon dynamics in the soil module of the land surface model ORCHIDEE (SVN r5165). Geoscientific Model Development, 11, 4711-4726. doi: 10.5194/gmd-11-4711-2018

- **Tifafi** M., Guenet B., **Hatté** C. (2018) Large Differences in Global and Regional Total Soil Carbon Stock Estimates Based on SoilGrids, HWSD, and NCSCD: Intercomparison and Evaluation Based on Field Data From USA, England, Wales, and France. *Global Biogeochemical Cycles* 32, 42-56 - doi: 10.1002/2017GB005678
- **Touzeau** A., **Landais** A., Morin S., Arnaud L., Picard G. (2018) Numerical experiments on isotopic diffusion in polar snow and firn using a multi-layer energy balance model. *Geosci. Model Dev*. 11(6), 2393-2418 - doi: 10.5194/gmd-11-2393-2018

Uemura R., Motoyama H., **Masson-Delmotte** V., **Jouzel** J., Kawamura K., Goto-Azuma K., Fujita S., Kuramoto T., Hirabayashi M., Miyake T., Ohno H., Fujita K., Abe-Ouchi A., Iizuka Y., Horikawa S., Igarashi M., Suzuki K., Suzuki T., Fujii Y. (2018) Asynchrony between Antarctic temperature and CO2 associated with obliquity over the past 720,000 years. *Nature Communications* 9, 961 - doi: 10.1038/s41467-018-03328-3

van Vliet-Lanoe B., Schneider J. L., Gu_mundsson Á., **Guillou** H., **Nomade** S., Chazot G., Liorzou C., Guegan S. (2018) Eemian estuarine record forced by glacio-isostasy (Southern Iceland)—link with Greenland and deep sea records Canadian. *Journal of Earth Sciences* 55, 154-171 - doi: 10.1139/cjes-2017-0126

Venancio I.M., Mulitza S., **Govin** A., Santos T.P., Lessa D.O., Albuquerque A.L.S., Chiessi C.M., Tiedemann R., Vahlenkamp M., Bickert T., Schulz M. (2018) Millennial- to Orbital-Scalp Responses of Western Equatorial Atlantic Thermocline Depth to Changes in the Trade Wind System Since the Last Interglacial. Paleoceanography and Paleoclimatology 33, 1490-1507.

- **Waelbroeck** C., Pichat S., Bohm E., **Lougheed** B.C., Faranda D., Vrac M., **Missiaen** L., **Vazquez Riveiros** N., Burckel P., Lippold J., Arz H.W., Dokken T., **Thil** F., **Dapoigny** A. (2018) Relative timing of precipitation and ocean circulation changes in the western equatorial Atlantic over the last 45 kyr. *Climate of the Past* 14, 1315-1330.
- Wary M., Eynaud F., **Kissel** C., Londeix L., Rossignol L., Lapuyade J., Castera M. H., Billy I. (2018) Spatio-temporal dynamics of hydrographic reorganizations and iceberg discharges at the junction between the Northeast Atlantic and Norwegian Sea basins surrounding Heinrich event 4. *Earth and Planetary Science Letters* 481, 236-245 - doi: 10.1016/j.epsl.2017.10.042

Webster J.M., Braga J.C., Humblet M., Potts D.C., Iryu Y., Yokoyama Y., Fujita K., Bourillot R., Esat T.M., Fallon S., Thompson W.G., Thomas A.L., Kan H., McGregor H.V., Hinestrosa G., Obrochta S.P., **Lougheed** B.C. (2018) Response of the Great Barrier Reef to sea-level and environmental changes over the past 30.000 years. *Nature Geosciences* 11, 426-432.

Werner M., **Jouzel** J., **Masson-Delmotte** V., Lohmann G. (2018) Reconciling glacial Antarctic water stable isotopes with ice sheet topography and the isotopic paleothermometer. *Nature Communications* 9, 3537 – doi: 10.1038/s41467-018-05430-y.

Wienberg C., Titschack J., Freiwald A., **Frank** N., Lundälv T., Taviani M., Beuck L., Schroder-Ritzrau A., Krengel T., Hebbeln D. (2018) The giant Mauritanian cold-water coral mound province: Oxygen control on coral mound formation. *Quaternary Science Reviews* 185, 135-152 - doi: 10.1016/j.quascirev.2018.02.012

- Wils K., Van Daele M., Lastras G., **Kissel** C., Lamy F., Siani G. (2018) Holocene Event Record of Aysén Fjord (Chilean Patagonia): An Interplay of Volcanic Eruptions and Crustal and Megathrust Earthquakes. *Journal of Geophysical Research: Solid Earth* 123, 324-343 - doi: 10.1002/2017JB014573

- **Wu** H.C., Dissard D., **Douville** E., **Blamart** D., Bordier L., Tribollet A., Le Cornec F., **Pons-Branchu** E., **Dapoigny** A., Lazareth C. (2018) Surface ocean pH variations since 1689 CE and recent ocean acidification in the tropical south Pacific. *Nature communications* 9, 2543 - doi:10.1038/s41467-018-04922-1

Wu J., **Rabouille** C., Charmasson S., Reyss J.L., Cagnat X. (2018) Constraining the origin of recently deposited particles using natural radionuclides ^{7}Be and $^{234}Th_{xs}$ in deltaic sediments. *Continental Shelf Research* 165, 106-119.

Yang J.W., Han Y., **Orsi** A.J., Kim S.J., Han H., Ryu Y., Jang Y., Moon J., Choi T., Hur S.D., Ahn J. (2018) Surface temperature in twentieth century at the Styx glacier, northern Victoria Land, Antarctica, from borehole thermometry. *Geophys. Res. Lett.* 45, 9834-9842.

Yu Z., Colin C., Ma R., Meynadier L., Wan S., Wu Q., Kallel N., Sépulcre S., **Dapoigny** A., **Bassinot** F. (2018) Antarctic intermediate water penetration into the Northern Indian Ocean during the last deglaciation. *Earth Planet. Sci. Lett.* 500, 67-75.

Autres publications

(Corrigendum, Addendum, articles EGU en "discussion", chapitre, article de rang B, prix et médailles)

Chen Y., Moufouma-Okia W., **Masson-Delmotte V.**, Zhai P., Pirani A. (2018) Recent Progress and Emerging Topics on Weather and Climate Extremes Since the Fifth Assessment Report of the Intergovernmental Panel on Climate Change, in: Gadgil, A., Tomich, T.P. (Eds.), Annual Review of Environment and Resources, Vol 43, pp. 35-59.

Frouin M., Lahaye C., **Valladas** H., Higham T., Delagnes A., Mercier N. (2018) Corrigendum to "Dating the Middle Palaeolithic deposits of La Quina Amont (Charente, France) using luminescence methods (vol 109, pg 30, 2017)". *Journal of Human Evolution* 124, 140-141.

Griggo C., de Souza I., Boëda E., **Fontugne** M., **Hatté C.**, Lourdeau A., Guidon N. (2018) La faune du Pléistocène supérieur – Holocène ancien de La Toca da Pena (Piaui, Brésil) – Etude paléontologique. Quaternaire, 29(3), 205-2016

Hershkovitz I., Duval M., Grun R., Mercier N., **Valladas** H., Ayalon A., Bar-Matthews M., Weber G.W., Quam R., Zaidner Y., Weinstein-Evron M. (2018) Response to Comment on "The earliest modern humans outside Africa". *Science* 362.

Jaillet S., **Pons-Branchu** E., Hoblea F., Berthet J., Deline P., Duvillard P.-A., Genuite K. (2018) The glacio-karstic depression of Mariet (Bauges occidentales, France): a marker of the wurmian glaciation in the Northern French Alps. *Geomorphologie-Relief Processus Environnement* 24, 107-120.

- **Juillet-Leclerc** A. (2019) The role of light as vital effect on coral skeleton oxygen isotopic ratio. Biogeosciences Discussion – doi: 10.5194/bg-2018-433

Masson-Delmotte V. (2018) parmi les dix scientifiques qui ont le plus marqué l'année

Rintoul S.R., Chown S.L., DeConto R.M., England M.H., Fricker H.A., **Masson-Delmotte** V., Naish T.R., Siegert M.J., Xavier J.C. (2018) Corrigendum to "Choosing the future of Antarctica (vol 558, 233, 2018)". Nature 562, E5-E5.

THÈSES SOUTENUES EN 2018

- thèse donnant lieu à une fiche ci-après

GUILPART Étienne — *soutenue le 23 janvier 2018*

Étude de la composition isotopique (deutérium et oxygène 18) de la vapeur d'eau dans l'atmosphère sur l'Ile de la Réunion : apport à la compréhension des processus humides atmosphériques en région tropicale

- TIFAFI Marwa — *soutenue le 5 avril 2018*

Different soil study tools (experimentation, databases comparison and modeling) to better understand the dynamics of carbon in soils

COULARIS Cindy — *soutenue le 23 juin 2018*

Dynamique et transfert du carbone dans le bassin versant de la Loire : traçage par les isotopes du carbone

- PERAL Marion — *soutenue le 9 octobre 2018*

Le rapport B/Ca des foraminifères : un proxy pour le cycle du carbone dans l'océan

- JREICH Rana — *soutenue le 28 novembre 2018*

Dynamique verticale du carbone dans les sols – Utilisation combinée des traceurs isotopiques et de méta-analyse statistique

DRUGAT Laurine — *soutenue le 17 décembre 2018*

Géochimie des spéléothèmes du sud-ouest de l'Europe (chronologie U/Th et ^{14}C, éléments traces, $^{87}Sr/^{88}Sr$, $^{18}O/^{16}O$, $^{13}C/^{12}C$) appliquée aux reconstitutions climatiques et environnementales à l'Holocène

Cafés-science de 2018

sous l'impulsion de l'équipe 2018 d'organisation des Cafés Sciences:
Sentia Goursaud, Kristan Cuny, Rana Jreich, Romain Euverte, Cécile Agosta, …

Traçage des sources sédimentaires et des polluants particulaires dans les rivières à partir de l'analyse de radionucléides (^{7}Be, ^{137}Cs, ^{210}Pb)
Olivier Evrard
le 6 février 2018

Les Populations du Proche-Orient au Paléolithique moyen
Hélène Valladas
le 6 mars 2018

Traçage des sources de sédiments dans les rivières de Nouvelle-Calédonie
Christophe Rabouille
le 3 avril 2018

Café Sciences « spécial stagiaires »
le 5 juin 2018

Le projet THEME : dendro-isotopie et cellule de Hadley
Valérie Daux et Monique Pierre
le 4 septembre 2018

Café Sciences « spécial doctorants »
le 6 novembre 2018

Les migrations des hominidés anciens dans le Sud-Est Asiatique: des hobbits surfers ?
Sébastien Nomade
le 4 décembre 2018

FICHES ILLUSTRANT LES ACTIVITÉS 2018

… sur la base des publications 2018

The triple oxygen isotope composition of phytoliths as a proxy of continental atmospheric humidity: insights from climate chamber and climate transect calibrations

Alexandre A., Landais A., …, Prié F., et al.

Biogeosciences, 15, 3223–3241 (2018), doi: 10.5194/bg-15-3223-2018
Financé par ANR HUMI1

Continental atmospheric relative humidity (RH) is a key climate parameter. Combined with atmospheric temperature, it allows us to estimate the concentration of atmospheric water vapor, which is one of the main components of the global water cycle and the most important gas contributing to the natural greenhouse effect. However, there is a lack of proxies suitable for reconstructing, in a quantitative way, past changes of continental atmospheric humidity. This reduces the possibility of making model–data comparisons necessary for the implementation of climate models.

Over the past 10 years, analytical developments have enabled a few laboratories to reach sufficient precision for measuring the triple oxygen isotopes, expressed by the ^{17}O-excess in water, water vapor and minerals. The ^{17}O-excess represents an alternative to deuterium-excess for investigating relative humidity conditions that prevail during water evaporation. Phytoliths are micrometric amorphous silica particles that form continuously in living plants. Phytolith morphological assemblages from soils and sediments are commonly used as past vegetation and hydrous stress indicators. In the present study, we examine whether changes in atmospheric RH imprint the ^{17}O-excess of phytoliths in a measurable way and whether this imprint offers a potential for reconstructing past RH. For that purpose, we first monitored the ^{17}O-excess evolution of soil water, grass leaf water and grass phytoliths in response to changes in RH (from 40 to 100 %) in a growth chamber experiment where transpiration reached a steady state. Decreasing RH from 80 to 40% decreases the ^{17}Oexcess of phytoliths by 4.1 per meg/% as a result of kinetic fractionation of the leaf water subject to evaporation. In order to model with accuracy the triple oxygen isotope fractionation in play in plant water and in phytoliths we recommend direct and continuous measurements of the triple isotope composition of water vapor. Then, we measured the ^{17}O-excess of 57 phytolith assemblages collected from top soils along a RH and vegetation transect in inter-tropical West and Central Africa. Although scattered, the ^{17}O-excess of phytoliths decreases with RH by 3.4 per meg/%. The similarity of the trends observed in the growth chamber and nature supports that RH is an important control of ^{17}O-excess of phytoliths in the natural environment.

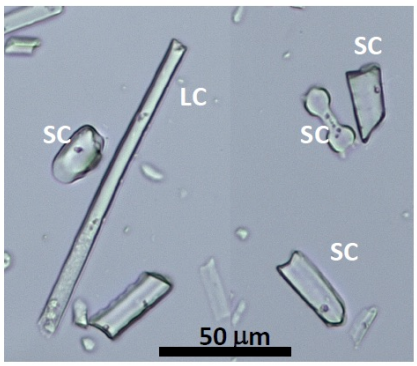

Figure: Phytolith types extracted from Festuca arundinaceae

Atmosphere-soil carbon transfer as a function of soil depth

Balesdent J., Basile-Doelsch I., Chadoeuf J., Cornu S., Derrien D., Fekiacova Z., Hatté C.

Nature, 559, 599-602 (2018), doi:10.1038/s41586-018-0328-3
Financé par ANR DEDYCAS et LEFE DYVERTIS

The exchange of carbon between soil organic carbon (SOC) and the atmosphere affects the climate and—because of the importance of organic matter to soil fertility—agricultural productivity. The dynamics of topsoil carbon has been relatively well quantified, but half of the soil carbon is located in deeper soil layers (below 30 centimeters), and many questions remain regarding the exchange of this deep carbon with the atmosphere. This knowledge gap restricts soil carbon management policies and limits global carbon models. Here we quantify the recent incorporation of atmosphere-derived carbon atoms into whole-soil profiles, through a meta-analysis of changes in stable carbon isotope signatures at 112 grassland, forest and cropland sites, across different climatic zones, from 1965 to 2015. We find, in agreement with previous work, that soil at a depth of 30–100 centimeters beneath the surface (the subsoil) contains on average 47 per cent of the topmost meters SOC stocks. However, we show that this subsoil accounts for just 19 per cent of the SOC that has been recently incorporated (within the past 50 years) into the topmost meter. Globally, the median depth of recent carbon incorporation into mineral soil is 10 centimeters.

Variations in the relative allocation of carbon to deep soil layers are better explained by the aridity index than by mean annual temperature. Land use for crops reduces the incorporation of carbon into the soil surface layer, but not into deeper layers. Our results suggest that SOC dynamics and its responses to climatic control or land use are strongly dependent on soil depth. We propose that using multilayer soil modules in global carbon models, tested with our data, could help to improve our understanding of soil–atmosphere carbon exchange.

Sedimentological and geochemical study of the Bongongo and Ngol travertines located at the Cameroon Volcanic Line

Bisse S.B., Ekomane E., Eyong J.T., Ollivier V., Douville E., Nganne M.J.M., Bitom L.D.

Journal of African Earth Sciences (2018) 143 201-214, doi:10.1016/j.jafrearsci.2018.03.028

A sedimentological and geochemical study was carried out on the travertines from Bongongo and Ngol locations along the Cameroon Volcanic Line. This work seeks to ascertain: (1) the origin and typology of the studied travertine deposits, (2) the palaeo-environmental depositional model and (3) the typical characteristic of the hydrothermal system. The distribution and typology of travertine deposits were performed from natural outcrops. Oxygen and carbon stable isotope methods have been employed in the detail study of representative travertine samples from Bongongo and Ngol. The different travertine deposits along Ngol stream valley occur around waterfall/cascade, slopes and pools. At Bongongo the travertine precipitation can be linked to temporal fluctuation of carbonate mineral saturation level in rising thermal fluids and the depth of the boiling zone. The hydrothermal system of Ngol and Bongongo has been clarified using results of geochemical analyses of stable isotope, which can be applied regionally. The studied travertines are characterized by $\delta^{18}O$ values from −8.4 to −6.4‰ V-PDB for Ngol and −5.8 to −5.9‰ V-PDB for Bongongo and $\delta^{13}C$ values from 0.4 to 0.5‰V-PDB for Ngol and from 1.1 to 2‰V-PDB for Bongongo, in accordance with global travertine deposit environments. The values of stable carbon isotopes analyses of Bongongo and Ngol travertines are very far from the isotopic composition of magmatic carbon. Based on the geothermal environment, the high temperature parent solution (31 °C and 49°C) and stable isotope study, it can be considered that the studied travertine from Bongongo and Ngol are characteristic of the thermogenic type (Fig.).

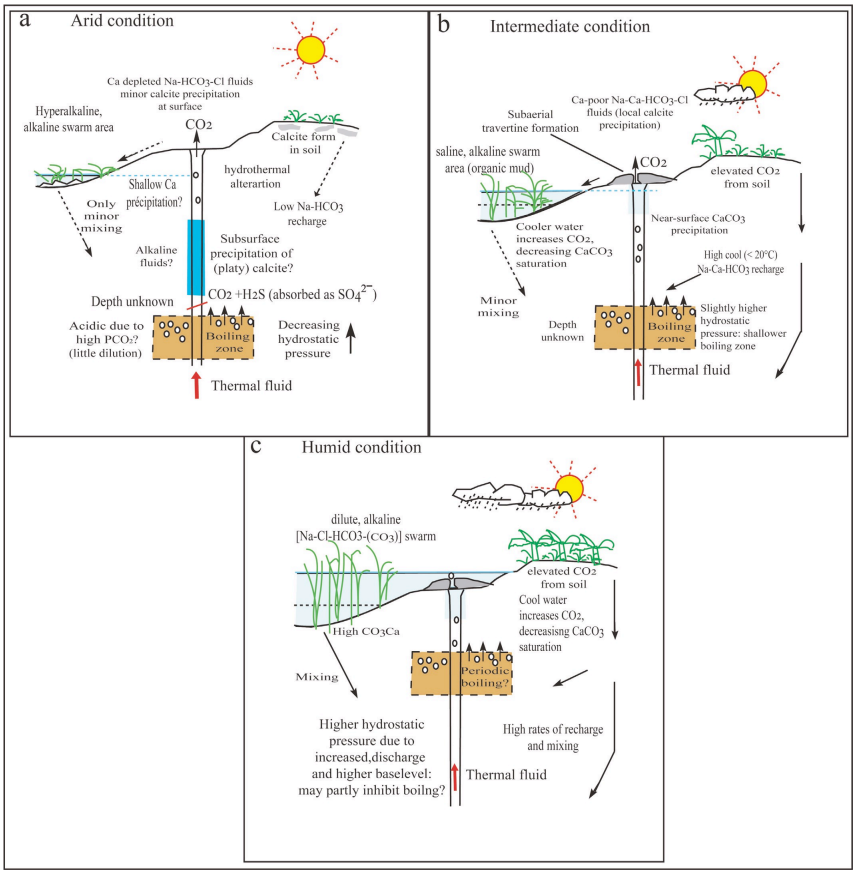

Figure: Schematic model to show the inferred processes and controls of carbonate precipitation at the Bongongo hot springs under different climate conditions and associated swamp levels.

Distribution and ecology of the *Globigerinoides ruber* — *Globigerinoides elongatus* morphotypes in the Azores region during the late Pleistocene-Holocene

Bonfardeci A., Caruso A., Bartolini A., Bassinot F., Blanc-Valleron M-M..

Palaeogeography, Palaeoclimatology, Palaeoecology (2018), 491, 92-111 - doi: 10.1016/j.palaeo.2017.11.052

Globigerinoides ruber is the dominant taxon in the North Atlantic Subtropical Gyre, nowadays limited to the north by the Azores Current. It is highly sensitive to recent and late Pleistocene Azores Front Current System variability. In this study, we analyse the distribution of five individual morphotypes of the G. ruber – G. elongatus plexus (G. ruber s.s., G. ruber cyclostoma type, G. elongatus, G. elongatus cf.1, G. elongatus pyramidical type) and G. ruber kummerform gr. in a core (ATA13-OF-KT1) collected southwest of the Azores islands and located in a strategical position near the present-day boundary of the Subtropical Gyre/Azores Front Current System (STG/AFCS). Micropaleontological and stable isotope analyses can provide new insights on the ecological preferences of the G. ruber chromotypes and some selected morphotypes (especially the less studied G. ruber cyclostoma type). Their distribution pattern shows cyclic oscillations linked to climatic variability at orbital and millennial scales. G. elongatus clearly dominated the G. ruber - G. elongatus assemblage during the interglacials, while G. ruber cyclostoma type reached their maxima abundances during glacial periods. Furthermore, changes in the relative abundance of warm (G. elongatus) and cool water (G. ruber cyclostoma type) morphotypes represent a powerful tool to track the position occupied by the Subtropical Gyre/Azores Current (STG/AC) boundary during the last 74.7 kyr.

Imprint of Holocene climate variability on CWC reef growth at the SW Rockall Trough margin, NE Atlantic

Bonneau L., …, Pons-Branchu E., Mienis F., Tisnérat-Laborde N., Blamart D., …, Douville E.

Geochem., Geophys., Geosyst. 19(8), 2437-2452(2018), doi:10.1029/2018GC007502

Project: ANR HAMOC with Lucile Bonneau (12 month-postdoc)

U-Th ages and Li/Mg derived temperatures were measured on coral fragments of *L. pertusa* and *M. oculata* collected from sediment cores from cold-water coral (CWC) mounds at 700-790 m water depth at the SW Rockall Trough margin. These data combined with previous ones from the same mound region allow not only to estimate the occurrence of CWC at the SW Rockall Trough margin during the Holocene and to constrain the environmental conditions driving variability in CWC growth. CWC abundance increases in the mid-Holocene (~6 ka) and is modulated by millennial-scale variability through-out the late Holocene. The mid-Holocene CWC proliferation coincides with the lowest IRD abundances and a major re-organization of the circulation at thermocline depth in the Rockall Trough, marked by the progressive replacement of the fresh-cold SubArctic Intermediate Water by the saltier and nutrient-rich Eastern North Atlantic Water. This event may have established a modern-like winter mixed layer and thermocline structure, generating suitable conditions for enhanced surface productivity, downslope transport of food particles, bottom current acceleration at mound depth and thus CWC growth. Several short time intervals of decreased CWC occurrences closely match prominent increases in North Atlantic drift ice and storminess in Northern Europe. We propose that high detrital supply and/or changes in the vertical density gradient associated to millennial-scale ice rafted detritus (IRD) events are the likely controlling factors for CWC growth and subsequently mound formation of the SW Rockall Trough margin.

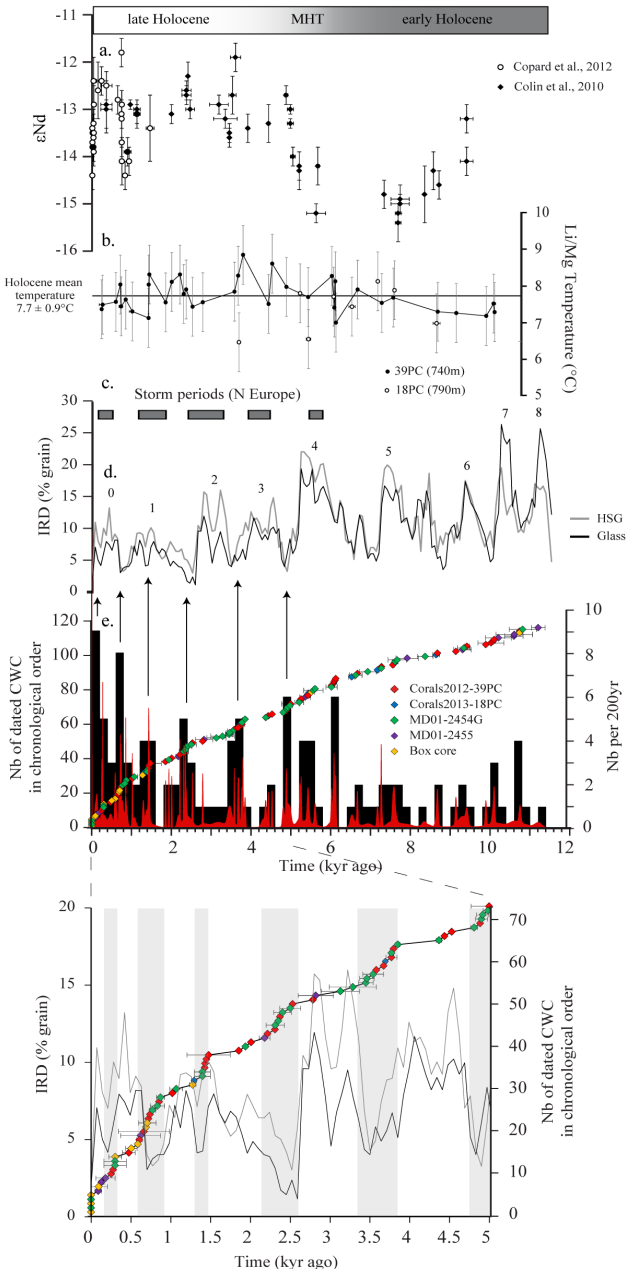

Figure: (a) εNd & (b) Li/Mg temperature obtained from CWC collected on the SW Rockall Bank; (c) Storm periods in Northern Europe; (d) IRD (Glass & Hematite Stained Grains: HSG) abundance in core VM29-191 (Bond et al., 1997) and (Sorel et al., 2012). (e) Compilation of U-Th datings.

Limitations to U/Th dating of reef-platform carbonate boulders produced by high-energy marine inundations in the Tuamotu Archipelago (French Polynesia)

Canavesio R., Pons-Branchu E., Yannick C.

Coral reefs, 37 (4), 1139-1155 (2018), doi:10.1007/s00338-018-1732-8

On intertropical coastlines, coral boulders located on the reef platform are often used to characterize high-energy marine inundations of the past. Precise U/Th coral dating provides opportunities to assess the timing and recurrence of these events. However, this method of dating is subject to several limitations, as revealed by studying live coral cover at five islands in French Polynesia, since the early 1990s. We show that live coral assemblages experience very different changes within the islands of the same archipelago. Moreover, our observations show that the passage of a cyclone causes almost complete disappearance of the most recent coral in the coral boulder formation zone. This analysis shows that the probability of taking coral samples that were alive on the day of the high-energy marine inundation is extremely low. We have clarified the limitations of this method based on the dating of coral assumed to be alive on the day of the well-documented high-energy marine inundation of 1903 AD. The dating of 24 samples taken from 22 boulders from 3 islands of the Tuamotu Archipelago shows that important parts of the coral were dead when displaced by the marine inundations, thereby overestimating the timing of the disturbance event. As such, U/Th coral dating has limited application for establishing the precise timing for high-energy marine inundations with a return period of less than a century, but may be useful for exploring infrequent and extreme events such as the cyclone that ravaged the Tuamotu atolls in 1903. Indeed, we observed that this cyclone is the one that produced the world's largest reef-platform coral boulders (more than 100 m^3). We also provide evidence of an earlier event in the center of the Tuamotu Archipelago, during the middle of the first century AD.

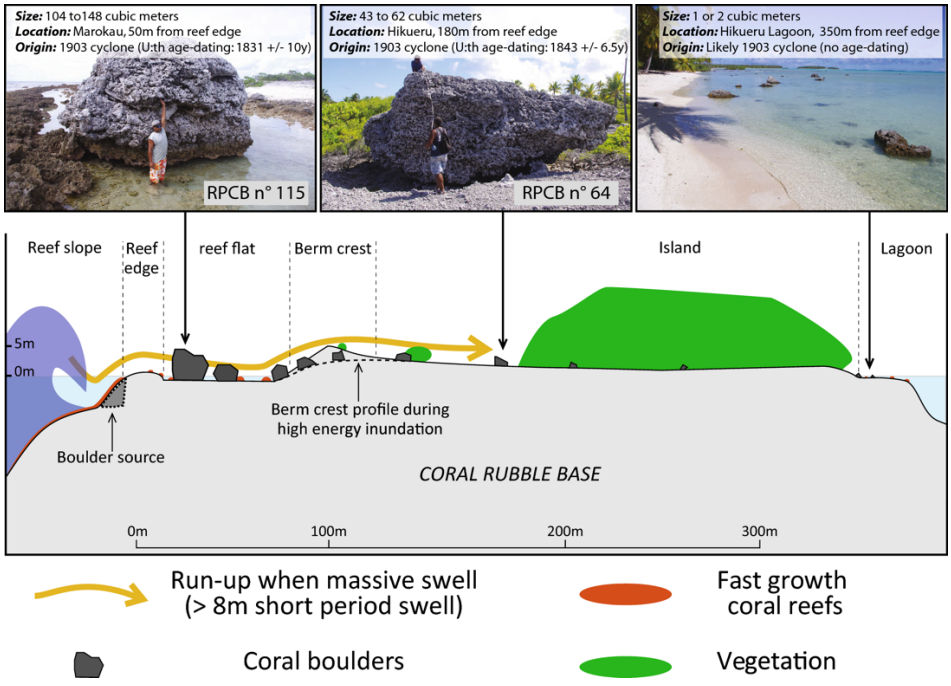

Figure: Profile and zonation of a cyclonic boulder field in the Tuamotu Archipelago

Archival processes of the water stable isotope signal in East Antarctic ice cores

Casado M., Landais A., … Touzeau A., Masson-Delmotte V., Jouzel J.

The Cryosphere, 12, 1745–1766 (2018), doi: 10.5194/tc-12-1745-2018
Financé par l'ERC Combiniso

The oldest ice core records are obtained from the East Antarctic Plateau. Water isotopes are key proxies to reconstruct past climatic conditions over the ice sheet and at the evaporation source. The accuracy of climate reconstructions depends on the knowledge of all processes affecting water vapor, precipitation and snow isotopic compositions. Fractionation processes are well understood and can be integrated in trajectory-based Rayleigh distillation and isotope enabled climate models. However, a quantitative understanding of processes potentially altering snow isotopic composition after deposition is still missing. In low-accumulation sites, such as those found in East Antarctica, these poorly constrained processes are likely to play a significant role and limit the interpretability of an ice core's isotopic composition.

By combining observations of isotopic composition in vapor, precipitation, surface snow and buried snow from Dome C, a deep ice core site on the East Antarctic Plateau, we found indications of a seasonal impact of metamorphism on the surface snow isotopic signal when compared to the initial precipitation. Particularly in summer, exchanges of water molecules between vapor and snow are driven by the diurnal sublimation–condensation cycles. Overall, between precipitation events, we observe modification of the surface snow isotopic composition. Using high-resolution water isotopic composition profiles from snow pits at five Antarctic sites with different accumulation rates, we identified common patterns which cannot be attributed to the seasonal variability of precipitation. These differences in the precipitation, surface snow and buried snow isotopic composition provide evidence of post-deposition processes affecting ice core records in low-accumulation areas.

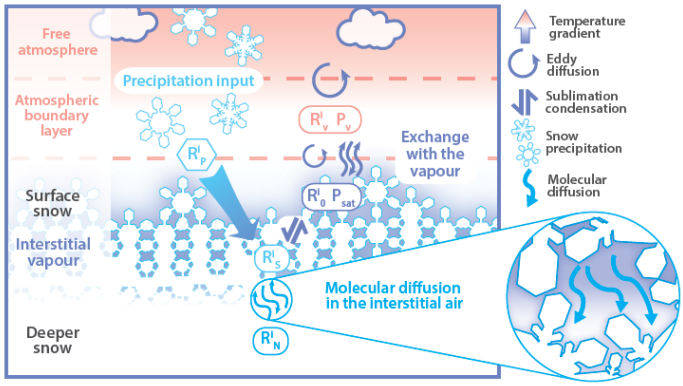

Figure: Scheme of the different contributions to snow isotopic composition (R^i_X stands for the composition of isotope i in phase X: P is precipitation, V is vapor, S is surface snow, N is the deeper snow, 0 is vapor at equilibrium with the snow and Pv and Psat are the water vapor partial pressure and the saturated vapor pressure, respectively). Above the surface, both the precipitation and the sublimation–condensation cycles can contribute to the surface composition; in the open-porous firn below the surface, ice crystals can exchange with the air through the pores and may be influenced by wind pumping. Deeper in the firn, molecular diffusion in the interstitial air affects the snow isotopic composition.

Circulation Changes in the Eastern Mediterranean Sea Over the Past 23,000 Years Inferred from Authigenic Nd Isotopic Ratios

Cornuault M., … Bassinot F., Revel M.

Paleoceanography and Paleoclimatology (2018) 33 (3), 264-280, doi: 10.1002/2017PA003227

The Eastern Mediterranean Sea (EMS) is a key region to study circulation change because of its own thermohaline circulation. In this study, we focused on intermediate/deep water circulation since the Last Glacial Maximum (LGM) including the sapropel S1 period. Two cores from the Levantine Sea and the Strait of Sicily, respectively, collected at 1,780 m and 771 m water depth, were studied using 143Nd/144Nd (εNd) of foraminiferal tests and leachates as well as benthic foraminiferal stable isotopes (δ13C, δ18O). This approach allowed the determination of variations in (1) the North Atlantic water contribution to the Mediterranean basin, (2) water exchanges at the Strait of Sicily, and (3) the influence of the Nile River over the last 23,000 years. During the LGM, high benthic foraminiferal δ13C values indicate well-ventilated intermediate and deep waters in the EMS. The εNd values were more radiogenic than at present, reflecting a smaller contribution of unradiogenic North Atlantic waters to the EMS due to reduced exchange at the Strait of Sicily. The sluggish circulation in the EMS initiated during deglaciation was further enhanced by increased Nile River freshwater inputs between 15 ka BP and the S1 period. Partial dissolution of Nile River particles contributed to an increase in EMS εNd. The large εNd gradient between the EMS and the Western Mediterranean Sea observed during LGM and S1 suggests that each basin had a distinct circulation mode. Decreasing εNd values at the Strait of Sicily after S1 reflected improved water exchange between both basins, leading to the modern circulation pattern.

.

The calcification depth and Mg/Ca thermometry of Pulleniatina obliquiloculata in the tropical Indo-Pacific: A core-top study

Dang H., …, Bassinot F., Wang T., Kissel C.

Marine Micropaleontology (2018) 145, 28-40, doi: 10.1016/j.marmicro.2018.11.001

A sub-surface dwelling planktonic foraminifer, Pulleniatina obliquiloculata, in particular its shell's geochemical properties such as stable oxygen isotopic composition and Mg/Ca ratios, are widely used to reconstruct past changes in the thermocline of tropical Indo-Pacific. However, the depth range that P. obliquiloculata population generally dwells or calcifies has been shown to significantly vary, depending on the regions and the seasons. In this study, δ18O and Mg/Ca of core-top P. obliquiloculata from the tropical Indo-Pacific are analyzed by means of comparison with modern hydrographic data. We apply a δ18O-based approach to decipher the varying apparent calcification depth (ACD) of this species for the tropical Indo-Pacific, and find that P. obliquiloculata's ACD varies between 50 and 150 m regionally, in connection with local oceanographic settings. At given ACD, exponential relationships between temperature and P. obliquiloculata Mg/Ca are determined as $Mg/Ca = 0.245 \pm 0.041 \exp.(0.088 \pm 0.009\,T)$ for these core-top samples. The sensitivity of P. obliquiloculata Mg/Ca to temperature is in good accordance with most previous findings, particularly the recent work using core-top samples from the western tropical Pacific. Taken together, our results not only improve the understanding of the calcification conditions of P. obliquiloculata, but also make it possible to better estimate the sub-surface temperature of the Indo-Pacific Warm Pool (IPWP) using Late-Quaternary sedimentary materials.

Comparisons of the performance of $\delta^{13}C$ and $\delta^{18}O$ of *F. sylvatica*, *P. sylvestris* and *Q. petraea* in the record of past climate variations

Daux V., Michelot-Antalik A., Lavergne A., Pierre M., Stievenard M. et al.

J. Geophys. Res. Biogeosci. 123, 1144-1160 (2018), doi: 10.1002/2017JG004203
Financé par le GIS-AFOCLIM

Climate reconstructions in temperate Europe have been widely based on oak species. However, other co-occurring species, largely distributed in Europe, may be used for recording climate variability. In this paper, we document the inter-trees and inter-species variations over 1960-2007 of oxygen and carbon isotopic compositions in ring cellulose of *F. sylvatica*, *P. sylvestris* and *Q. petraea* co-occurring in the Fontainebleau forest (France; Figure). Our results indicate that large levels of series replication (11 trees on average) are required to generate isotopic mean series representative of the populations. Calculated mean isotopic ratios in pine are higher than in the deciduous species, and we hypothesize that these contrasts result from differences in stomatal conductance, phenology and canopy structure, and, for oxygen, also in water uptake depth and isotopic exchange rate. We find that $\delta^{18}O$ and $\delta^{13}C$ chronologies are significantly correlated to one another in the three species and respond primarily to air moisture and T_{max}, which indicates that stomatal conductance, was an important driver of changes in both types of records. We determine that the correlations were strong with the May to July climate variables in *F. sylvatica*, and with the July and August ones in *Q. petraea* and *P. sylvestris*. We show that the oxygen records are systematically more coherent than those of carbon. This study demonstrates that $\delta^{18}O$, and to a lesser extent $\delta^{13}C$, from the three different species are reliable proxies for reconstructing past hydroclimatic variations in Europe.

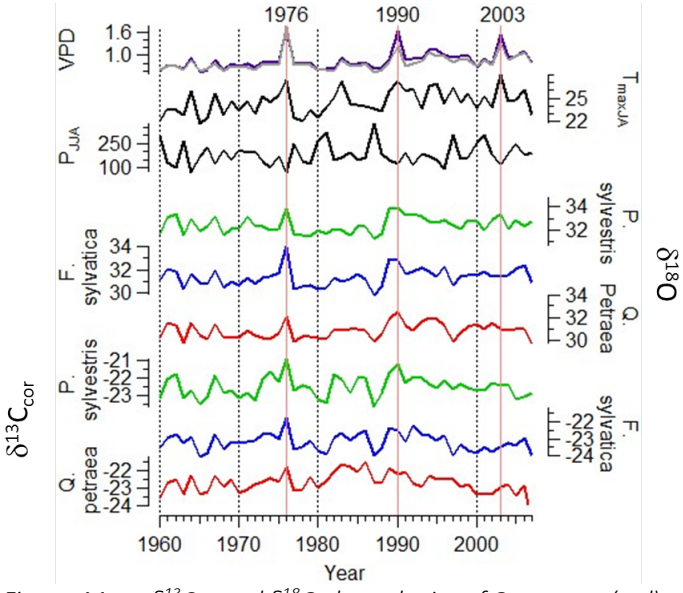

Figure: Mean $\delta^{13}C_{cor}$ and $\delta^{18}O$ chronologies of Q. petraea (red), F. sylvatica (blue) and P. sylvestris (green) from Fontainebleau forest, precipitation over June-August (in mm), maximum temperature averaged over July-August (T_{maxJA} in °C), vapor pressure deficit (VPD in kPa) averaged over July-August (purple) or June-August (grey) over the years 1960 to 2007. Years 1976, 1990 and 2003, which have experienced extremely high summer temperature and VPD are shown by vertical red lines. Extremely low precipitation was also registered in 1976 and 1990.

On the use of $\delta^{18}O_{atm}$ for ice core dating

Extier T., Landais A., Bréant C., Prié F., Bazin L., Dreyfus G., Roche D., Leuenberger M.

QSR, 185, 244-257 (2018), doi: 10.1016/j.quascirev.2018.02.008
Issu du projet : Labex LP1

Deep ice core chronologies have been improved over the past years through the addition of new age constraints. However, dating methods are still associated with large uncertainties for ice cores from the East Antarctic plateau where layer counting is not possible. Indeed, an uncertainty up to 6 ka is associated with AICC2012 chronology of EPICA Dome C (EDC) ice core, which mostly arises from uncertainty on the delay between changes recorded in $\delta^{18}O_{atm}$ and in June 21st insolation variations at 65°N used for ice core orbital dating. Consequently, we need to enhance the knowledge of this delay to improve ice core chronologies. Here we present new high-resolution EDC $\delta^{18}O_{atm}$ record (153-374 ka) as well as new $\delta O_2/N_2$ measurements (163-332 ka) performed on well-stored ice to provide continuous records of $\delta^{18}O_{atm}$ and $\delta O_2/N_2$ between 100 and 800 ka.

The comparison of $\delta^{18}O_{atm}$ with the composite $\delta^{18}O_{calcite}$ from East Asian speleothems shows that both signals present similar orbital and millennial variabilities, which may represent shifts in the InterTropical Convergence Zone position, themselves associated with Heinrich events. We thus propose to use the $\delta^{18}O_{calcite}$ as target for $\delta^{18}O_{atm}$ orbital dating. Such a tuning method improves the ice core chronology of the last glacial inception compared to AICC2012 by reconciling the NGRIP and mid-latitude climatic records. It is especially marked during Dansgaard-Oeschger 25 where the proposed chronology is 2.2 ka older than AICC2012. This $\delta^{18}O_{atm}$ – $\delta^{18}O_{calcite}$ alignment method applied to the period between 100-640 ka further improves the EDC ice core chronology, especially over MIS 11, and leads to lower ice age uncertainties compared to AICC2012.

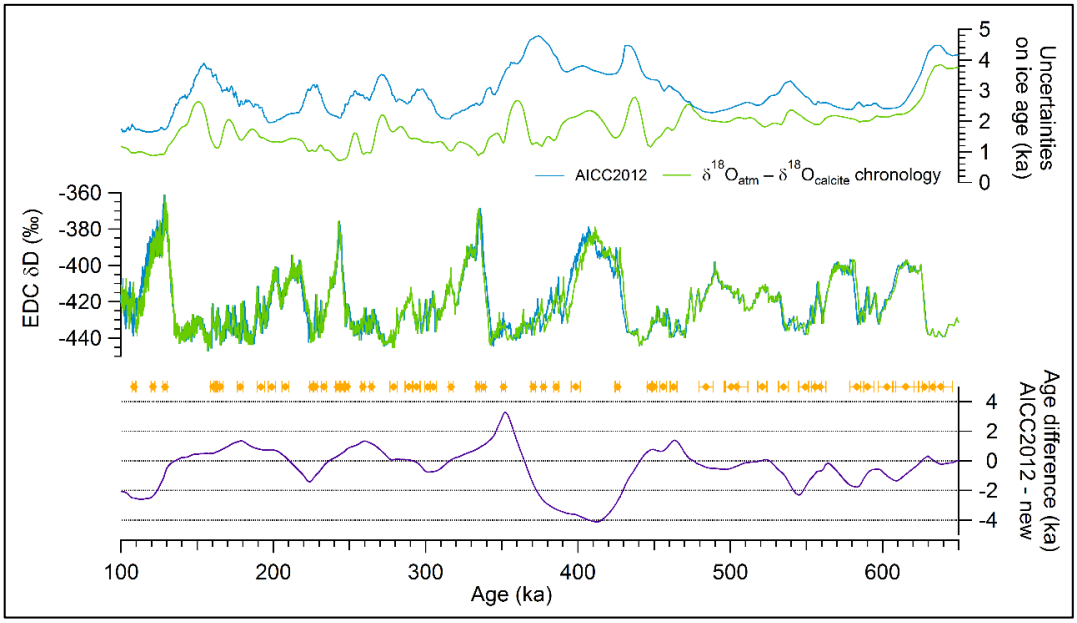

Figure: Top: Representation of the uncertainties associated with the ice age of AICC2012 (blue: Bazin et al., 2013) and δ18Oatm – δ18Ocalcite (green) chronologies. Middle: δD evolution between 100-640 ka on AICC2012 (blue: Jouzel et al., 2007) and on the new EDC chronology (green). The orange diamonds represent the markers used for the alignment between δ18Oatm and δ18Ocalcite. Bottom: The age difference between AICC2012 and the δ18Oatm – δ18Ocalcite chronology (designed as "new") is represented.

Variability of the Indonesian Throughflow in the Makassar Strait over the Last 30 ka

Fan W., … Bassinot F., X Han, Y. Bian.

Scientific Reports (2018) 8, 5678

The hydrological characteristics, including temperatures and salinities, of the upper water over the last 30 ka from two sites connected by the Indonesian Throughflow (ITF) across the Makassar Strait are reconstructed and compared. The thermocline hydrological gradient in the strait was larger during 13.4~19 ka BP and 24.2~27 ka BP than that in the Holocene. The weakened ITF during those periods in the last glacial period, corresponding to the decreased trade wind stress under an El Niño-like climate mean state, likely accounts for the increased thermocline gradient. The thermocline water temperature variabilities of the two sites, in particular the highest peaks at ~7 ka BP, are different from the records of the open western Pacific. Reoccurrence of the South China Sea Throughflow and thus a decreased surface throughflow along the Makassar Strait perhaps led to a warmer peak of thermocline temperature at ~7 ka BP than at ~11 ka BP.

Tritium records to trace stratospheric moisture inputs in Antarctica

Fourré E., Landais A., Cauquoin A., Jean-Baptiste P., Lipenkov V., Petit J.-R.

Journal of Geophysical Research Atmospheres (2018) DOI: 10.1002/2018JD028304

Better assessing the dynamic of stratosphere-troposphere exchange is a key point to improve our understanding of the climate dynamic in the East Antarctica Plateau, a region where stratospheric inputs are expected to be important. Although tritium (3H or T), a nuclide naturally produced mainly in the stratosphere and rapidly entering the water cycle as HTO, seems a first-rate tracer to study these processes, tritium data are very sparse in this region. We present the first high resolution measurements of tritium concentration over the last 50 years in three snow pits drilled at the Vostok station. Natural variability of the tritium records reveals two prominent frequencies, one at about 10 years (to be related to the solar Schwabe cycles) and the other one at a shorter periodicity : despite dating uncertainty at this short-scale, a good correlation is observed between 3H and Na+ and an anti-correlation between 3H and δ18O measured on an individual pit. The outputs from the LMDZ Atmospheric General Circulation Model including stable water isotopes and tritium show the same 3H-δ18O anti correlation and allow further investigation on the associated mechanism. At the interannual scale, the modelled 3H variability matches well with the SAM (Southern Annular Mode) index. At the seasonal scale, we show that modelled stratospheric tritium inputs in the troposphere are favored in winter cold and dry conditions.

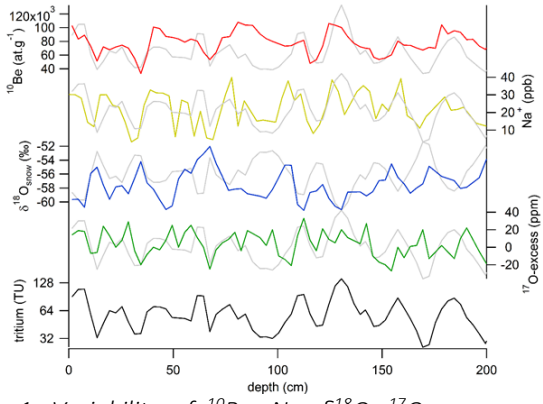

Fig 1: Variability of ^{10}Be, Na, $\delta^{18}O$, ^{17}O-excess and tritium (corrected from the influence of the bomb test peak) on the 2008 Vostok snow pit on a depth scale. For the 4 upper panels, the tritium concentration is also displayed in light grey (reverse axis for the third panel) for comparison with the other proxies.

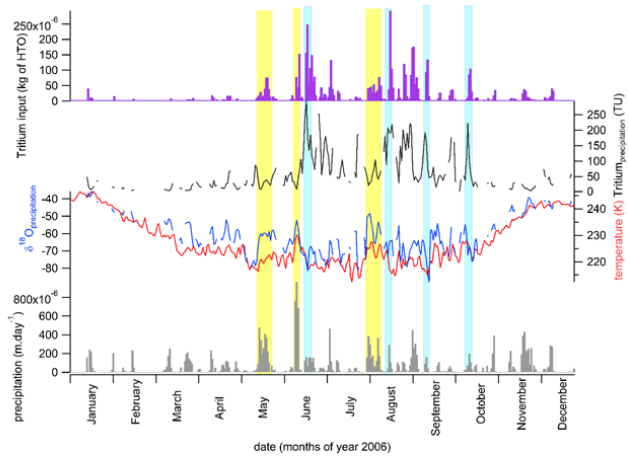

Fig 2: Modeled variations of tritium, δ18O, temperature, and precipitation amount during year 2006 from the LMDZ-iso at the Vostok station. Light blue: significant tritium input during cold periods. Yellow: larger amount of precipitation but little tritium input, in winter milder temperatures and higher δ18O episodes.

Radiocarbon measurements of small-size foraminiferal samples with the MIni CArbon DAting System (MICADAS) at the University of Bern: implications for paleoclimate reconstructions

Gottschalk J., Szidat S., Michel E., Mazaud A. et al.

Radiocarbon 60, 469-491 (2018), doi: 10.1017/RDC.2018.3

Radiocarbon (^{14}C) measurements of foraminifera often provide the only absolute age constraints in marine sediments. However, they can be challenging as their reliability and accuracy can be compromised by reduced availability of adequate sample material. New analytical advances using the MIni CArbon DAting System (MICADAS) allow ^{14}C dating of very small samples, circumventing size limitations inherent to conventional ^{14}C measure-ments with accelerator mass spectrometry (AMS). Here we use foraminiferal samples and carbonate standard material to assess the reproducibility and precision of MICADAS ^{14}C analyses, quantify contami-nation biases, and determine foraminiferal ^{14}C blank levels (Figure). The reproducibility of conventional ^{14}C ages for our planktic (benthic) foraminiferal samples from gas measurements is 200 (130) yr, and has good precision as illustrated by the agreement between both standards and their reference values as well as between small gas- and larger graphitized foraminiferal samples (within 100±70 yr). We observe a constant contamination bias and slightly higher ^{14}C blanks for foraminifera than for carbonate reference materials, limiting significant gas ^{14}C age determinations for foraminifera from our study sites (carbonate blanks) to ~38 (~45) kyr. Our findings underline the significance of MICADAS gas analyses for ^{14}C on smaller-than-conventional sized foraminiferal samples for paleoclimate reconstructions and dating.

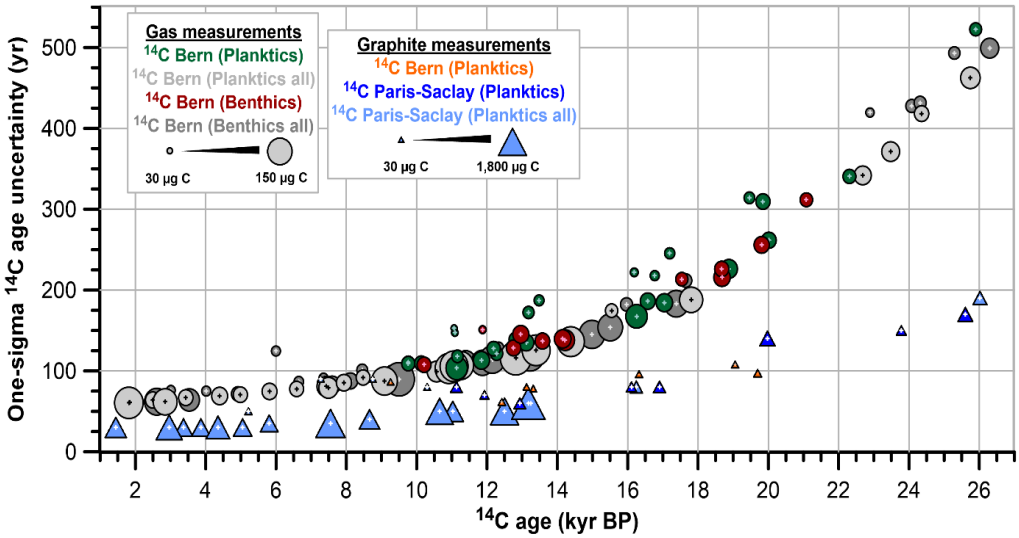

Figure: One-sigma ^{14}C age uncertainties of planktic and benthic foraminifera from sediment core MD12-3396Q measured as gas (circle) and as graphite (triangle) at the University of Bern (MICADAS AMS) and the University of Paris-Saclay (ARTEMIS Pelletron AMS). Symbol size varies with sample size. Note that ^{14}C age uncertainties are to some extent dependent on the protocols of normalization and data correction used in different laboratories.

$^{40}Ar/^{39}Ar$ age of Cryptochron C2r.2r-1 as recorded in a lava sequence within the Ko`olau Volcano (Hawaii, USA)

Guillou H., Scao V., Nomade S.

Quaternary Geochronology 43,91-101 (2018), doi: 10.1016/j.quageo.2017.10.005

The $^{40}Ar/^{39}Ar$ method was used to refine the dating of a volcanic sequence drilled in the Ko`olau volcano which recorded a period of anomalously shallow inclinations. Previously, this sequence was dated using the unspiked K-Ar method at ≈ 2.1 Ma (Laj et al., 2000). This age was questioned by Ozawa et al. (2005) based on unspiked K-Ar ages of 2.40 and 2.41 Ma for two stratigraphically younger lava flows. Our new $^{40}Ar/^{39}Ar$ isochron results date this period of low inclination between 2.52 ± 0.10 and 2.40 ± 0.17 Ma. The combination of our two most reliable ages allows us to propose an age of 2.46 ± 0.13 Ma for the magnetic anomaly that we attribute to the cryptochon C2r.2r-1. This age agrees with previous estimates on the Halawa section of 2.46 ± 0.12 Ma (Singer, 2014) and the São Gonçalo profile of 2.46 ± 0.08 Ma (Holm et al., 2008; Knudsen et al., 2009). Our $^{40}Ar/^{39}Ar$ ages confirm the unspiked K-Ar dating results of Ozawa et al. (2005), which were corrected for the mass-fractionation effect. Along with published data, our new ages allow to bracket the Makapuu late-shield stage between 2.6 and 2.2 Ma (figure).

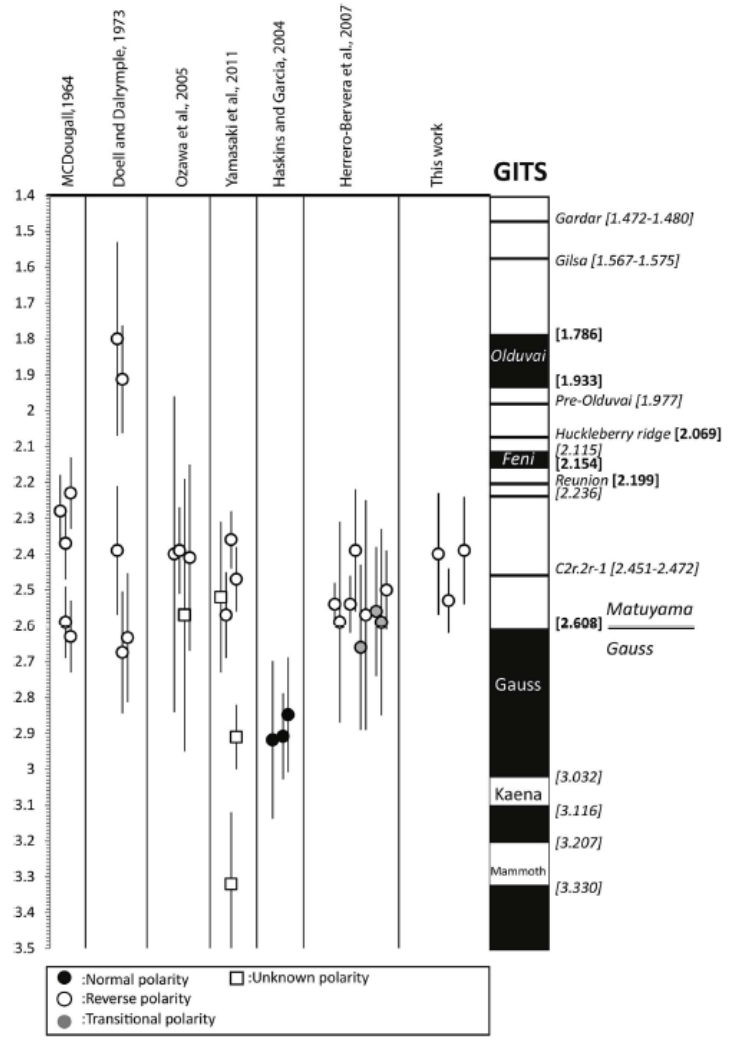

Figure: Comparison of published ages from the Ko`olau volcano and those obtained in this study with the geomagnetic instability timescale indicated (GITS; Singer, 2014).

The earliest modern humans outside Africa

Hershkovitz et al. including Valladas H.

Science 359, 456–459 (2018), doi: 10.1126/science.aap8369

To date, the earliest modern human fossils found outside of Africa are dated to around 90,000 to 120,000 years ago at the Levantine sites of Skhul and Qafzeh. A maxilla and associated dentition recently discovered at Misliya Cave, Israel), was dated at 177,000 to 194,000 years ago (Fig. 1, suggesting that members of the Homo sapiens clade left Africa earlier than previously thought. This finding changes our view on modern human dispersal and is consistent with recent genetic studies, which have posited the possibility of an earlier dispersal of Homo sapiens around 220,000 years ago. The Misliya maxilla is associated with full-fledged Levallois technology in the Levant (Fig. 2), suggesting that the emergence of this technology is linked to the appearance of Homo sapiens in the region, as has been documented in Africa.

Figure 1: Various views of the Misliya 1 hemimaxilla

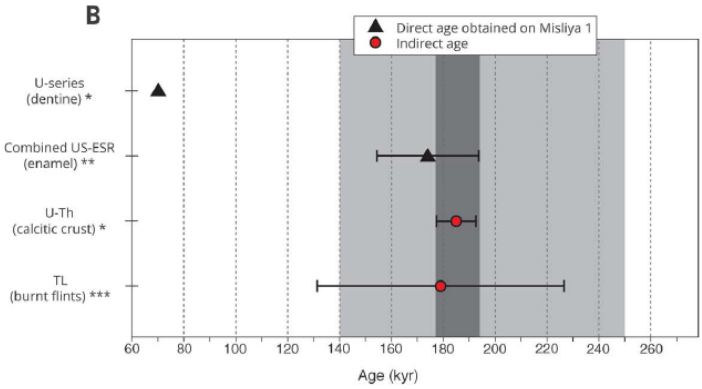

Figure 2: Lower Middle Palaeolithic artefacts

Earliest known hominin activity in the Philippines by 709 thousand years ago

Ingicco T.,…, Nomade S., Pereira A., et al.

Nature (2018) 557, 233-237

Over 60 years ago, stone tools and remains of megafauna were discovered on the Southeast Asian islands of Flores, Sulawesi and Luzon, and a Middle Pleistocene colonization by Homo erectus was initially proposed to have occurred on these islands. However, until the discovery of Homo floresiensis in 2003, claims of the presence of archaic hominins on Wallacean islands were hypothetical owing to the absence of in situ fossils and/or stone artefacts that were excavated from well-documented stratigraphic contexts, or because secure numerical dating methods of these sites werelacking. As a consequence, these claims were generally treated with scepticism.

Here we describe the results of recent excavations at Kalinga in the Cagayan Valley of northern Luzon in the Philippines that have yielded 57 stone tools (Fig.) associated with an almost- complete disarticulated skeleton of Rhinoceros philippinensis, which shows clear signs of butchery, together with other fossil fauna remains attributed to stegodon, Philippine brown deer, freshwater turtle and monitor lizard. All finds originate from a clay-rich bone bed that was dated to between 777 and 631 thousand years ago using electron-spin resonance methods that were applied to tooth enamel and fluvial quartz. This evidence pushes back the proven period of colonization of the Philippines by hundreds of thousands of years, and furthermore suggests that early overseas dispersal in Island South East Asia by premodern hominins took place several times during the Early and Middle Pleistocene stages. The Philippines therefore may have had a central role in southward movements into Wallacea, not only of Pleistocene megafauna, but also of archaic hominins.

Figure: Lithic artefacts from Kalinga. a, Cortical flake on chert (II-2014-J1-362; length (L) = 100 mm, breadth (B) = 55 mm, thickness(T) = 33 mm). b, Possible hammerstone on dacite (II-2014-J1-371), although its highly eroded aspect precludes any definitive conclusion. Arrows indicate crushed areas interpreted as the result of precussions. c, Siret kombewa flake on jasper (II-2014-J1-391; L = 40 mm, B = 18 mm, T = 8 mm) that has a longitudinal and oblique fracture on the inferior two-thirds of the left side resulting from a knapping accident while flaking. d, Double-backed flake on flint (II-2014-J1-519). e, Core on quartz (II-2014-J1-396), with clear marks of knapping on an anvil, and itsdiachritic diagram. Arrows indicate the percusion axes.

Tritium and radiocarbon levels in the Rhône river delta and along the French Mediterranean coastline

Jean-Baptiste P., Fontugne M., Fourré E., et al.

Journal of Environmental Radioactivity 187, 53-64 (2018), doi: 10.1016/j.jenvrad.2018.01.031

The Rhône is characterized by a heavy concentration of nuclear-based industries including nuclear power stations and nuclear sites housing civilian and military facilities. Here, we report the results of a four-year survey (2010-2013) of tritium and radiocarbon levels in a variety of matrices within the Rhône delta and along the French Mediterranean coastline (Fig.1). The aim of the study is to create a spatial reference framework of environmental levels of these two radionuclides, which are the most prevalent in liquid radioactive effluents from nuclear power stations. Although both tritium and radiocarbon levels in the analyzed samples are very low and can only be detected using ultra-sensitive analytical techniques, they clearly show the influence of the tritium and radiocarbon discharges carried by the Rhône plume along the Mediterranean coast (Fig. 2). The tritium content of suspended matter and sediments of the Rhône is a special case, which shows elevated tritium values not seen in other French rivers with similar nuclear facilities. The north-south spatial distribution of this tritium anomaly shows that these trace values are at their highest in the upper Rhône, close to the Swiss border and upstream of Creys Malville, the northernmost nuclear power station on the Rhône. This points to a legacy of past tritium releases by the watchmaking industry. A dedicated study would be needed to clearly identify the source and the exact nature of this contamination.

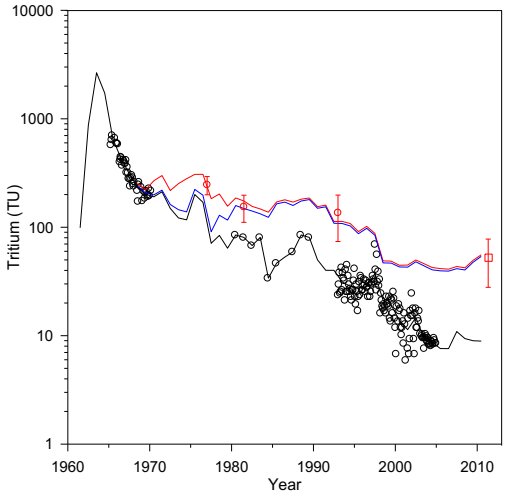

Figure 2: Reconstruction of the Rhône's water ^{3}H content downstream of the nuclear facilities using upstream Rhône background data (black line) with direct liquid ^{3}H discharge data (blue line) and additional indirect inputs due to gaseous discharges (red curve).

Figure 1 : Tritium (TU) in white font and ^{14}C (pmC) in red font in Mediterranean surface water in March 2011

New determination of the ^{3}He mixing ratio in the Earth's lower atmosphere from an international tritium intercomparison exercise

Jean-Baptiste P., Fourré E., Cassette P.

Applied Geochemistry (2018) doi.org/10.1016/j.apgeochem.2018.09.003

The light isotope of helium, ^{3}He, is essentially a primordial substance entrapped within the Earth's interior during the formation of the planet. It is released into the atmosphere by volcanic/magmatic activity, and eventually escapes to outer space. ^{3}He is also produced by the radioactive beta-decay of tritium. Hence measurements of ^{3}He can be used to derive the concentration of tritium. The so-called "^{3}He ingrowth" uses a mass spectrometer to detect the amount of ^{3}He that accumulates in a sample during a given period of storage. The ^{3}He measurements are classically calibrated against an air standard. The method thus relies on the accurate knowledge of the atmospheric mixing ratio of ^{3}He. This value is based on mass spectrometric measurements with gravimetrically or volumetrically prepared ^{3}He standard mixtures. Here, we apply the ^{3}He ingrowth method in reverse, using a solution of tritiated water prepared for an international comparison of tritium activity measurements to precisely determine the ^{3}He mixing ratio of our air standard. The measured atmospheric mixing ratio of ^{3}He, based on a series of ten measurements, is [^{3}He]=7.12 ± 0.06 ppt (Fig.). This value is between 1% and 2% lower than previous determinations reported in the literature. However, all results remain statistically consistent. The adoption of this value removes the systematic 2% positive offset noted by Clarke et al. (1976) between their results based on the 3He ingrowth method and the Miami Tritium Laboratory beta –particle counting system.

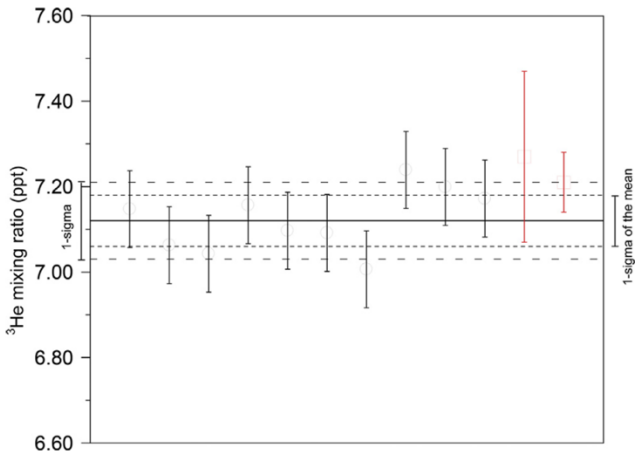

Figure: Results of the ten mass spectrometric measurements of the atmospheric ^{3}He mixing ratio carried out in this study (black). The red bars correspond to atmospheric mixing ratios reported in the literature by direct measurements and by combining the determination of the atmospheric 4He mixing ratio with the ^{3}He/^{4}He ratio of air

Helium and neon in the accreted ice of Lake Vostok

Jean-Baptiste P., Fourré E. et al.

Geophysical Res. Lett. (2018) doi.org/10.1029/2018GL078068

We analyzed helium and neon in 24 samples from between 3,607 and 3,767 m (i.e., down to 2 m above the lake-ice interface) of the accreted ice frozen to the ceiling of Lake Vostok. Within uncertainties, the neon budget of the lake is balanced, the neon supplied to the lake by the melting of glacier ice being compensated by the neon exported by lake ice. The helium concentration in the lake is about 12 times more than in the glacier ice, with a measured $^{3}He/^{4}He$ ratio of 0.12 ± 0.01 Ra (Fig. 1, 2). This shows that Lake Vostok's waters are enriched by a terrigenic helium source.

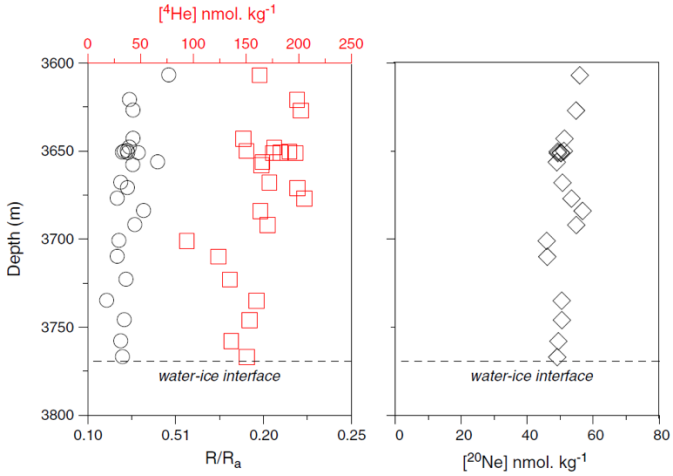

Figure 1: ^{4}He, ^{20}Ne and $^{3}He/^{4}He$ vertical profiles

The $^{3}He/^{4}He$ isotope ratio of this helium source was determined. Its radiogenic value (0.057 × Ra) is typical of an old continental province, ruling out any magmatic activity associated with the tectonic structure of the lake. It corresponds to a low geothermal heat flow estimated at 51 mW/m^{2}.

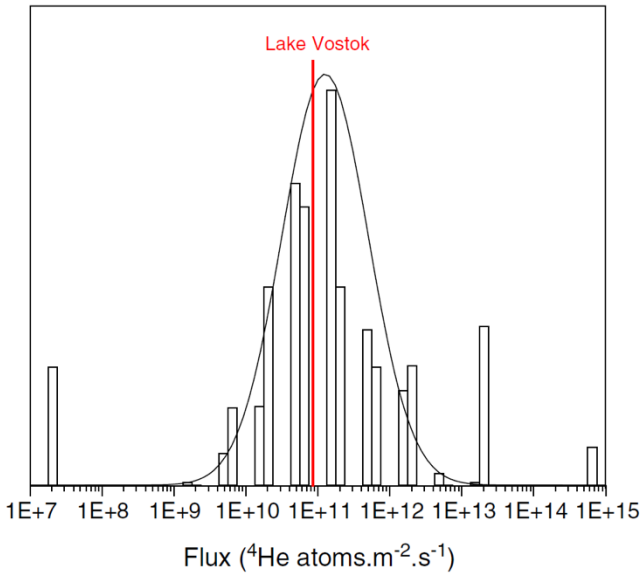

Figure 2: Histogram of continental degassing helium fluxes (Torgersen, 2010), with the plot of the corresponding lognormal distribution. He flux for Lake Vostok corresponds to the residence time of 13,300 years determined by Bell et al. (2002)

Glacier extent in sub-Antarctic Kerguelen archipelago from MIS 3 period: Evidence from ^{36}Cl dating

Jomelli V., … Landais A., et al.

Quaternary Science Reviews, 183, 110–123 (2018), doi: 10.1016/j.quascirev.2018.01.008

Documenting sub-Antarctic glacier variations during the last glacial maximum is of major interest to better understand their sensitivity to atmospheric and oceanic temperature changes in conjunction with Antarctic ice sheet changes. However, data are sparse because evidence of earlier glacier extents is in most sub-Antarctic islands located offshore. Here, we present 22 cosmogenic ^{36}Cl surface exposure ages obtained from 5 sites at Kerguelen to document the glacial history (Figure). The ^{36}Cl ages from 'roche moutonnée' surfaces, erratics and boulders collected on moraines span from 41.9 ± 4.4 ka to 14.3 ± 1.1 ka. Ice began to retreat on the eastern part of the main island before 41.4 ± 4.4 ka. Slow deglaciation occurred from ~41 to ~29 ka. There is no evidence of advances between 29 ka and the Antarctic Cold Reversal (ACR) period (~14.5–12.9 ka). During the ACR, however, the Bontemps and possibly Belvedere moraines were formed by the advance of a Cook Ice Cap outlet glacier and a local glacier on the presqu'île Jeanne d'Arc, respectively. This glacier evolution differs from that of glaciers in New Zealand and in Patagonia. These asynchronous glacier changes in the sub-Antarctic region are in agreement with sea surface temperature changes around Antarctica, which suggest differences in the climate evolution of the Indo-Pacific and Atlantic sectors of Antarctica.

Figure: Location of ^{36}Cl ages on Belvedere moraine site. The 1σ uncertainties in the individual ^{36}Cl boulder ages account for analytical and production rate uncertainties, while the uncertainty in the mean includes standard deviation, analytical and production rate uncertainties. The sample in italic was rejected as an outlier based on the Chi2 test.

Bayesian selection of mixed covariates from a latent layer: application to hierarchical modeling of soil carbon dynamics

Jreich R., Hatté C., Balesdent J., Parent É.

Journal de la Société Française de Statistique, 2018, 159 (2), 128-155
Thèse phare CEA et projet ANR DEDYCAS

Soil carbon is important not only to ensure food security via soil fertility, but also to potentially mitigate global warming via increasing soil carbon sequestration. There is an urgent need to understand the response of the soil carbon pool to climate change and agricultural practices. Biophysical models have been developed to study Soil Organic Matter (SOM) for some decades. However, there still remains considerable uncertainty about the mechanisms that affect SOM dynamics from the microbial level to global scales. In this paper, we propose a statistical Bayesian selection approach to study which forcing conditions influence soil carbon dynamics by looking at the depth distribution of radiocarbon content for 159 profiles under different conditions of climate (temperature, precipitation, etc.) and environment (soil type, land-use). Stochastic Search Variable Selection (SSVS) is here applied to latent variables in a hierarchical Bayesian model. The model describes variations of radiocarbon content as a function of depth and potential covariates such as climatic and environmental factors. SSVS provides a probabilistic judgment about the joint contribution of soil type, climate and land use on soil carbon dynamics. We also discuss the practical performance and limitations of SSVS in presence of categorical covariates and collinearity between covariates in the latent layers of the model.

A new paradigm for $\delta^{18}O$ in coral skeleton oxygen isotope fractionation response to biological kinetic effects

Juillet-Leclerc A., Rollion-Bard C., Reynaud S., Ferrier-Pagès C.

Chemical Geology (2018) 483, 131-140.
Issu du projet : ASTICO

La compréhension de la réelle signification de $\delta^{18}O$ de l'aragonite des coraux ne peut être atteinte qu'à l'échelle micrométrique grâce aux analyses au SIMS (Ion Mass Spectrometry), effectuées en collaboration avec Claire Rollion-Bard (IPGP). Ces mesures s'effectuent sur des échantillons de coraux de cultures obtenues au CSM (Centre Scientifique de Monaco) dans des conditions contrôlées, en particulier de température et de lumière. Ce dernier facteur est le plus souvent négligé et ne peut être observé que sur des cultures car, sur le terrain, il ne peut être séparé de la température.
Les dernières recherches publiées (Juillet-Leclerc et al., 2018) ont mis en évidence des fractionnements isotopiques à l'échelle micrométrique sur des coraux *Acropora* cultivés dans des conditions croisées de 3 températures, 23, 25 et 28°C et de deux lumières, 200 and 400 µmol photon m^{-2} s^{-1} (LL et HL). Ces analyses effectuées seulement sur des fibres (une des deux microstructures mises en évidence dans l'aragonite des coraux) ont révélé que les fractionnements isotopiques de $\delta^{18}O$ résultent de mécanismes cinétiques causés par la présence de protéines différentes suivant le cycle nuit-jour (Figure 1). La mise en évidence des fractionnements opérant la nuit et le jour sous deux intensités lumineuses révèlent des mécanismes complexes (Figure 2).

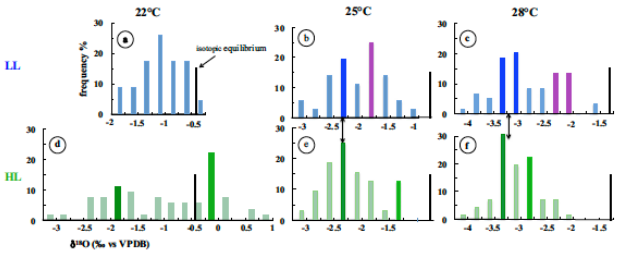

Figure 1: Histograms of $\delta^{18}O$ obtained on colonies grown in each condition with a bin width of 0.25‰. The frequency is represented as a percentage relative to the entire dataset. The vertical black bar corresponds to the calculated oxygen isotope equilibrium value corrected from seawater $\delta^{18}O$. Values corresponding to cultures conducted under LL are blue and green under HL. The isotopic bars corresponding to the isotope values most depleted in ^{18}O are violet under LL and sparkling green under HL and are associated with daytime fibers. The isotopic bars corresponding to the isotope values less depleted in ^{18}O are dark blue under LL and dark green under HL and are associated to nighttime fibers. Black arrows highlight similar lower $\delta^{18}O$ bars for LL and HL, underlining that the high bars corresponding to the isotope values most depleted in ^{18}O are only temperature dependent

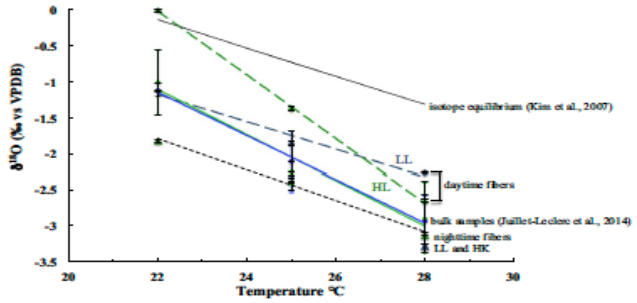

*Figure 2: The dashed black $\delta^{18}O$ vs temperature calibration corresponds to nighttime aragonite (blue triangles correspond to nighttime deposit after LL daytime and green triangles to nighttime deposit after HL daytime), $\delta^{18}O$=−0.19*SST+2.96. Daytime fibers are represented by the dashed dark blue and dark green lines, blue diamonds correspond to LL $\delta^{18}O$=−0.19*SST+4.15, N=3, R2=0.99, p < 0.05 and green ones to HL, $\delta^{18}O$=−0.21*SST+2.94. The black line of equilibrium corresponds to the theoretical $\delta^{18}O$ value at equilibrium including seawater $\delta^{18}O$, $\delta^{18}O$=−0.19*SST+5.75. The isotopic values of micrometric samples are compared to calibrations of bulk aragonite, the blue line corresponding to LL, $\delta^{18}O$=−0.30*SST+5.41 and the green one under HL condition, $\delta^{18}O$=−0.31*SST+5.75.*

The role of light as vital effect on coral skeleton oxygen isotopic ratio

Juillet-Leclerc A.

Biogeoscience Discussion In Press (2018), doi:10.5194/bg-2018-433

Light, an environmental parameter playing a crucial role in coral aragonite growth and $\delta^{18}O$ formulation, is always neglected in the geochemical literature. However, by revisiting already published studies, we demonstrate that light might be considered as a vital effect affecting coral aragonite $\delta^{18}O$. We stress that annual $\delta^{18}O$–annual temperature calibrations of all considered coral genera may be compared because their assessment assumes homogenous light levels. Temperature prevails on $\delta^{18}O$ because it influences $\delta^{18}O$ in two ways: 1) it acts as is thermodynamically predicted implying a $\delta^{18}O$ decrease; 2) it enhances photosynthesis causing $\delta^{18}O$ increase. When the highest annual temperature occurs simultaneously with the highest annual irradiation, the annual $\delta^{18}O$ amplitude is shortened. The annual $\delta^{18}O$–annual temperature calibration is also explained by the relative distribution of microstructures, centers of calcification or COC and fibers, according to morphology, and in turn taxonomy. We also investigate monthly $\delta^{18}O$–monthly temperature calibrations of Porites grown at the same sites. Multiple evidence show that temperature is the prevailing environment forcing on $\delta^{18}O$ and that the mixture of temperature and light also determines the relative distribution of microstructures, explaining the relationships between Porites calibration constants. By examining monthly and annual $\delta^{18}O$–monthly and annual temperature calibrations, we reveal that monthly calibration results from the superimposition of seasonal and annual variability over time. Seasonal $\delta^{18}O$ strongly impacted by seasonal light fluctuations, may be obtained by removing interannual $\delta^{18}O$ only weakly affected by light. Such features necessitate the reconstitution of tools frequently utilised, such as the coupled $\delta^{18}O$ – Sr/Ca or pseudo-coral concepts.

.

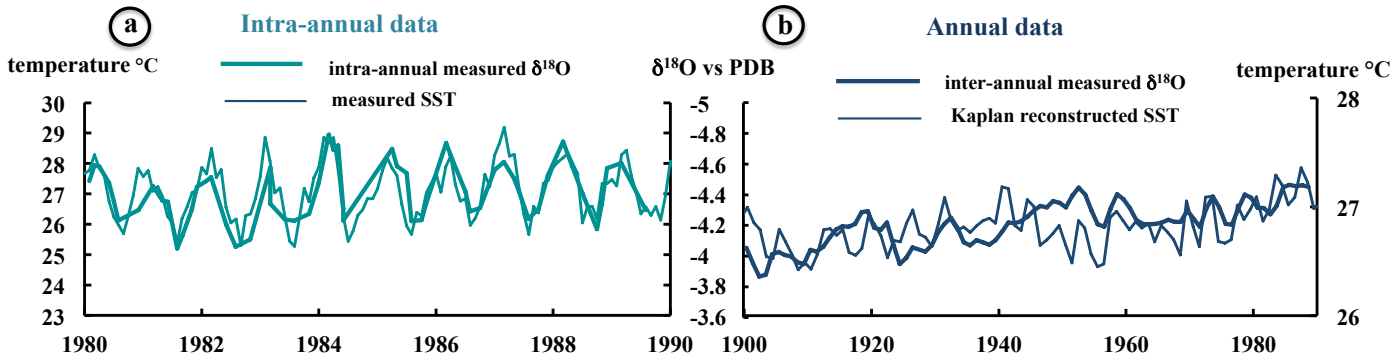

Figure: comparison of $\delta^{18}O$ measured on coral core collected at Moorea (French Polynesia) (Boiseau et al., 1998) and measured and estimated temperatures: a, between 1980 and 1990, seasonal measured data compared to instrumental seawater temperature (Boiseau et al., 1998). b, over the last century, annual averaged measured data, originated from the same data series than seasonal data, compared to estimated temperature in the (1°, 1°) grid containing Moorea (Kaplan et al., 1998). The two curves are displayed to obtain the best matching. Isotopic scale of the two isotopic profiles is common to the two profiles, while temperature scales cover 7°C and 2°C respectively. There is a mismatch between annual and monthly calibrations given on a unique isotopic scale, illustrating the non-linearity between monthly and annual $\delta^{18}O$ profiles over time.

Magnetic Fingerprints of Modern Sediments in the South China Sea Resulting From Source-to-Sink Processes

Kissel C., Sarnthein M., Laj C., Wang P.X., Wandres C., Egli R.

Geochemistry, Geophysics, Geosystems, 19, 1979-1993 (2018), doi: 10.1029/2018GC007571

Financé par LIA French-Chinese MONOCL (Monsoon, Ocean and Climate), LEFE-Monocl (2015-2017)

The South China Sea (SCS), the largest marginal sea in eastern Asia, between the Pacific and Indian oceans, forms a perfect natural laboratory to study source-to-sink processes of detrital particles. Previous studies (Kissel et al., 2016, 2017) have shown that the magnetic composition of the riverine sediments is significantly variable from north to south. On the basis of this evidence, we have examined a full set of magnetic properties for a number of core tops taken at water depth of mostly between 800 and 3,500 m.

Different proportions of magnetite/hematite are observed with a progressive southward increase in hematite content (Figure). This reflects the changes already observed in the rivers from Luzon-Taiwan-Pearl River in the north to Mekong-Borneo in the south. This gradient allows us to define the terrestrial origin of the sediments. However, the contrast between north and south is weakened at sea, indicating that the present distribution of magnetic minerals in the SCS results both from the trapping of the river-borne sediments on the shelf and from an active transport along the slope and in the deep basin. In the northern basin, the transport results from surface currents in the northern part of the SCS, involving the Luzon coastal current, from the Kuroshio current, and from the deep-water flow invading also this area. Mixing might occur in the northwestern part via cyclonic eddies mixing surface and deep waters.

In the southern basin, the clear signature of central and north Borneo rivers and of the Mekong is mixed with northern-source-like material. It is most likely related to an active southward transport of northern-sourced terrigenous sediments on the shelf during winter, when the surface current is strong, as well as by the deep-water masses.

For the first time, we characterize a wide spectrum of magnetic properties of modern marine sediment in the SCS. Our results give important insights into the modern pathways of sediment particles, depicting the source-to-sink processes that affect the terrigenous sediment load.

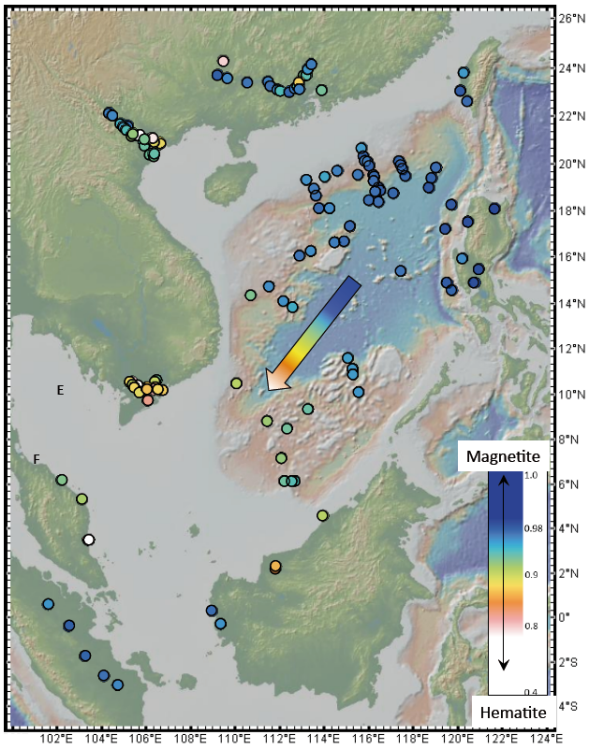

Figure: Magnetic coercivity spectrum of both river samples and core-tops in the South China Sea. End-members are magnetites (blue) and hematite (toward yellow and red).

Holocene Hydroclimate Variability in Central Scandinavia Inferred from Flood Layers in Contourite Drift Deposits in Lake Storsjön

Labuhn I., Hammarlund D., Chapron E., Czymzik M., Dumoulin J.-P., Nilsson A., Régnier E., Robygd J., von Grafenstein U.

Quaternary, 2018, 1(1), 2
Financé par Franco-Suédois ISOSCAN

Despite the societal importance of extreme hydroclimate events, few palaeoenvironmental studies of Scandinavian lake sediments have investigated flood occurrences. Here we present a flood history based on lithological, geochemical and mineral magnetic records of a Holocene sediment sequence collected from contourite drift deposits in Lake Storsjön (63.12° N, 14.37° E). After the last deglaciation, the lake began to form around 9800 cal yr BP, but glacial activity persisted in the catchment for ~250 years. Element concentrations and mineral magnetic properties of the sediments indicate relatively stable sedimentation conditions during the Holocene. However, human impact in the form of expanding agriculture is evident from about 1100 cal yr BP, and intensified in the 20th century. Black layers containing iron sulphide appear irregularly throughout the sequence (Fig). Elevated frequencies of black layer occurrence between 3600 and 1800 cal yr BP reflect vegetation changes in the catchment as well as large-scale climatic change. Soil erosion during snowmelt flood events increased with a tree line descent since the onset of the neoglacial period (~4000 cal yr BP). The peak in black layer occurrence coincides with a solar minimum ~2600 cal yr BP, which may have accentuated the observed pattern due to the prevalence of a negative NAO index, a longer snow accumulation period and consequently stronger snowmelt flood.

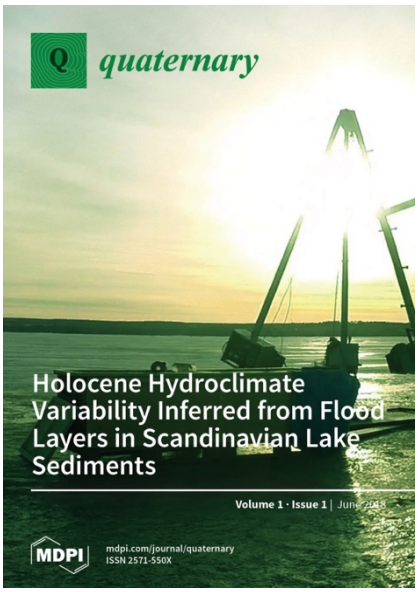

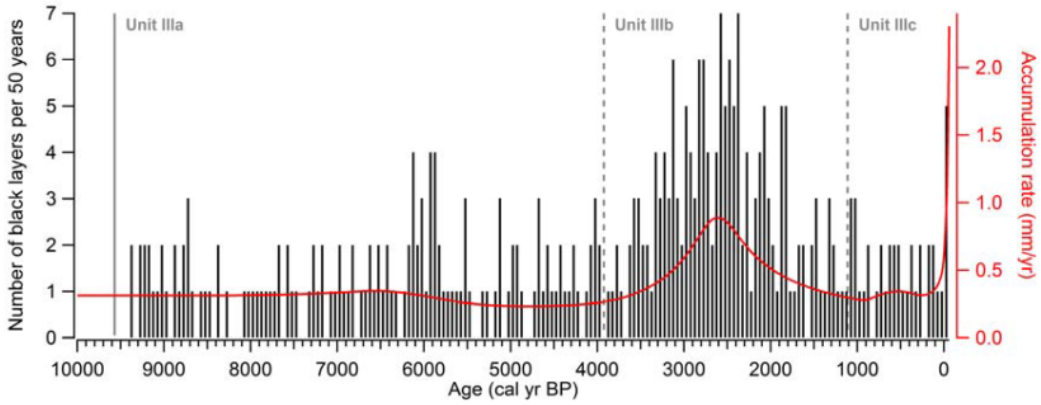

Figure: Numbers of black layers per 50-year interval in the sediment sequence (black bars) and accumulation rate (red curve).

On the similarity and apparent cycles of isotopic variations in East Antarctic snow pits

Laepple T., Münch T., Casado M., Hoerhold M., Landais A., Kipfstuhl S.

The Cryosphere, 12, 169–187 (2018), doi: 10.5194/tc-12-169-2018
Financé par COMBINISO

Stable isotope ratios $\delta^{18}O$ and δD in polar ice provide a wealth of information about past climate evolution.
Snow-pit studies allow us to relate observed weather and climate conditions to the measured isotope variations in the snow. They therefore offer the possibility to test our understanding of how isotope signals are formed and stored in firn and ice. As $\delta^{18}O$ and δD in the snowfall are strongly correlated to air temperature, isotopes in the near-surface snow are thought to record the seasonal cycle at a given site. Accordingly, the number of seasonal cycles observed over a given depth should depend on the accumulation rate of snow. However, snow-pit studies from different accumulation conditions in East Antarctica reported similar isotopic variability and comparable apparent cycles in the $\delta^{18}O$ and δD profiles with typical wavelengths of ~20 cm. These observations are unexpected as the accumulation rates strongly differ between the sites, ranging from 20 to 80 mm water equivalent. yr^{-1}.
Here, we systematically analyse the properties and origins of $\delta^{18}O$ and δD variations in high-resolution firn profiles from eight East Antarctic sites. First, we confirm the suggested cycle length of ~20 cm by counting the isotopic maxima. Spectral analysis further shows a strong similarity between the sites but indicates no dominant periodic features. Furthermore, the apparent cycle length increases with depth for most East Antarctic sites, which is inconsistent with burial and compression of a regular seasonal cycle. We show that these results can be explained by isotopic diffusion acting on a noise-dominated isotope signal. The firn diffusion length is rather stable across the Antarctic Plateau and thus leads to similar power spectral densities of the isotopic variations. This in turn implies a similar distance between isotopic maxima in the firn profiles. Our results explain a large set of observations discussed in the literature, providing a simple explanation for the interpretation of apparent cycles in shallow isotope records, without invoking complex mechanisms. Finally, the results underline previous suggestions that isotope signals in single ice cores from low-accumulation regions have a small signal-to-noise ratio (Fig) and thus likely do not allow the reconstruction of interannual to decadal climate variations.

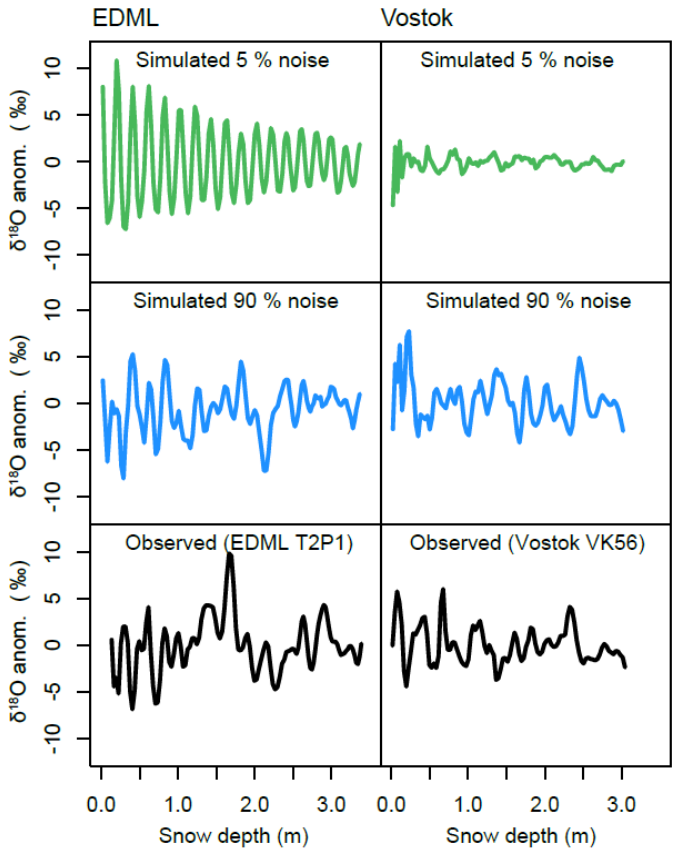

Figure: Visual comparison of measured and simulated profiles for EDML (left) and Vostok (right panel)

Ice core evidence for decoupling between mid-latitude atmospheric water cycle and Greenland temperature during the last deglaciation

Landais A., Capron E., Masson-Delmotte V., …, Minster B., Prié F.

Clim. Past, 15, 3223–3241 (2018), doi: 10.5194/cp-2018-65
Financé par COMBINISO

The last deglaciation represents the most recent example of natural global warming associated with large-scale climate changes. In addition to the long-term global temperature increase, the last deglaciation onset is punctuated by a sequence of abrupt changes in the Northern Hemisphere. Such interplay between orbital- and millennial-scale variability is widely documented in paleoclimatic records but the underlying mechanisms are not fully understood. Limitations arise from the difficulty in constraining the sequence of events between external forcing, high- and low- latitude climate and environmental changes.

Greenland ice cores provide sub-decadal-scale records across the last deglaciation and contain fingerprints of climate variations occurring in different regions of the Northern Hemisphere. Here, we combine new ice d-excess and ^{17}O-excess records, tracing changes in the mid-latitudes, with ice $\delta^{18}O$ records of polar climate. Within Heinrich Stadial 1, we demonstrate a decoupling between climatic conditions in Greenland and those of the lower latitudes. While Greenland temperature remains mostly stable from 17.5 to 14.7 ka, significant change in the mid latitudes of northern Atlantic takes place at ~16.2 ka, associated with warmer and wetter conditions of Greenland moisture sources. We show that this climate modification is coincident with abrupt changes in atmospheric CO_2 and CH_4 concentrations recorded in an Antarctic ice core. Our coherent ice core chronological framework and comparison with other paleoclimate records suggest a mechanism involving two-step freshwater fluxes in the North Atlantic associated with a southward shift of the intertropical convergence zone.

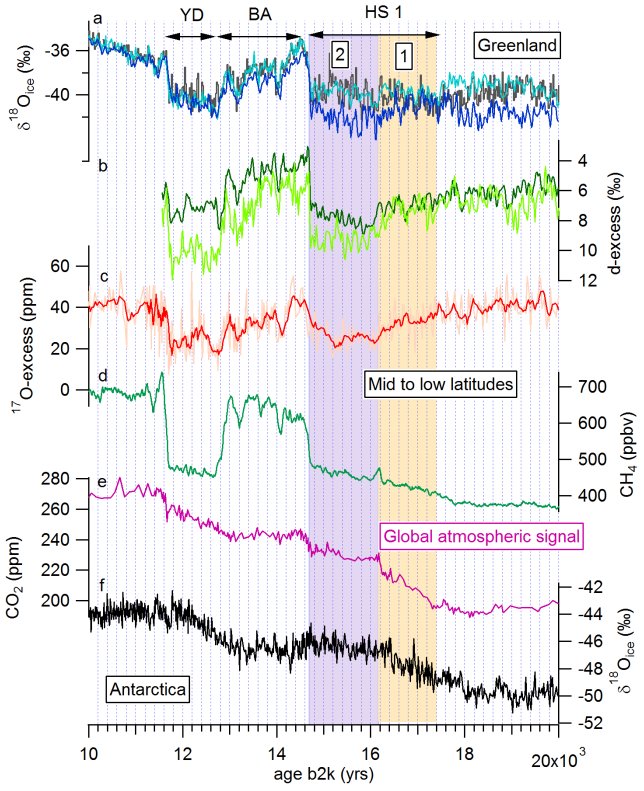

Figure: A synthesis of ice core records over the last deglaciation displayed on the respective GICC05 and AICC2012 timescales with an identification of two phases (1, orange box and 2, purple box) within Heinrich Stadial 1 (HS1).

Past summer temperatures inferred from dendrochronological records of *Fitzroya cupressoides* on the eastern slope of the northern Patagonian Andes

Lavergne A., Daux V., Pierre M., Stievenard M., Srur A. M., Villalba R.

J. Geophys. Res. Biogeosci. 123(1), 32-45 (2018), doi : **10.1002/2017JG003989**
Financé par Lefe-PATISO

Estimating summer temperature fluctuations over long timescales in southern South America is essential for better understanding the past climate variations in the Southern Hemisphere. Here we develop robust 212 years long basal area increment (BAI) and $\delta^{13}C$ chronologies from living temperature-sensitive *Fitzroya cupressoides* on the eastern slope of the northern Patagonian Andes (41°S). After removing the increasing trend from the growth records likely due to the CO_2 fertilization effect, we test the potential to reconstruct past summer temperature variations using BAI and $\delta^{13}C$ as predictors. The reconstruction based on $\delta^{13}C$ records has the strongest predictive skills and explains as much as 62% of the total variance in instrumental summer temperature (n = 81, p < 0.001). The temperature signal recorded in tree-ring growth is not substantially different to that present in $\delta^{13}C$ and consequently does not provide additional information to improve the regression models. Our $\delta^{13}C$-based reconstruction shows cold summer temperatures in the second part of the 19th century and in the mid-20th century followed by a warmer period (Fig). Notably, the 20th and the early 21st centuries were warmer (+0.6°C) than the 19th century. Reconstructed summer temperature variations are modulated by low-latitude (El Niño–Southern Oscillation) and high-latitude (Southern Annular Mode) climate forcing. Our reconstruction based on $\delta^{13}C$ agrees well with previous ring width based temperature reconstructions in the region and comparatively enhances the low-frequency variations in the records. The present study provides the first reconstruction of summer temperature in South America south of 40°S for the period 1800–2011 entirely based on isotopic records.

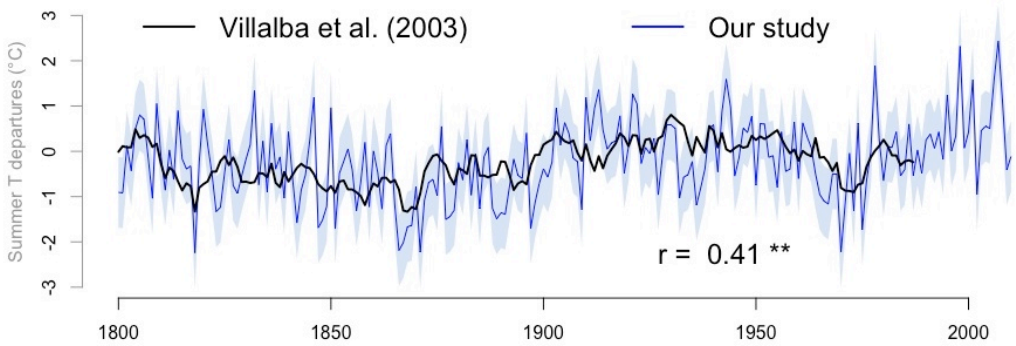

*Figure: Comparison between different summer temperature reconstructions in the region. The Villalba et al. (2003) reconstruction is based on the first principal component of tree-ring width records from Nothofagus pumilio (r^2 = 0.55). * indicates that the correlation is significant at 95%.*

A review of the geologic sections and the faunal assemblages of Aurelian Mammal Age of Latium (Italy) in the light of a new chronostratigraphic framework

Marra F., Nomade S., Pereira A., et al.

Quaternary Science Reviews 181, pages 173-199 (2018), doi: 10.1016/j.quascirev.2017.12.007

The Aurelian Mammal Age for peninsular Italy was introduced on the basis of faunal assemblages mainly recovered at sites along the Via Aurelia west of Rome. These sites exposed a set of sedimentary deposits currently attributed to the Aurelia and to the Vitinia Formations correlated with MIS 9 and MIS 7, respectively. In the present paper we reconstruct the geologic-stratigraphic setting in the western sector of Rome within the wider context of glacio-eustatically controlled, geochronologically constrained aggradational successions defined for this region (Fig.). We present a chronostratigraphic study based on dedicated field surveys that, combined with five new $^{40}Ar/^{39}Ar$ ages and eighteen trace-element and EMP glass analyses of volcanic products, allow us to revise age and correlation with the Marine Isotopic Stages for 10 sites out of 12 previously attributed to the Aurelia Formation and the Torre in Pietra Faunal Unit. In particular, we demonstrate a MIS 13/MIS 11 age for several sections along the Via Aurelia between Malagrotta and Castel di Guido. Based on this new geochronological framework, the first occurrences of Canis lupus and Vulpes vulpes in Italy are antedated to MIS 11, within the Fontana Ranuccio Faunal Unit of the Galerian Mammal Age, consistent with the wider European context. This contribution is intended as the groundwork for a revision of the Middle Pleistocene Mammal Ages of the Italian peninsula, according to the improved chronostratigraphy of the geological sections hosting the faunal assemblages.

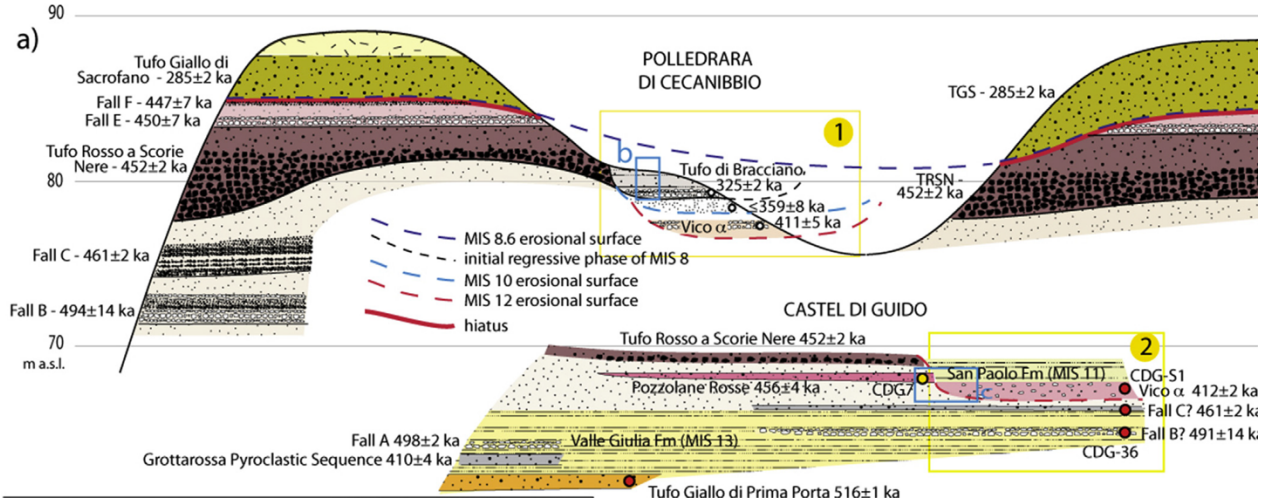

Figure: Stratigraphy of La Polledrara di Cecanibbio and Castel di Guido reconstructed through the integration of dedicated field surveys in the surrounding areas with literature and archive data from the archaeological sites (yellow boxes: 1 from Pereira et al., 2017a; 2: original data by G. Boschian

Downcore variations of sedimentary detrital ($^{238}U/^{232}Th$) ratio: implications on the use of $^{230}Th_{xs}$ and $^{231}Pa_{xs}$ to reconstruct sediment flux and ocean circulation

Missiaen L., Pichat S., Waelbroeck C., Douville É., Bordier L., Dapoigny A., Thil F., Foliot L., Wacker L.

Geochemistry, Geophysics, Geosystems, Vol. 19, 2560-2573, 2018

Excess ^{231}Pa and ^{230}Th ($^{231}Pa_{xs}$ and $^{230}Th_{xs}$) can be used to reconstruct past oceanic sedimentation (^{230}Th-normalized flux) and circulation changes (($^{231}Pa/^{230}Th)_{xs,0}$, hereafter Pa/Th). These quantities are determined by computing the detrital and authigenic contributions from bulk sediment measurement. The method relies on the use of a chosen constant value of the detrital ($^{238}U/^{232}Th$) activity ratio (hereafter $(U/Th)_{det}$). In this study, we have extracted the detrital fraction of the sediments from North Atlantic deep-sea core SU90-08 (43°03'1N, 30°02'5W, 3,080 m) and determined its $(U/Th)_{det}$ value over the last 40 ky. We find that $(U/Th)_{det}$ varied significantly through time with a minimum value of 0.4 during the Holocene and a maximum value of 0.7 during the Last Glacial Maximum (LGM). The sensitivity of sedimentary ^{230}Th-normalized flux and Pa/Th is tested for our study site and for other North Atlantic sites. We show that the sensitivity is highly dependent on the core location and its terrigenous material supply. The ^{230}Th-normalized flux and Pa/Th signals are very robust in cores with low detrital contributions, whereas they are very sensitive to $(U/Th)_{det}$ changes in cores with higher detrital contribution. In the latter case, changes in ^{230}Th-normalized flux and Pa/Th due to the choice of a constant $(U/Th)_{det}$ can largely exceed the uncertainty on the ^{230}Th-normalized flux and Pa/Th, inducing potential biases in the amplitude and temporal variability of reconstructed sedimentation and ocean circulation changes.

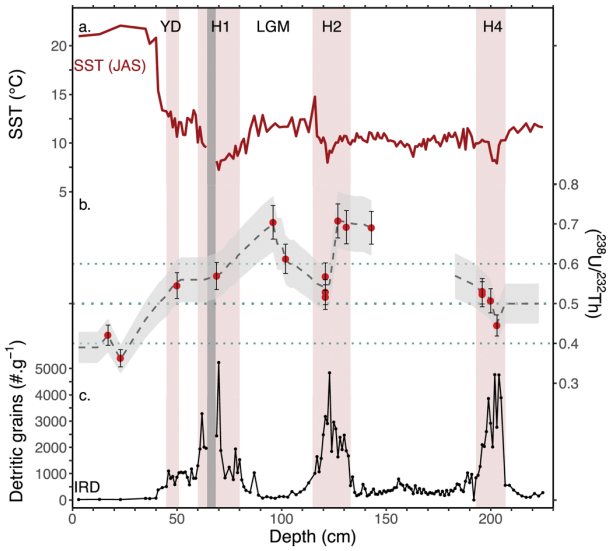

Fig. 1. *SU90-08 downcore variations. (a) Summer sea surface temperature reconstructed from planktonic foraminifer assemblages. (b) ($^{238}U/^{232}Th$) of the leaching residues (red dots) and associated standard deviation (2σ), interpolated $(U/Th)_{det}$ time series (dashed line) and associated 2σ (grey envelope). The dotted blue lines correspond to the most commonly used $(U/Th)_{det}$ and associated uncertainty. (c) IRD content as number of >150 μm detritic grains per gram of dry sediment. The Younger Dryas and Heinrich layers are highlighted by red bands based on IRD abundance. The vertical grey band corresponds to a sediment hiatus.*

Neolithic water management and flooding in the lesser Caucasus (Geogia)

Ollivier V ., Fontugne M., Hamon C., Decaix A., Hatté C., Jalabadze M.

Quaternary Science Reviews (2018), 197, 267-287
Financé par ANR KURA

River management is generally thought to have started at 5500 cal. BC within the development of eastern Neolithic societies. In the Lesser Caucasus, evidence of early river management has been discovered around the famous Neolithic sites of Shulaveri, Gadachrili Gora, and Imiris Gora in Georgia. Here we report a preliminary data set indicating that river management was set up at 5900 cal. BC leading to the flooding, destruction, and local abandonment of the hydraulic infrastructures of the Gadachrili village between 5750 and 5430 cal. BC. The hydraulic infrastructures were developed during a more humid period encompassing the 8200 cal. BP (6200 cal. BC) climatic event, probably to optimize agricultural yield. It potentially led to the first prehistoric engineering accident for which there is evidence, which may have been followed by the reorganization of the occupation and/or to architectural modifications.

Reservoir ages in the western tropical north Atlantic from one coral off Martinique Island

Paterne M., Feuillet N., Cabioch G., Cortijo E., Blamart D., Weill-Accardo J., Bonneau L., Colin C., Douville E., Pons-Branchu E.

Radiocarbon, 60, 639-652 (2018), doi : 10.1017/RDC.2017.118
Financé par INSU/LEFE-ARRA

Sea surface reservoir ages (R) are reported from ^{14}C measurements of the annual growth bands of coral *Siderastrea siderea* collected on the Atlantic coast off Martinique *Is*., in the Lesser Antilles volcanic arc (Fig. 1). Mean values of R are similar between 1835 and 1845 during pre-anthropogenic times at 385 ± 30 years and between 1895 and 1905 at 382 ± 20 years when there was a huge eruption from the Montagne Pelée volcano in 1902-1903. They are very similar to values of R in the Caribbean Sea, Mexico Gulf and Florida Strait. Limited ^{14}C aging of sea surface (~40 years) may be due to enhanced volcanic activity, although within the statistical variability.

Variability of R is slightly greater during 1835-1845 than during 1895- 1905 (Fig. 2). It is linked to a moderate increase of $\Delta^{14}C$ of 5‰, strengthened by a clear increase of $\delta^{18}O$ of 0.4‰. This is attributed to a decrease of the northward SEC advection of the old South Atlantic Waters into the western tropical North Atlantic and Caribbean Sea and relative enhanced westward flux of the tropical North Atlantic surface waters, the southern waters having lower values of ^{14}C and $\delta^{18}O$ than the North Atlantic ones. From 1835 to1845, the fraction of the South Atlantic Waters transported up to Martinique *Is*. was reduced from 25% to 15%..

EAW: East Atlantic current; CC: Caribbean current; GS: Gulf Stream. The 1000m isobath is represented.

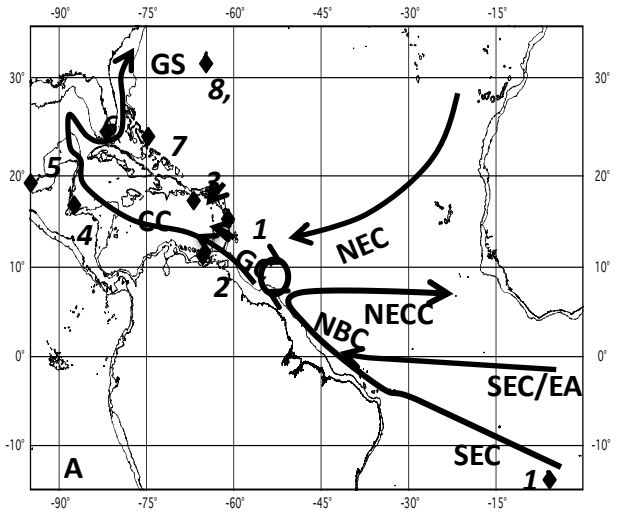

Figure 1: Location of the samples used in this study and schematic patterns of the oceanic currents. 1: Martinique 2: Cariaco basin; 3: Puerto-Rico; 4: Belize; 5: Gulf of Mexico; 6: Florida; 7: Bahamas; 8: Bermuda North shore; 9: Bermuda South shore; 10: Santa Helena. NEC: North Equatorial current; NECC: North equatorial undercurrent; NBC: North Brazil current; GC: Guiana Current; SEC: South Equatorial current;

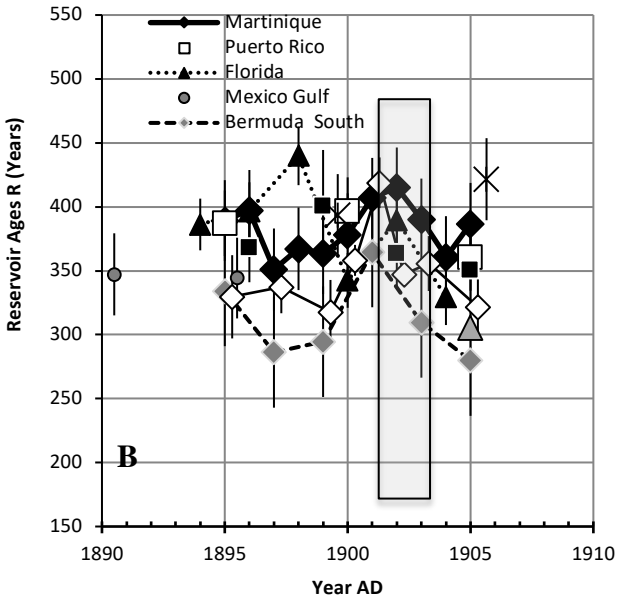

Figure 2: Values of the sea surface reservoir ages R (years) off Martinique and at the sites located on Figure 1 as a function of calendar years (AD). Grey box figures out the 2yr long eruption of Montagne Pelée.

Updated calibration of the clumped isotope thermometer in planktonic and benthic foraminifera

Peral M., Daëron M., Blamart D., Bassinot F., Dewilde F., Smialkowski N., Isguder G., …, Kissel C., Michel E., Vázquez Riveiros N., Waelbroeck C.

Geochimica et Cosmochimica Acta 239, 1-16 (2018), doi: 10.1016/j.gca.2018.07.016

Accurate reconstruction of past ocean temperatures is of critical importance to paleoclimatology. Carbonate clumped isotope thermometry ("Δ47") is a relatively recent technique based on the strong relationship between calcification temperature and the statistical excess of ^{13}C–^{18}O bonds in carbonates. Its application to foraminifera holds great scientific potential, particularly because Δ47 paleotemperature reconstructions do not require assumptions regarding the ^{18}O composition of seawater. However, there are still relatively few published observations investigating the potential influence of parameters such as salinity or foraminiferal size and species. We present a new calibration data set based on 234 replicate analyses of 9 planktonic and 2 benthic species of foraminifera collected from recent core-top sediments, with calcification temperatures ranging from −2 to 25 °C. We observe a strong relationship between Δ47 values and independent, oxygen-18 estimates of calcification temperatures (Fig.):

$$\Delta47 = 41.63 \times 103/T2 + 0.2056$$

The formal precision of this regression (± 0.7–1.0 °C at 95 % confidence level) is much smaller than typical analytical errors. Our observation confirms the absence of significant species-specific biases or salinity effects. We also investigate potential foraminifer size effects between 200 and >560 µm in 6 species, and conclude that all size fractions from a given core-top location and species display statistically undistinguishable Δ47 values. These findings provide a robust foundation for future inter-laboratories comparisons and paleoceanographic applications.

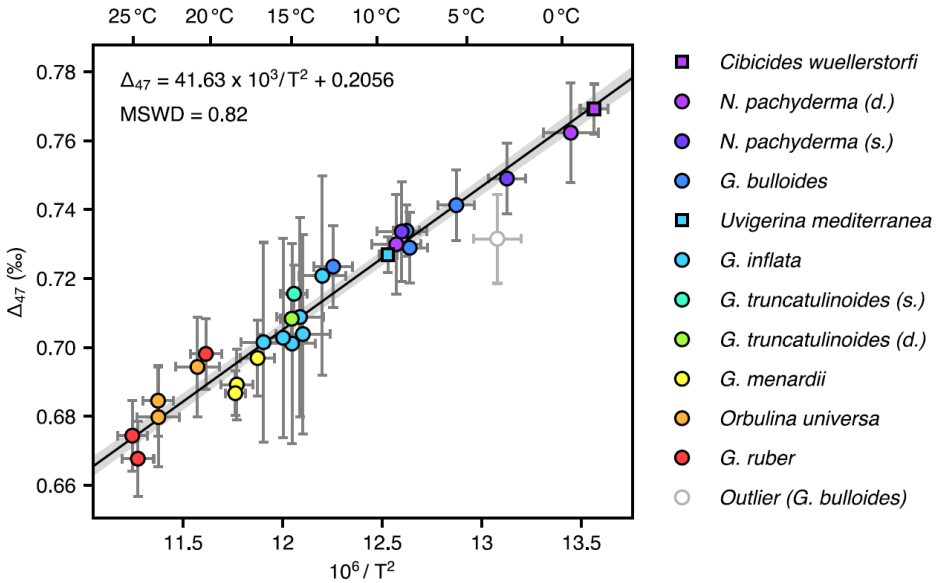

Figure: Δ47 values (mean and 2SE) compared to isotopic temperatures (mean and 2SE) obtained with Kim and O'Neil, 1997 for planktonic (circle) and benthic (square) foraminifera samples, combining all size fraction. The calibration regression (black line) is calculated following York et al. (2004) with 95% confidence level (grey band).

Integrated geochronology of Acheulian sites from the southern Latium (central Italy): Insights on human environment interaction and the technological innovations during the MIS 11-MIS 10 period

Pereira A., Nomade S., … Scao V. et al.

Quaternary Science Reviews 187, pages 112-129, (2018), doi: 10.1016/j.quascirev.2018.03.021

We have explored the multimethod approach combining 40Ar/39Ar on single crystal, ESR on bleached quartz, and ESR/U-series on teeth to improve the age of four neighbours "Acheulian" sites of the Frosinone Province (Latium, Italy): Fontana Ranuccio, Cava Pompi (Pofi), Isoletta, and Lademagne. Ages obtained by the three methods are in mutual agreement and confirm the potential of dating with confidence Middle Pleistocene sites of Italy using these methods. At Fontana Ranuccio, the 40Ar/39Ar age (408 ± 10 ka, full external error at 2s, Fig. 1) obtained for the archaeological level (unit FR4) and geochemical analyses of glass shards performed on the Unit FR2a layer allow us to attribute the studied volcanic material to the Pozzolane Nere volcanic series, a well known caldera-forming event originated from the Colli Albani volcanic district. These new data ascribe the Fontana Ranuccio site, as well as the eponym faunal unit, to the climatic optimum of Marine Isotope Stage (MIS) 11. Ages obtained for the Cava Pompi, Isoletta, and Lademagne sites cover a relativelyshort period of time between 408 ka and 375 ka, spanning MIS 11 climatic optimum to the MIS 11/10 transition. Analysis of small collections of lithic industries, bifacial tools, and small cores technologies from Isoletta, Lademagne, and the neighbour site of Ceprano-Campogrande shows common technical strategies for the period comprised between MIS 11 and MIS 9 (410-325 ka), such as the elaboration of flaked elephant bone industries found over the whole Latium region. However, some features found only in the Frosinone province area, like large-sized bifaces, suggest particular regional behaviours.

.

The presence of one Levallois core in the oldest layer of Lademagne (i.e. > 405 ± 9 ka) suggests a punctual practice of this technology, also proposed as early as MIS 10/11 in the neighbour site of Guado San Nicola (Molise) in central Italy.

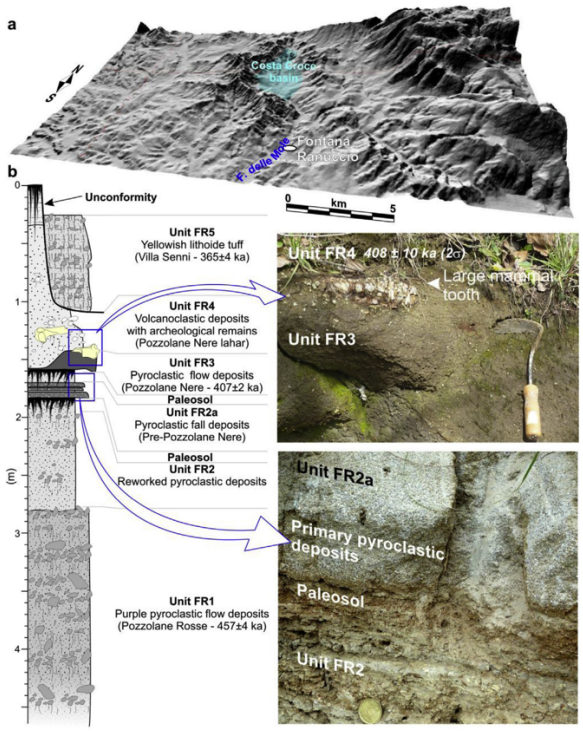

Fig. 1 : Geomorphological and stratigraphic setting of Fontana Ranuccio site a) 3D digital terrain model of the area surrounding the archaeological site. b) Simplified stratigraphic succession and pictures of the main sedimentary units outcropping at site. Note that the thickness of the Unit FR5, carved into the older ones, is not to scale and it can be on the order of ca. 4 m

Towards speciation of organically bound tritium and deuterium: quantification of non-exchangeable forms in carbohydrate molecules

Péron O., Fourré E. et al.

Chemosphere 196, 120-128 (2018) doi:10.1016/j.chemosphere.2017.12.136

An original methodology to quantitatively explore exchangeability of hydrogen isotopes in carbohydrate molecules is proposed. To access the speciation of organically bound hydrogen isotopes, isotopic exchanges were carried out under a soft path regime in the vapor phase at 20°C with set (D, T/H) vapor pressure ratios (Fig. 1). When steady states were reached, the fraction of exchangeable hydrogen of microcrystalline cellulose, alpha-cellulose and wheat grains were obtained and ranged from 13 to 31% (versus a theoretical value of 30%). In cellulose, and more specifically in microcrystalline cellulose, the molecular hydrogen bonds as well as the different conformations of the network seemed to decrease the hydroxyl groups of glucose units available for isotopic exchange. On the contrary, the assumed enzymatic hydrolysis of the constitutive molecules of wheat starch into low-molecular weight carbohydrate molecules enhanced the exchangeable pool. An average value of the activity between non-exchangeable organically bound tritium (NE-OBT) and non-exchangeable organically bound hydrogen was calculated for wheat grains = 0.55 ± 0.03 Bq.g^{-1} of hydrogen atoms (Fig. 2).

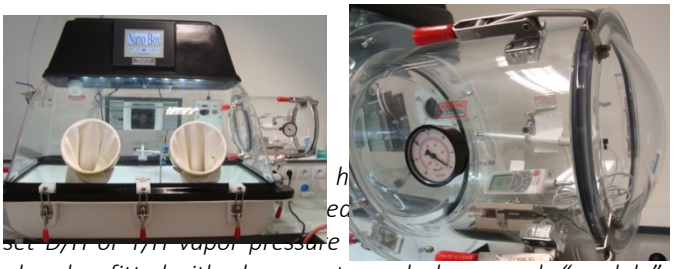

h
ec
set D/H or T/H vapor pressure
glove box fitted with a hygrometer and a homemade "module".

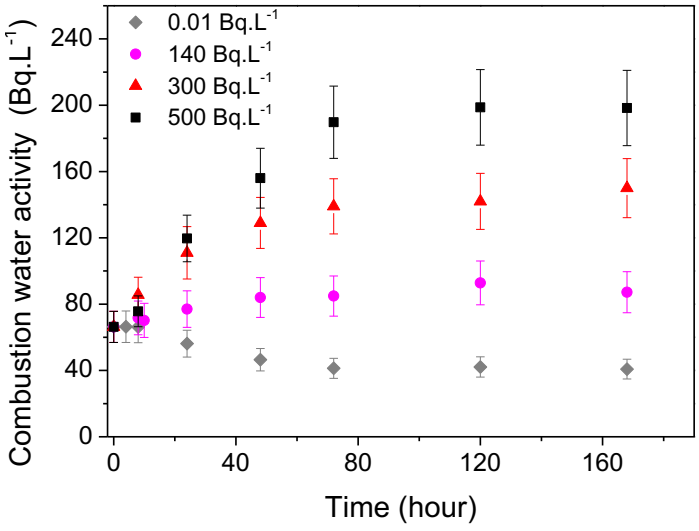

Figure 2: Tritium activities of combustion waters (OBT levels of wheat grains) versus contact time with saline solutions at 0.01, 140, 300 and 500 Bq.L-1.

Groundwater flowpaths and residence times inferred by ^{14}C, ^{36}Cl and ^{4}He isotopes in the Continental Intercalaire aquifer (North Western Africa)

Petersen J. O., Deschamps P., Hamelin B., Fourré E. et al.

Journal of Hydrology 560, 11-23 (2018), doi: 10.1016/j.jhydrol.2018.03.003

In a semi-arid to arid climate context, dependency on groundwater resources may lead to overexploitation and deterioration of water quality. The Continental Intercalaire (CI) aquifer is one such continental-scale aquifer (more than a million of km^2), which is mainly confined, poorly recharged but intensely abstracted. To date, the management of this resource relies on hydrogeological modeling and key parameters such as recharge/discharge rate and groundwater dynamics. We use a combination of residence time indicators (^{14}C, ^{36}Cl, ^{4}He) and stable isotopes of water (^{2}H and ^{18}O) to give greater constraint on the groundwater residence time in the CI. In previous studies, ^{14}C measurements and steady state modeling indicate a residence time of less than 100 ka whereas in others, ^{36}Cl measurements and transient scenarios modeling suggest a longer residence time (>500 ka).

In the Tunisian recharge area, detectable ^{14}C indicate sporadic recharge episodes (3–7 ka and 29–43 ka), whereas ^{4}He and ^{36}Cl concentrations in central areas suggest very old (<2 Ma) groundwaters.

We characterize five distinct flowpaths reaching the Tunisian discharge area using their isotopic signatures. According to our mixing model, the average contribution from the main recharge area, the Algerian Atlas Mountains, is around 88%.

This value is close to hydrogeological models. Conversely, the contribution from the Dahar Mountains is lower than in the hydrogeological modeling (2% against 10%) whereas the Tinhert shows a greater contribution (10% against 1%).

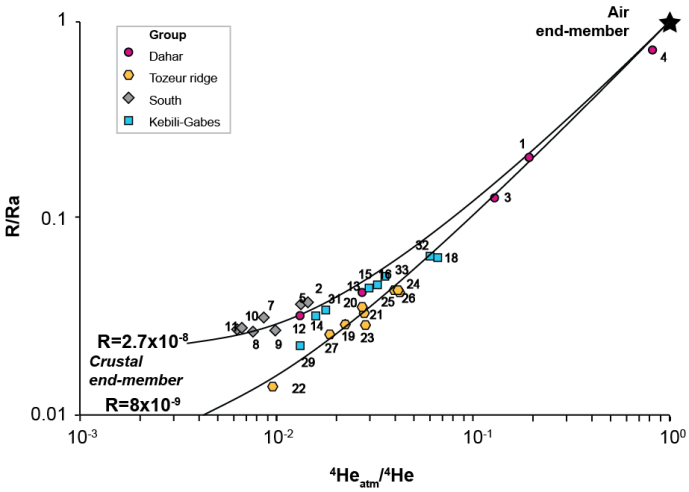

Figure: $^{4}He_{atm}$ is the sum of the solubility component at estimated recharge temperature (15°C) and the excess air deduced from ^{20}Ne and unfractionated excess air model. The two solid curves represent binary mixing between the atmospheric end-member and a crustal end-member. Ra = atmospheric $^{3}He/^{4}He$ ratio ($1.38x10^{-6}$).

First evidence of a mid-Holocene earthquake-triggered megaturbidite south of the Chile Triple Junction

Piret L., Bertrand S., Kissel C., De Pol-Holz, R., Tamayo Hernando, A., Van Daele, M.

Sedimentary Geology, in press (2018), doi:10.1016/j.sedgeo.2018.01.002
Financé par LEFE-PACHIDERME

Megaturbidites have been the focus of many paleoseismic and paleo-environmental studies because they can provide evidence for catastrophic and/or hazardous events with potentially major paleo-environmental implications. During a recent research cruise in Baker fjord, Chile (47°54' S – 74°30' W), a megaturbidite was described between the Northern and Southern Patagonian Icefields (Fig). Based on the turbidite's location, a possible origin was the early Holocene drainage of megalake General Carrera producing a Glacial Lake Outburst Flood (GLOF) that drained through Baker fjord. However, seismic activity must also be considered as a potential trigger mechanism, due to the fjords proximity to the Liquiñe-Ofqui Fault Zone (LOFZ) and the Chile Triple Junction.

Here, we aim to determine the depositional processes of the megaturbidite and identify the turbidite's origin, undertaking a multi-proxy analysis of sediment core MD07-3121 (PACHIDERME cruise on board the R. V. *Marion Dufresne*), including sedimentology (grain size, magnetic properties, loss-on-ignition, foraminifera counts), bulk organic geochemistry, and radiocarbon dating, and we analysed bathymetric maps and sub-bottom profiles. Our grain-size results display a diagnostic fining-up trend and show evidence of seiching in the 7.33 m thick megaturbidite. The age of the event (5513–5211 cal yr BP) contradicts the hypothesis of an early Holocene GLOF origin. Bulk organic geochemical results indicate that the sediments that compose the turbidite are clearly of marine origin, which further goes against a GLOF origin. In addition, the megaturbidite is underlain by a 11.36 m thick mass transport deposit (MTD), also composed of marine sediments. According to the sub-bottom profiles, the MTD and the megaturbidite originate from the reworking of thick packages of sediment previously deposited on nearby sills and on the fjord's flanks. Furthermore, similar coeval deposits are found in two adjacent sub basins. We therefore interpret these deposits to be triggered by an earthquake during the late mid-Holocene. This study reveals the first earthquake-triggered megaturbidite south of the Chile Triple Junction.

Figure: Bathymetry of Baker fjord in the vicinity of the coring site. The multibeam echosounder data from the MR08-06 cruise on board R/V Mirai are in bright colors and the SHOA based bathymetry in lighter colors. Two sub-bottom profiles were obtained in the study area during the PACHIDERME cruise (Kissel et al., 2007).

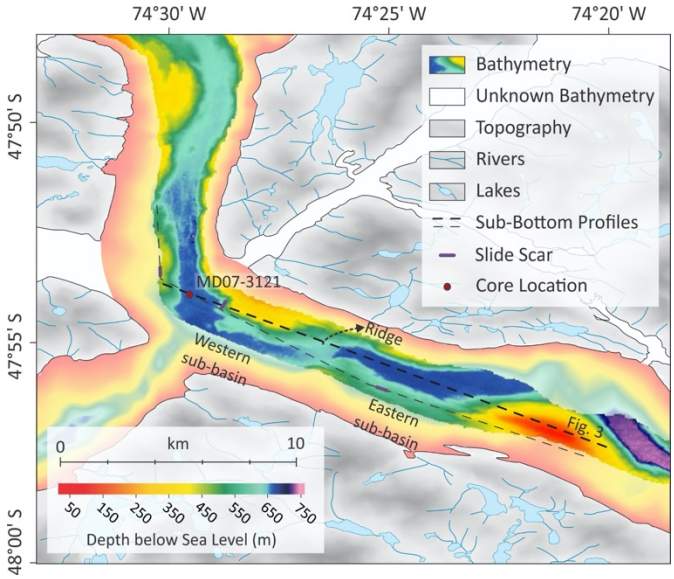

^{14}C in urban secondary carbonate deposits: a new tool for environmental studies

Pons-Branchu E., Bergonzini L., Tisnérat-Laborde N., …, Roy-Barman M.

Radiocarbon, 2018; 60(4), 1269 – 1281, DOI:10.1017/RDC.2018.25
Project: Aqueducs et Fontaines (Fondation des sciences du patrimoine)

Secondary carbonate deposits (similar to speleothems) in urban undergrounds, have been recently highlighted as powerful archives for reconstruction of the historical anthropogenic imprint on the environment. The precise chronology of these secondary carbonate deposits is a key issue for the accurate time reconstruction of environmental conditions. We present three ^{14}C data sets for urban speleothem-like deposits that developed in contrasted man made environments.

The first one was sampled in an underground technical gallery of the Palace of Versailles (France), and the other two in a manhole (Saint-Martin spring) of a historical underground aqueduct in Paris (France; Fig.). The comparison of these records with the bomb peak and relative chronology (laminae counting) allowed us to identify: i) fast carbon transfer from the atmosphere to the urban underground; ii) a high proportion of dead carbon and a high damping effect in relation to possible old carbon stored within urban soils and/or the influence of local fossil carbon burning. This study also shows that the lamination of these deposits is bi-annual in these highly urbanized sites.

Figure: Saint Martin spring and the CaCO3 crust sampled, SM B core and picture of thin section within the laminated level.

$\delta^{13}C$ signal of earthworm calcite granules: A new proxy for palaeoprecipitation reconstructions during the Last Glacial in western Europe

Prud'homme C., Lécuyer C., Antoine P., Hatté C. et al.

Quaternary Science Reviews 179, 158-166 (2018), doi: 10.1016/j.quascirev.2017.11.017
Financé par ANR ACTES

Quantification of paleoprecipitation during the Last Glacial is a key element to reconstruct palaeoclimates. Recently, fossil calcite granules have been identified in loess sequences with high contents in specific horizons. In this study, we explored for the first time the potential of this new bio-indicator as a climatic proxy for precipitation in western Europe during the Last Glacial. We extracted 30 granules from eleven samples belonging to three tundra gleys and two brown soils from the Nussloch loess sequence previously dated between 50 and 20 ka. Stable carbon isotope measurements were performed on each granule and duplicated. Throughout the studied section, $\delta^{13}C$ values range from -15.4 to -10.3‰ for tundra gleys and from -14.9 to -9.5‰ for brown soils. By taking into account the fractionation factor between the carbon ingested by the earthworm and the carbon output of the granules, the $\delta^{13}C$ values of these granules reflect the composition of the C3 plant vegetation cover. Thus, we estimated the $\delta^{13}C$ of the plants with a mean value of -24.3 ± 0.9‰ for tundra gleys and -24.1 ± 0.9‰ for brown soils, which are in agreement with values obtained from organic matter preserved in sediments. Palaeoprecipitation range over both tundra gley horizons and brown soils were estimated at about 333 [159-574] mm/yr by using an empirical relationship determined between present-day plant leaf isotopic discrimination and the mean annual precipitation. This original preliminary study highlights the potential of earthworm calcite granule $\delta^{13}C$ measurements as a new proxy for paleoprecipitation during the Last Glacial interstadials in continental environments.

Climate and tectonic-driven sedimentary infill of a lagoon as revealed by high resolution seismic and core data (the Nador lagoon, NE Morocco)

Raji O., Dezileau L, …, von Grafenstein U., A.Poujol

Marine Geology 398, 99-111 (2018), https://doi.org/10.1016/j.margeo.2018.01.010
Financé par CNRS et CEA Mistrals (Paleomex)

Lagoonal systems are vulnerable environments in the present day context of global climate change. The study of their sedimentary infill is critical to understand marine and continental factors controlling their evolution, and in so doing, evaluate their future behaviour and potential management. In that context, Mediterranean lagoons are particularly important due to their social and economic values. The Nador lagoon, located along the Western Mediterranean coast, is the largest Moroccan lagoon. In order to study its sedimentary infill, very high-resolution seismic reflection data were acquired, providing for the first time an image of the architecture of the infilling Holocene deposits. The combination between sediment core information and seismic data allows the reconstruction of the lagoon history over the last millennium. We demonstrate that the time between the 15th and 19th century has been a key period in the lagoon evolution. Sand bodies of marine origin dominated the sedimentary infill of the lagoon during that time (Fig). We propose that this stage of the Nador lagoon, the evolution and infilling is closely linked both to the local tectonic and Little Ice Age climatic contexts. These results are important to understand the mode of evolution of other comparable lagoons along microtidal coasts.

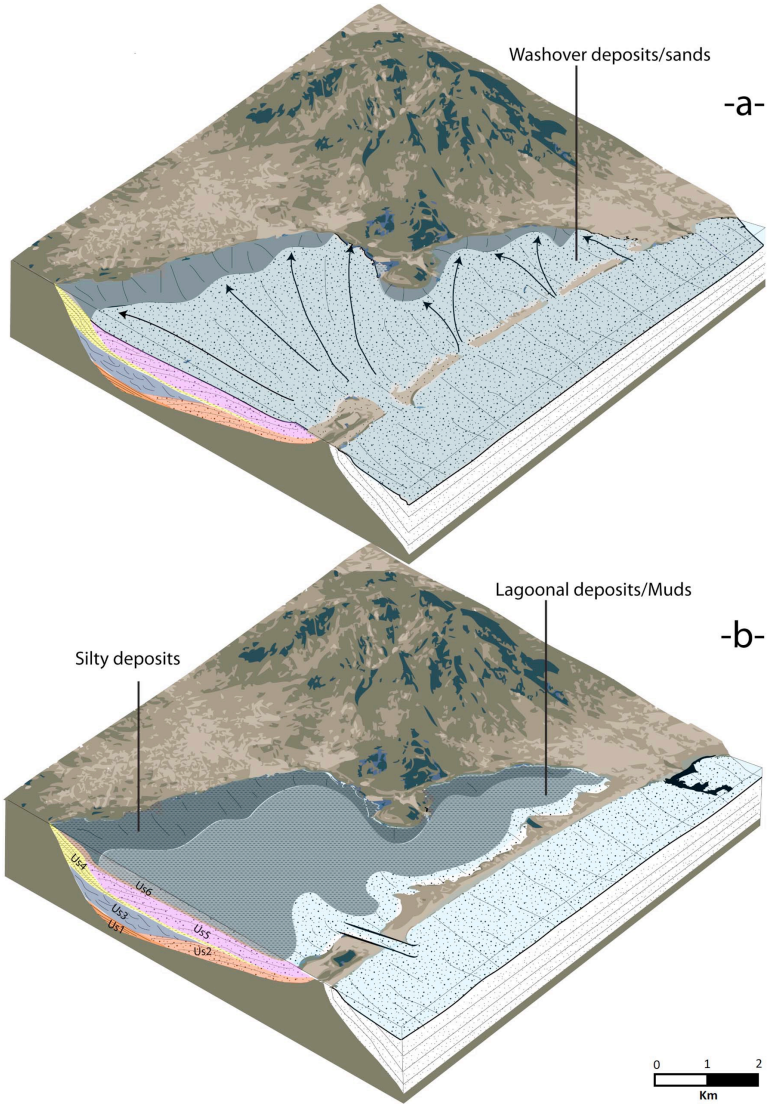

Figure: Diagram showing the abnormal expansion of marine sands (a) compared to the current situation of the NW part of the Nador Lagoon (b). A narrow barrier, breached under the action of storm waves into several short barriers separated by inlets can explain the large distance of marine sediment transportation (a).

6600 years of earthquake record in the Julian Alps (Lake Bohinj, Slovenia)

Rapuc W., Sabatier P…, Régnier E., Daut G., Von Grafenstein U.

Sedimentology 65, 1777–1799 (2018), doi: 10.1111/sed.12446
Financé par CNRS et CEA via Mistrals (Paleomex)

Sequences of lake sediments often form long and continuous records that may be sensitive recorders of seismic shaking. A multi-proxy analysis of Lake Bohinj sediments associated with a well-constrained chronology was conducted to reconstruct Holocene seismic activity in the Julian Alps (Slovenia). A seismic reflection survey and sedimentological analyses identified 29 homogenite-type deposits related to mass-wasting deposits. The most recent homogenites can be linked to historical regional earthquakes (i.e. 1348 AD, 1511 AD and 1690 AD) with strong epicentral intensity [greater than 'damaging' (VIII) on the Medvedev–Sponheuer–Karnik scale]. The correlation between the historical earthquake data set and the homogenites identified in a core isolated from local stream inputs, allows interpretation of all similar deposits as earthquake related. This work extends the earthquake chronicle of the last 6600 years in this area with a total of 29 events recorded. The early Holocene sedimentary record is disturbed by a seismic event (661794 cal yr BP) that reworked previously deposited sediment and led to a thick sediment deposit identified in the seismic survey. The period between 3500 cal yr BP and 2000 cal yr BP is characterized by a major destabilization in the watershed by human activities that led to increases in erosion and sedimentation rates. This change increased the lake's sensitivity to recording an earthquake (earthquake-sensitivity threshold index) with the occurrence of 72 turbidite-type deposits over this period. The high turbidite frequency identified could be the consequence of this change in lake earthquake sensitivity and thus these turbidites could be triggered by earthquake shaking, as other origins are discarded. This study illustrates why it is not acceptable to propose a return period for seismic activity recorded in lake sediment if the sedimentation rate varies significantly.

FAME (v1.0): a simple module to simulate the effect of planktonic foraminifer species-specific habitat on their oxygen isotopic content

Roche D., Waelbroeck C., Metcalfe B., Caley T.

Geoscientific Model Development (2018) 11, 3587-3603

The oxygen-18 to oxygen-16 ratio recorded in fossil planktonic foraminifer shells has been used for over 50 years in many geoscience applications. However, different planktonic foraminifer species generally yield distinct signals, as a consequence of their specific living habitats in the water column and along the year. This complexity is usually not taken into account in model–data integration studies. To overcome this shortcoming, we developed the Foraminifers As Modeled Entities (FAME) module. The module predicts the presence or absence of commonly used planktonic foraminifers and their oxygen-18 values. It is only forced by hydrographic data and uses a very limited number of parameters, almost all derived from culture experiments. FAME performance is evaluated using the Multiproxy Approach for the Reconstruction of the Glacial Ocean surface (MARGO) Late Holocene planktonic foraminifer calcite oxygen-18 and abundance datasets. The application of FAME to a simple cooling scenario demonstrates its utility to predict changes in planktonic foraminifer oxygen-18 to oxygen-16 ratio in response to changing climatic conditions.

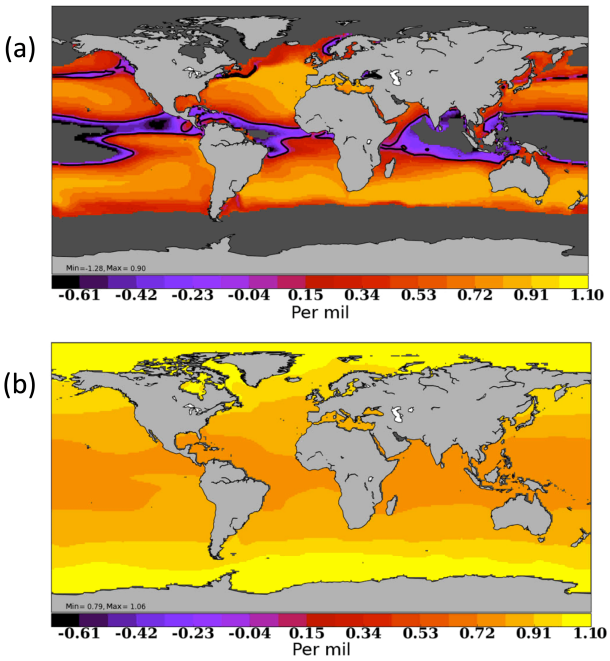

Fig. 1. *Calcite $\delta^{18}O$ response to a horizontally and vertically homogeneous 4 °C cooling applied to the WOA13 dataset. Results are expressed in permil for G. bulloides (a) and for the classically computed equilibrium surface calcite $\delta^{18}O$ (b).*

Increased production of cosmogenic 10Be recorded in oceanic sediment sequences: Information on the age, duration, and amplitude of the geomagnetic dipole moment minimum over the Matuyama–Brunhes transition

Simon Q., …, Bassinot F., et al.

Earth and Planetary Science Letters, 489, 191-202 (2018).

New high-resolution authigenic 10Be/9Be ratio (Be-ratio) records covering the last geomagnetic reversal, i.e. the Matuyama–Brunhes transition (MBT), have been obtained and set on a time scale using benthic (Cibicides wuellerstorfi) records Fig.). The geographic distribution of the four studied sites allows global comparison between the North Atlantic, Indian and Pacific Oceans. All Be-ratio records contain a two-fold increase triggered by the geomagnetic dipole moment (GDM) collapse associated with the MBT. The stratigraphic position of the Be-ratio spike, relative to marine isotope stages, allows establishment of a robust astrochronological framework for the MBT, anchoring its age between 778 and 766 ka (average mid-peaks at 772 ka), which is consistent with all other available 10Be-proxy records from marine, ice and loess archives. The global 10Be atmospheric production doubling represents an increase of more than 300 atoms m−2 s−1 that is compatible with the increased magnitude of atmospheric 10Be production obtained by simulations between the present GDM and a null-GDM. The minimum 10Be-derived GDM average computed for the 776–771 ka interval is Am2, in agreement with model simulations and absolute paleointensities of transitional lava flows.

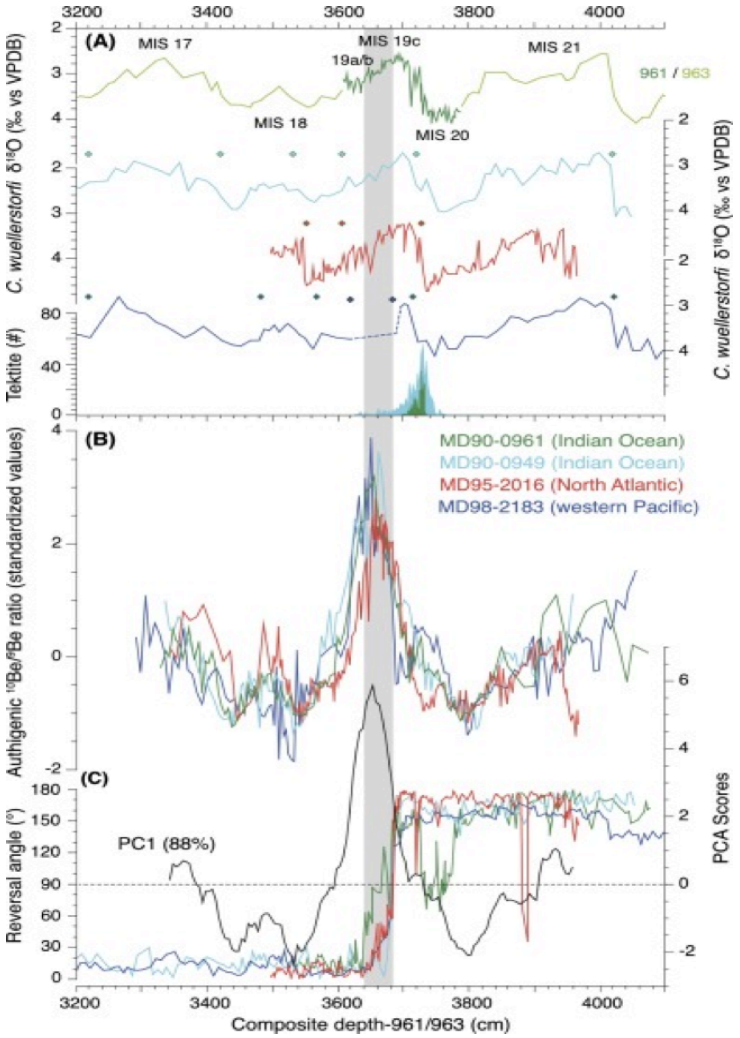

Figure: Results plotted on a common depth scale. (A) δ18O records synchronized to a common depth scale (MD90-961/963 as a target) using minimal tie points numbers (indicated by diamonds). (B) Be-ratios from each core standardized over the same composite depth for the same time period, i.e. 700–850 ka. (C) Scores of the first principal component (PC1 explains 88% of the variance) from a principal component analysis on the four Be-ratio series studied, and reversal angles defining the transitional field depth intervals in each core (Valet et al., 2016). The grey band highlights the transitional fields between full polarity states, as indicated by reversal angles between 30° and 150°.

Increased nutrient supply to the Southern Ocean during the Holocene and implications for atmospheric CO_2 levels

Studer A.S., ..., Michel E., Jaccard, S.L., Lippold, J.A., Mazaud, A., et al.

Nature Geoscience, 11(10), 756-760 (2018), doi.org/10.1038/s41561-018-0191-8

A rise in the atmospheric CO_2 concentration of ~20 parts per million over the course of the Holocene has long been recognized as exceptional among interglacials and is in need of explanation. Previous hypotheses involved natural or anthropogenic changes in terrestrial biomass, carbonate compensation in response to deglacial outgassing of oceanic CO_2, and enhanced shallow water carbonate deposition.

Here, we compile new and previously published fossil-bound nitrogen isotope records from the Southern Ocean (Fig.). Precisely, the nitrogen (N) isotope composition of exported organic matter reflects the degree to which the gross nitrate supply is assimilated by phytoplankton growth (nutrient excess). $\delta^{15}N$ increases as nitrate is consumed and surface nitrate concentration declines.

Here, nitrogen isotope records from the Southern Ocean document a $\delta^{15}N$ decrease through the Holocene. This Holocene decline in Southern Ocean microfossil-bound $\delta^{15}N$ is best interpreted as an increase in the proportion by which the nitrate supply to the surface ocean exceeded its demand by phytoplankton, resulting in a rise in surface nitrate concentration. It suggests an acceleration of nitrate supply to the Southern Ocean surface from underlying deep water.

This change would have weakened the ocean's biological pump that stores CO_2 in the ocean interior, via an increased leakage of biologically stored CO_2 from the Southern Ocean which possibly explains the Holocene atmospheric CO_2 rise.

Over the Holocene, the circum-North Atlantic region cooled, and the formation of North Atlantic Deep Water appears to have slowed. Thus, the 'seesaw' in deep ocean ventilation between the North Atlantic and the Southern Ocean that has been invoked for millennial-scale events, deglaciations and the last interglacial period may have also operated, albeit in a more gradual form, over the Holocene.

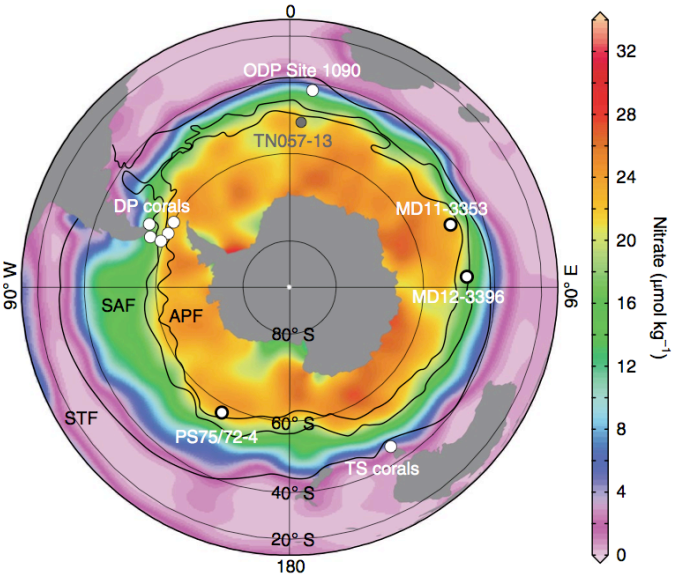

Figure: Sediment core and deep sea coral locations relative to austral summer surface nitrate concentrations and oceanic fronts.

Core locations of the diatom-bound $\delta^{15}N$ and opal flux records are shown in white with a black rim, locations of ODP Site 1090 foraminifera-bound $\delta^{15}N$ record and of the coral-bound $\delta^{15}N$ measurements are shown in white, and sediment core TN057-13 is shown in dark grey. APF, Antarctic Polar Front; SAF, Subantarctic Front; STF, Subtropical Front.

Large difference in global and regional total soil carbon stock estimates on SoilGrids, HWSD, and NCSCD: Intercomparison and evaluation based on field data from USA, England, Wales and France

Tifafi M., Guenet B., Hatté C.

Global Biogeochemical Cycles 32, 42-56 (2018), doi : 10.1002/2017GB005678
Thèse UVSQ ED129, projet ANR DedyCA

Soils are the major component of the terrestrial ecosystem and the largest organic carbon reservoir on Earth. However, they are a nonrenewable natural resource and especially reactive to human disturbance and climate change. Despite its importance, soil carbon dynamics is an important source of uncertainty for future climate predictions and there is a growing need for more precise information to better understand the mechanisms controlling soil carbon dynamics and better constrain Earth system models. The aim of our work is to compare soil organic carbon stocks given by different global and regional databases that already exist. We calculated global and regional soil carbon stocks at 1 m depth given by three existing databases (SoilGrids, the Harmonized World Soil Database, and the Northern Circumpolar Soil Carbon Database). We observed that total stocks predicted by each product differ greatly: it is estimated to be around 3,400 Pg by SoilGrids and is about 2,500 Pg according to Harmonized World Soil Database. This difference is marked in particular for boreal regions where differences can be related to high disparities in soil organic carbon concentration. Differences in other regions are more limited and may be related to differences in bulk density estimates. Finally, evaluation of the three data sets versus ground truth data shows that (i) there is a significant difference in spatial patterns between ground truth data and compared data sets and that (ii) data sets underestimate by more than 40% the soil organic carbon stock compared to field data.

Numerical experiments on vapor diffusion in polar snow and firn and its impact on isotopes using the multi-layer energy balance model Crocus in SURFEX v8.0

Touzeau A., Landais A., Morin S., Arnaud L., Picard G.

Geosc. Model Dev., 11, 2393-2418 (2018), doi: 10.5194/gmd-11-2393-2018
Financé par l'ERC Combiniso

To evaluate the impact of vapor diffusion on isotopic composition variations in snow pits and then in ice cores, we introduced water isotopes in the detailed snowpack model Crocus. At each step and for each snow layer, (1) the initial isotopic composition of vapor is taken at equilibrium with the solid phase, (2) a kinetic fractionation is applied during transport, and (3) vapor is condensed or snow is sublimated to compensate for deviation to vapor pressure at saturation.
We study the different effects of temperature gradient, compaction, wind compaction, and precipitation on the final vertical isotopic profiles (Fig.). We also run complete simulations of vapor diffusion along isotopic gradients and of vapor diffusion driven by temperature gradients at GRIP, Greenland and at Dome C, Antarctica over periods of 1 or 10 years. The vapor diffusion tends to smooth the original seasonal signal, with an attenuation of 7 to 12% of the original signal over 10 years at GRIP. This is smaller than the observed attenuation in ice cores, indicating that the model attenuation due to diffusion is underestimated or that other processes, such as ventilation, influence attenuation. At Dome C, the attenuation is stronger (18%), probably because of the lower accumulation and stronger $\delta^{18}O$ gradients.

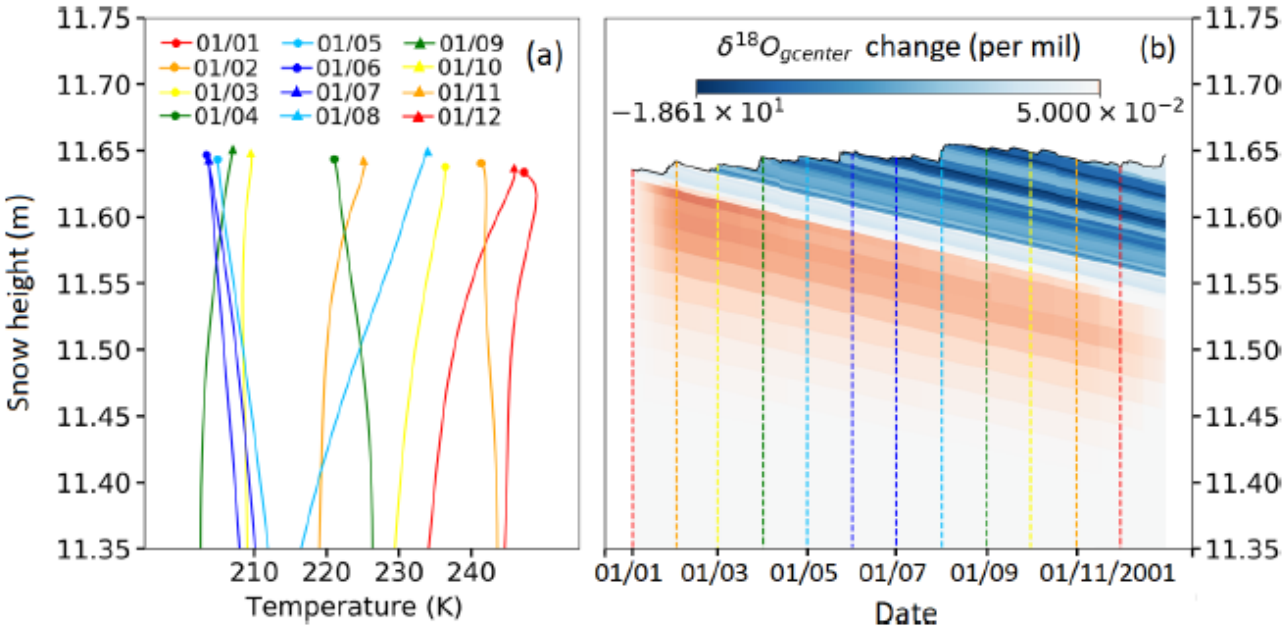

Figure: Cumulative change in $\delta^{18}O$ values at the grain center (relative to t0) over 6 months. Simulation with snowfall with varying $\delta^{18}O$ (function of T_{air}), vapor transport active, wind, and weight compaction active.

Relative timing of precipitation and ocean circulation changes in the western equatorial Atlantic over the last 45 kyr

Waelbroeck C., Pichat S., Böhm E., Lougheed B.C., Faranda D., Vrac M., Missiaen L., Vazquez Riveiros N., Burckel P., Lippold J., Arz H.W., Dokken T., Thil F., Dapoigny A.

Climate of the Past (2018) 14, 1315-1330

Thanks to its optimal location on the northern Brazilian margin, core MD09-3257 records both ocean circulation and atmospheric changes. The latter occur locally in the form of increased rainfall on the adjacent continent during the cold intervals recorded in Greenland ice and northern North Atlantic sediment cores (i.e. Greenland stadials). These rainfall events are recorded in MD09-3257 as peaks in ln(Ti/Ca). New sedimentary Pa/Th data indicate that mid-depth western equatorial water mass transport decreased during all the Greenland stadials of the last 40 kyr. Using cross-wavelet transforms, we assess the relative phase between the MD09-3257 sedimentary Pa/Th and ln(Ti/Ca) signals. We show that decreased water mass transport between a depth of ~1300 and 2300m in the western equatorial Atlantic preceded increased rainfall over the adjacent continent by 120 to 400 yr at Dansgaard–Oeschger (D–O) frequencies, and by 280 to 980yr at Heinrich-like frequencies. We suggest that the large lead of ocean circulation changes with respect to changes in tropical South American precipitation at Heinrich-like frequencies is related to the effect of a positive feedback involving iceberg discharges in the North Atlantic. In contrast, the absence of widespread ice rafted detrital layers in North Atlantic cores during D–O stadials supports the hypothesis that a feedback such as this was not triggered in the case of D–O stadials, with circulation slowdowns and subsequent changes remaining more limited during D–O stadials than Heinrich stadials.

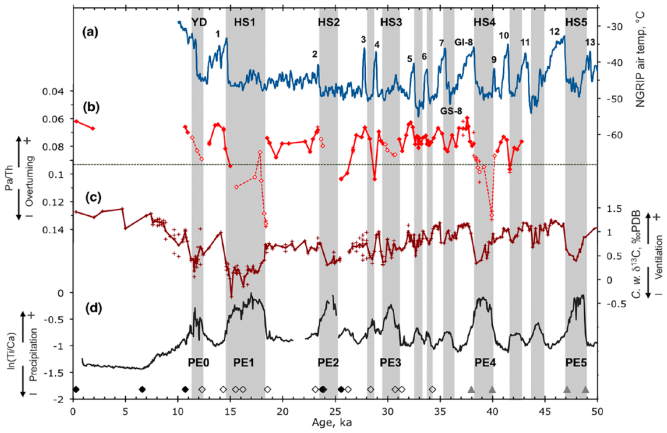

Fig. 1. *MD09-3257 Pa/Th, ln(Ti/Ca) and composite C. wuellerstorfi $\delta^{13}C$ ($\delta^{13}C_{Cw}$) records versus age. (a) NGRIP air temperature versus the GICC05 age scale. (b) MD09-3257 Pa/Th record. Empty symbols denote data points that may be affected by terrigenous fluxes. (c) MD09-3257 and GeoB3910-2 composite $\delta^{13}C_{Cw}$ record. (d) MD09-3257 ln(Ti/Ca). Diamonds above the x axis indicate calibrated radiocarbon dates in MD09-3257 (filled symbols) and GeoB3910-2 (empty symbols). Triangles indicate alignment tie points to South American speleothem $\delta^{18}O$. Grey bands delineate precipitation events recorded in MD09-3257 ln(Ti/Ca).*

Spatio-temporal dynamics of hydrographic reorganizations and iceberg discharges at the junction between the Northeast Atlantic and Norwegian Sea basins surrounding Heinrich event 4

Wary M., Eynaud F., Kissel C., et al.

Earth Planet. Sci. Lett., 481, 236-245 (2018), doi : 10.1016/j.epsl.2017.10.042

Dansgaard–Oeschger and Heinrich events constitute ones of the most enigmatic features of the last glacial period. Many studies have focused on their characteristic millennial climatic variability, testing atmospheric/cryospheric/oceanic couplings, but major uncertainties and discrepancies still remain.
Here, we present new very high temporal resolution (from 4 to 38 years on average depending on proxies) records from the 37–40ka cal BP section of core MD99-2281 located southwest off Faeroes, stemming from the same multiproxy approach conducted on the 35–41ka cal BP interval of core MD99-2285 located north-east off Faeroes (Fig.).

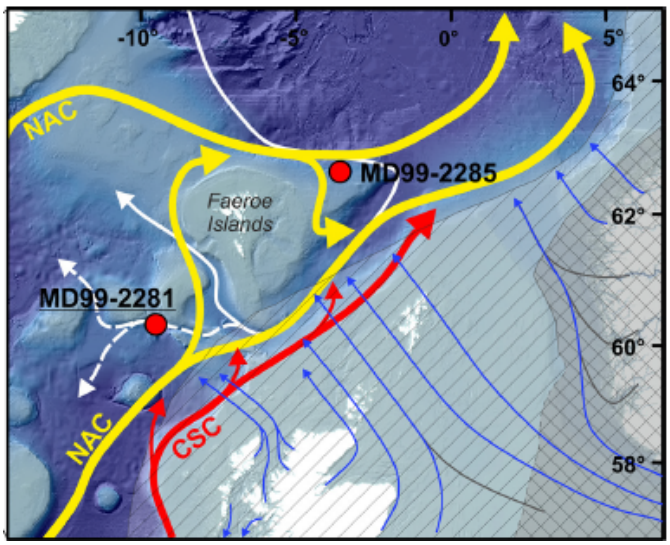

Figure: Map of the study area showing the location of cores MD99-2281 and MD99-2285 with respect to the North Atlantic current (yellow arrows), the major European ice sheet (grey with blue arrows indicating the paleo-ice streams) and the deep currents (white arrows).

A new scenario, robustly supported by paleo-reconstructions coupled with freshwater hosing experiments simulating Heinrich-type perturbations, has recently emerged. Reconciling most of the up to now hypothesized theories, it suggests the occurrence of a regional seesaw between a cooled-down North Atlantic Ocean and warmed-up Nordic Seas during cold atmospheric phases, in relation to enhanced subsurface advection of warm Atlantic waters re-emerging in the Norwegian Sea. The associated ocean warming, thus reaching Nordic basins at a critical location beyond the Faeroe-Shetland sill, is proposed to be involved in the concomitant release of European icebergs. Here we further investigate this promising scenario over the 35–41ka BP interval by (i) outlining its precise spatial pattern in a crucial area, i.e. the junction between the North Atlantic and the Norwegian Sea close to European ice-sheets, (ii) resolving its very fine temporal and regional evolution during critical transitions associated with the onset of warm advection, i.e. Greenland Interstadial to Greenland Stadial and Greenland Interstadial to Heinrich Stadial, and (iii) assessing its impact on the spatio-temporal dynamic of iceberg discharges from the European and Laurentide ice-sheets during cold stadial episodes especially including Heinrich event4.

Holocene Event Record of Aysén Fjord (Chilean Patagonia): an Interplay of Volcanic Eruptions, Crustal and Megathrust Earthquakes

Wils K., Van Daele M., Lastras G., Kissel C., et al.

J. Geophys. Res. Solid Earth. 123, 324-343 (2018), doi: 10.1002/2017JB014573, (2018).
Financé par LEFE-PACHIDERME

The seismic hazard at subduction zones not only originates from megathrust earthquakes occuring regularly, but also from intraplate earthquakes such as intra-oceanic and crustal earthquakes. Megathrust earthquakes might affect large areas, but large crustal earthquakes can lead to higher seismic intensities close to the epicenter and thus more severe damage, albeit over a more restricted area. Therefore, it is crucial to distinguish between both subduction and other earthquake sources in order to perform an adequate hazard assessment and evaluate which source mechanism forms the most imminent threat for any region in the world.

Chile is known to be one of the most seismically active countries in the world. Early 2007, the Aysén region in southern Chile was affected by a crustal seismic swarm with the epicentre of the largest earthquake (Mw 6.2) in Aysén Fjord. Seismic intensities became so high that hundreds of onshore mass movements were triggered, several of which entered into the fjord, resulting in mass transport deposits (MTDs) preserved at the fjord bottom. Here we present a Holocene record of paleo-earthquakes in the previously unstudied Patagonian fjordland based on MTD stratigraphy. High-resolution seismic data retrieved using two different seismic systems (sparker and TOPAS) reveal multiple older MTDs on different stratigraphic levels. Correlation of the seismic stratigraphy with sedimentological data obtained from a long Calypso core (MD07-3117) allows conclusion on the seismic origin of these deposits (Fig.). Additionally, radiocarbon dating permits constructing an age model, validated by tephrochronology, providing an age for the different MTD levels. We thus present a highly detailed paleoseismological history of the Aysén region, including at least six major Holocene earthquakes, one of which is likely related to a known megathrust earthquake. Other earthquakes are related to activity of the Liquiñe-Ofqui Fault Zone (LOFZ), forming the main source of seismic hazard in the area. We can infer a general average recurrence time for LOFZ earthquakes of ~2,100 years in the vicinity of Aysén Fjord with clustered events during the early and late Holocene. Finally, we argue that cascading events (causal link between volcanic and seismic events) may be a frequent phenomenon along the LOFZ.

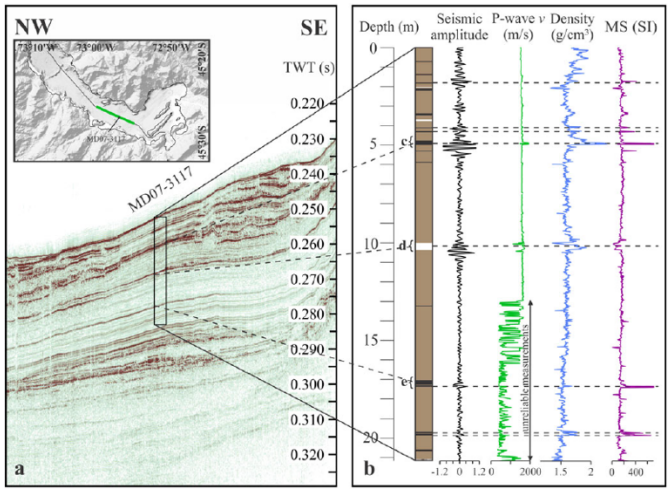

Figure: Correlation between MD07-3117 and the seismic data. (a) Extent of the core drawn on TOPAS profile 209_000 (vertical scale in two-way travel time, TWT) withthe location of the seismic line and the core with respect to the fjord given in the top left corner; (b) schematic lithology of the core (brown represents mud, black intervals are either a tephra or turbidite, and white are pumice layers) together with a seismic wiggle (black) and MSCL measurements of P wave velocity (green), core density (blue), and MS (purple). P wave velocity in the bottom 8 m of the core is not correct due to erroneous measurements.

Surface ocean pH variations since 1689 CE and recent ocean acidification in the tropical south Pacific

Wu H.C., Dissard D., Douville E., Blamart D., …, Pons-Branchu E., Dapoigny A., Lazareth C.

Nature communications 9 (1) 2543(2018), doi: 10.1038/s41467-018-04922-1

Projects: AO-IPSL-2014; ANR-Labex L-IPSL(Henry Wu – Post-doc 24 months) & ANR CARBORIC

Increasing atmospheric CO_2 from man-made climate change is reducing surface ocean pH. Due to limited instrumental measurements and historical pH records in the world's oceans, seawater pH variability at the decadal- and centennial scale remain largely unknown and requires documentation. We present evidences of striking secular trends of decreasing pH since the late 19th century with pronounced interannual to decadal-interdecadal pH variability in the South Pacific Ocean from 1689 to 2011 CE (Fig. 1). High-amplitude oceanic pH changes, likely related to atmospheric CO_2 uptake and seawater dissolved inorganic carbon fluctuations, reveal a coupled relationship to sea surface temperature variations and highlight the marked influence of El Niño/Southern Oscillation and Interdecadal Pacific Oscillation (Fig.2).

We suggest changing surface winds strength and zonal advection processes as the main drivers responsible for regional pH variability up to 1881 CE, followed by the prominent role of anthropogenic CO_2 in accelerating the process of ocean acidification.

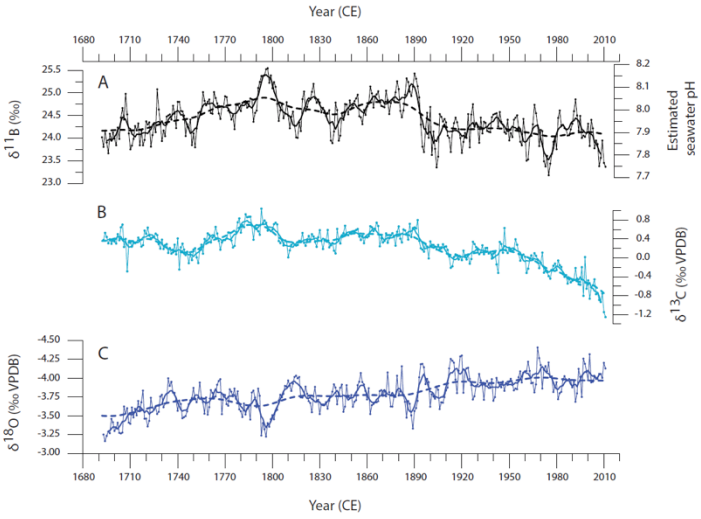

Figure 1: Diploastrea heliopora coral proxy records and $\delta^{11}B$-pH reconstruction. New Caledonia D. heliopora annually-resolved records over the period 1689-2011 CE from precisely dated $^{230}Th/U$-age. A. Coral $\delta^{11}B$ signature (left y-axis) with estimated seawater pH (pH_{SW}) on the right y-axis. B.) Coral $\delta^{13}C$ (‰ VPDB). C. $\delta^{18}O$ (‰ VPDB) ratios.

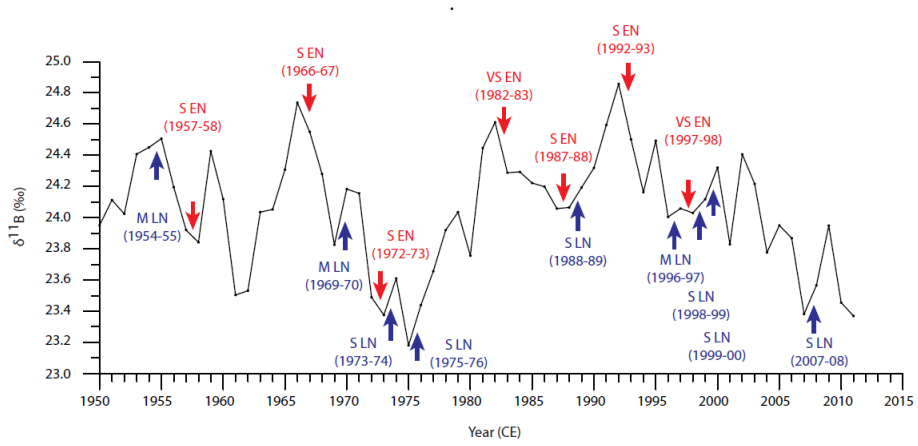

Figure 2: New Caledonia coral $\delta^{11}B$ and ENSO events. The New Caledonia coral $\delta^{11}B$ record from 1950-2011 CE with recent ENSO events identified. The severity of the listed El Niño (EN) or La Niña (LN) events are identified by the Oceanic Niño Index (ONI) from the 3-month running mean SST34 anomaly that is above or below the 0.5°C threshold for a period of at least 5 months in the Niño 3.4 region based on ERSST version 4 (Huang et al., 2014). The threshold of ENSO event is broken down into categories of moderate -M- (±1.0-1.4 ºC), severe -S-(±1.5-2.0 ºC), and very severe -VS- (> ±2.0 °C)

… projets de thèse et de post-doctorat

Le rapport B/Ca des foraminifères : un proxy pour le cycle du carbone dans l'océan.

Peral, Marion

PhD thesis from University Paris-Saclay (Orsay) ; Thesis advisors : D. Blamard, M. Daeron and F. Bassinot.

Around 1 Ma, during the "Mid-Pleistocene Transition" (MPT), the main period of glacial/interglacial cycles shifted from 40 kyr to 100 ky, while the orbitaly-driven insolation forcing remained unchanged. Understanding the mechanisms driving this major climatic transition and the respective roles played by external forcing and internal feedbacks constitute one of the top priorities for paleoclimatologists and climate modelers. In the oceanic domain, the MPT manifests clearly as a change in the frequency and amplitude of biocarbonate oxygen isotopes (d18O) variations. This transition is generally interpreted as reflecting changes in the oceanic temperature and/or in the continental ice sheet volume, although it has not been possible so far to precisely quantify these two effects. In order to resolve this issue, we propose to take advantage of "clumped isotope paleothermometry", a relatively new technique based on precise measurements of statistical anomalies (Δ47) in the isotopic composition of carbonates. Clumped isotope analyses of planktonic (surface) and benthic (deep) foraminifers retrieved from sediment cores located at different latitudes and within different oceanic basins will aim for the following objectives: (1) to quantify changes of oceanic temperature and ice sheet volume across the MPT; (2) to analyze lead/lag phasing between those parameters; (3) to study in some detail the temporal structure of the MPT and document the first apparition of massive glacial ice sheets typical of the Late Quaternary climate. Overall, these reconstructions will provide quantitative data on key physical parameters, to be integrated in present and future climate models.
This PhD work (still in progress) has made it possible to obtain a new calibration data set based on a large number of analyses performed on 9 planktonic and 2 benthic species of foraminifera obtained from recent core-top sediments, and covering temperatures of -2◦C to 25◦C. A robust relationship exists between Δ47 values and independent temperature estimates with a formal regression precision better than ± 1 ◦C (95% CL). It is important to note that the slope is comparable to recent studies and that these new observations confirm the absence of significant species-specific biases and salinity effects (Tripati et al., 2010; Grauel et al., 2013). The PhD work also made it possible to investigate potential foraminifer size effects between 200 and > 560 µm in 6 species, and conclude that all size fractions from a given core-top location and species display statistically undistinguishable Δ47 values. Because of its standardisation and its precision, this calibration should provide a strong foundation for future inter-comparison and paleoceanographic applications
This calibration will be applied to Δ47 from a marine series in the Mediterranean sea (Montalbano Jonico) and from a pelagic core in the Madagascar Strait covering the MPT.

… autres projets

Projets EAIIST, ASUMA, Antarctic-SNOW, ADELISE

Agosta C., Bréant C., Cattani O., Fourré E., Goursaud S., Landais A., Leroy Dos Santos C., Masson-Delmotte V., Minster B., Orsi A., Prié F.

Issu du projet : Eaiist, Asuma, Antarctic-SNOW, Adelise (2014-2018)

Ces projets visent à fournir une image quantitative de la variabilité climatique et environnementale des derniers siècles en Antarctique de l'Est, une région très mal documentée et très vulnérable. Deux régions sont visées par ces projets : la Terre Adélie au-dessus de la base française de Dumont d'Urville et le plateau Est Antarctique. La Terre Adélie est une zone fortement affectée par les vents catabatiques, dans laquelle le bilan d'accumulation de surface est très mal défini. Par sa situation géographique, le plateau Est-Antarctique est la région la plus froide au monde. La calotte de glace antarctique est la plus grande réserve mondiale d'eau douce (équivalente à 60 m de niveau marin) et elle est particulièrement vulnérable aux augmentations de température et aux modifications du cycle de l'eau.

Pendant l'été austral 2016-2017 un raid scientifique a permis d'installer des stations météos et de relever l'accumulation de surface en Terre Adélie depuis la base côtière de Dumont d'Urville jusqu'au plateau Est Antarctique. De nombreuses carottes de glace ont été forées pour une analyse en isotopes de l'eau au LSCE (thèses de Sentia Goursaud et de Christophe Leroy Dos Santos) qui révèle pour la première fois une variabilité inter-annuelle avec une signature forte de l'effet de transport en plus du signal habituel de température. Cette même saison, un instrument de spectroscopie laser installé pour 40 jours à la station de Dumont d'Urville a montré la valeur ajouté des mesures en continu de la composition isotopique de la vapeur d'eau pour interpréter les enregistrements des carottes de glace courtes dans la région pour reconstruire la variabilité climatique et du cycle de l'eau (thèse de Camille Bréant). Cette étude pilote a permis de valider l'installation pendant 2 ans (2018 à 2020) d'instruments similaires sur les sites de Dumont d'Urville et de Dome C. De plus, de 2018 à 2020, une traverse scientifique unique reliera les 1760 km entre les sites de Dome C et de Pôle Sud. Les instruments à déployer sur cette traverse pour la mesure des isotopes de l'eau en conditions extrêmes ont été développés et calibrés au LSCE (thèse de Christophe Leroy Dos

Les données acquises dans le cadre de ces projets sont utilisés pour valider le modèle de climat régional développé sur l'Antarctique, MAR, dans le cadre du post-doc de Cécile Agosta. En particulier, l'étude couplée modèle – données démontre l'importance de prendre en compte l'effet de neige soufflée dans les bilans de masse de surface de la calotte antarctique.

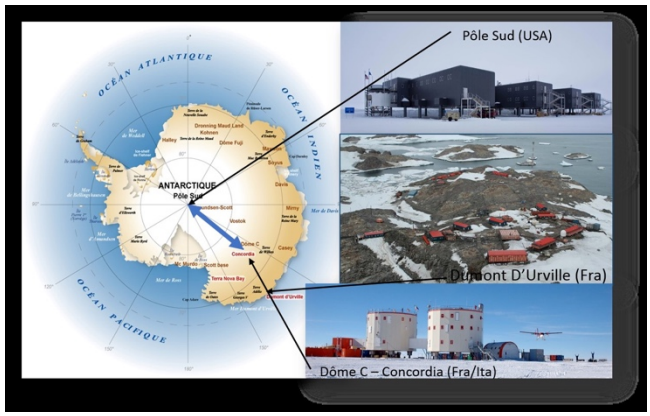

Figure: Localisation des sites d'intérêt pour les projets EAIIST, ASUMA, Antarctic-SNOW et Adelise

MONOPOL / Paleovariabilité de la mousson indienne (ANR Blanc 2012)

Bassinot, F. (LSCE) and a consortium of scientists from 6 French laboratories (CEREGE, EPOC, GEOPS, IPGP, MNHN, LSCE).

9 publications de rang A (5 articles en préparation), 15(18) présentations dans des congrès internationaux (nationaux) ; 6 thèses.

ANR-MONOPOL, 11 BS5-6 02401

The main objectives of the ANR-MONOPOL project were to better constrain the natural evolution of Indian Monsoon at different timescales (100 – 100,000 years) and to decipher its impact on Himalaya's erosion through the study of sedimentary cores retrieved in the Bay of Bengal during a dedicated cruise of the French R/V Marion Dufresne.

A consortium of scientists from six French laboratories and three Chinese institutes has analyzed the material retrieved. Technics and expertise cover the full range of marine sediment studies: micropaleontology (pollens, foraminifers, coccoliths), radiochronological dating (^{210}Pb, ^{14}C), cutting-edge sedimentological approaches (XRD-mineralogy, microstructure and grain size determination through RX-imaging and laser granulometry, XRF core-scanning), magnetic properties (susceptibility, magnetic mineralogy, remanent magnetization), isotopic and elemental determination of detrital sources and dynamics of water masses (eg. Sr/Sr and eNd analyses on dissolved material, detrital fraction and foraminifer tests), elemental and isotopic tracers of past hydrographic changes ((δ^{18}O, δ^{13}C, Mg/Ca-thermometry and B/Ca on planktonic and benthic foraminifers).

To summarize key achievements, the MONOPOL project made it possible to better understand modern repartition and ecology of planktonic foraminifers in the Bay of Bengal and -by comparison with recent GEOTRACE data – it has revealed for the first time the unsuspected seasonal variability of concentration and isotopic composition of dissolved Nd. The multi-proxy analysis of sedimentary series made it possible to reconstruct centennial/millennial hydrograph variability (salinity, temperature) and the dynamics of the Indian vegetation in response to monsoon changes, revealing the strong impact of high-latitude remote-connections. At long timescales, we reconstructed thermal variability of low-latitude Indian Ocean surface water across the major Mid-Pleistocene transition, around 1 Ma. On a sedimentological point of view, we were able to better understand mechanisms at play in the initiation and evolution of the active channel/levee system, highlighting the impact of monsoon imprint and sea level changes on that sedimentary dynamics. The impact of man activity, through deforestation, has also been pointed out to explain the most recent changes observed (last 2 millennia).

The material retrieved during the MONOPOL project has been used for 10 master and 6 PhD research projects. Results have been presented at 15 national and 15 international congresses and have been published in 5 scientific papers in international peer-reviewed journals. Two manuscripts have been recently submitted and five additional manuscripts are currently in preparation and will be submitted for a publication in 2017/2018.

INSU-LEFE : MAGICS - MAGnesium thermometer Improvement for assessing Climate Sensitivity

Bassinot, F. and collaboration with GEOPS (S. Sépulcre) and CEREGE (T. de Garidel)

projet INSU/LEFE/IMAG0-MAGICS, 2016-2018

Un point d'achoppement important du débat sur l'amplitude du réchauffement climatique futur repose sur la difficulté d'estimer la sensibilité climatique (Roe et Baker, 2007), c.à.d. le changement de température global associé à un doublement de la concentration atmosphérique en CO_2. Pour mieux contraindre ce paramètre clé, une des approches les plus prometteuses consiste à exploiter les reconstructions paléocéanographiques en comparant les changements passés de la température océanique (en particulier les eaux de surface dans la bande tropicale) avec les variations de gaz à effet de serre (GES) reconstruites à partir de l'étude des bulles d'air piégées dans les glaces. Ce type d'approche requiert la compilation de base de données de paléotempératures fiables et cohérentes, couvrant des périodes clés dont, en particulier, le Dernier Maximum Glaciaire (DMG), pour lesquelles nous disposons de données de GES issues des carottes de glace.

Le projet MAGICS comporte trois volets principaux :

(1) développer une stratégie permettant d'intégrer au mieux les données de Mg/Ca issues de différents laboratoires (i.e. obtenues à partir de protocoles d'analyses différents) et leur appliquer une conversion en température aussi cohérente et robuste que possible ;

(2) obtenir un nouveau jeu de données, contrôlé taxonomiquement, permettant de conclure quant au rôle potentiel de la salinité sur le thermomètre Mg/Ca et consolider, si nécessaire, l'approche de correction proposée par Mathien-Blard et Bassinot (2009);

(3) appliquer les stratégies développées dans le projet MAGICS aux données Mg/Ca collectées par le groupe MARGO (MARGO, 2009) et lors du récent programme ANR-EL PASO afin d'affiner la reconstruction des différences de températures océaniques de surface entre le DMG et l'actuel, avec un focus particulier sur la bande intertropicale et la Warm Pool du Pacifique ouest pour vérifier l'hypothèse d'une amplitude de ?T supérieure à celle admise actuellement. Se servir de ces données pour affiner l'estimation de la sensibilité climatique.

MAGICS s'appuie sur une collaboration entre le LSCE, GEOPS et le CEREGE et le travail de thèse de X. Pang (collaboration franco-chinoise avec l'Université Nationale des Géosciences de Pékin).

Développement de spectromètres laser ultra-précis dédiés à la mesure des anomalies isotopiques

Daëron M., Kassi S., Stoltmann T., Casado M., Landais A., Kerstel E.

Les techniques de mesure des rapports isotopiques par spectrométrie d'absorption laser ont connu de rapides progrès depuis une dizaine d'années. Ces techniques offrent des avantages spécifiques par rapport à la spectrométrie de masse “traditionnelle”, comme par exemple la capacité de faire une distinction entre deux isotopologues de masses quasi-identiques, comme $^{16}O^{13}C^{16}O$ et $^{16}O^{12}C^{17}O$. Cela étant, la plupart des instruments laser commerciaux privilégient aujourd'hui la simplicité d'utilisation et la capacité à effectuer des mesures in situ en continu. Pour ce qui concerne la mesure des rapports isotopiques, les instruments commerciaux les plus modernes restent encore en retrait en termes de précision aux spectromètres de masse les plus performants. Le LSCE et le LIPhy (Laboratoire Interdisciplinaire de Physique, UMR 5588) collaborent depuis plusieurs années dans le but de développer des spectromètres laser capables de mesurer les concentrations relatives des isotopologues du CO_2 et de l'eau avec des précisions extrêmes, de 0,001 à 0,01 ‰. Pour le CO_2 par exemple, ce type d'instrument permettra de mesurer, pour un échantillon donné, la composition isotopique traditionnelle ($\delta^{13}C$, $\delta^{18}O$), l'anomalie d'oxygène-17 ($\Delta^{17}O$), ainsi que le “clumping isotopique” associé à certains isotopologues (Δ16O13C18O, Δ18O12C18O). La capacité à mesurer toutes ces grandeurs simultanément, sans préparation chimique lourde, présente un grand intérêt scientifique dans le cadre des études géologiques et environnementales, car chacune de ces variables isotopiques est influencée par des paramètres naturels différents. Ce type de mesures ouvre ainsi des perspectives nouvelles pour étudier le cycle du carbone (ex : analyse du CO_2 atmosphérique) ou les mécanismes climatiques à l'échelle des temps géologiques (ex : par l'analyse de roches carbonatées ou de bio-carbonates). Nos prototypes actuels, développés dans le cadre de deux thèses (T. Stoltmann, M. Casado), ont déjà permis de redéfinir l’état de l’art des mesures par CRDS (cavity ring-down spectroscopy), et nous sommes sur le point de réaliser nos premières mesures isotopiques

Impact de l'acidification et du réchauffement des océans sur les écosystèmes coralliens

Douville E. et al.

Fin de l'expédition TARA-Pacific (Mai 2016 – Octobre 2018), France 2 (Télématin 09.11.18)

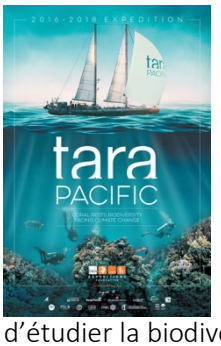

TARA-Pacific, qui a débuté le 28 mai 2016, s'est terminé le Samedi 27 Octobre 2018 après 2 ans et demi de navigation avec le retour médiatique de TARA à Lorient. Cette expédition, coordonnée par Serges Planes (CNRS), Denis Allemand (CSM) et Romain Troublé (TARA), a pour motivation générale d'étudier la biodiversité des récifs coralliens actuels et passés sur l'intégralité de l'océan Pacifique par une approche « transversale » impliquant des experts de différents horizons scientifiques. Les chercheurs souhaitent en particulier faire un bilan de l'état de santé actuel des récifs tropicaux et évaluer leur capacité de résilience et d'adaptation face aux changements globaux dus à l'ère industrielle. Pour réaliser ces études d'impact, le Centre Scientifique de Monaco (CSM) en étroite collaboration avec le LSCE, ont organisé à bord du TARA le prélèvement par forage de nombreuses carottes de corail. Le bilan est aujourd'hui extrêmement positif puisque 35 carottes de corail couvrant les 2 derniers siècles ont été prélevées sur 32 îles ou atolls de l'océan Pacifique. Dans le cadre d'une convention CSM-CEA qui sera signée en décembre 2018 pour la période (2018-2022), nous proposons de valoriser ces prélèvements et donc de reconstruire à l'échelle annuelle, voire saisonnière, l'évolution historique de la température et du pH-DIC (cycle du carbone) de l'océan Pacifique et de comparer les données géochimiques obtenues avec celles liées aux propriétés de croissance des colonies de corail *Porites* et *Diploastrea* prélevées.

https://www.france.tv/france-2/telematin/805937-environs-des-excursions-scientifiques-pour-sauver-les-coraux.html

Ce travail implique à la fois des analyses géochimiques de pointe ($\delta^{11}B$ et B/Ca pour le pH, les éléments traces et les rapports Li/Mg et Sr/ca pour la température, certains métaux lourds ou polluants pouvant également affecté la santé des coraux et les isotopes stables du C et de l'O pour tenir compte de la bio-minéralisation ou de l'effet Suess. Ces analyses seront logiquement réalisées sur les spectromètres de masse de nouvelle génération du LSCE (ICP-QMS, MC-ICPMS et IRMS). Ces travaux seront accompagnés d'une analyse qualitative (DRX/MEB) et d'une analyse de la densité (Tomographie/Radiographie-X) permettant le comptage des bandes annuelles (modèle de croissance des coraux tropicaux) et l'établissement des paramètres de croissance (densité, extension linéaire, taux de calcification).

Ces travaux autour des éléments traces (B/Ca, Li/Mg, Sr/Ca, etc.) et des isotopes du B nous permettront de reconstruire l'évolution historique de la température et de la chimie des carbonates pour l'océan Pacifique. Et ces données géochimiques, comparées à celles physiologiques, apporteront des informations uniques sur la résilience des coraux face aux changements globaux.

Updated calibration of Δ_{47} thermometry ("clumped isotopes") in foraminifera

Peral M., Daëron M., Blamart B., Bassinot F., Dewilde F., Smialkowski N., Isguder G., Bonnin J., Jorissen F., Kissel C., Michel E., Vázquez Riveiros N., Waelbroeck C.

In review (Geochimica et Cosmochima Acta)

Accurate reconstruction of past ocean temperatures is of critical importance to paleoclimatology. Carbonate clumped isotope thermometry ("Δ_{47}") is based on the strong relationship between calcification temperature and the statistical excess of ^{13}C-^{18}O bonds in carbonates. Its application to foraminifera holds great scientific potential, particularly because it does not require assumptions regarding the ^{18}O composition of seawater. We present a new calibration data set based on 9 planktonic and 2 benthic species of foraminifera collected from recent core-top sediments, with calcification temperatures ranging from -2 to 25 °C. We observe a robust relationship between Δ_{47} values and independent estimates of calcification temperatures, with a formal regression precision of ± 0.7–1.0 °C (95 % confidence). Our observations confirm the absence of significant species-specific biases or salinity effects. This calibration provides a strong foundation for inter-laboratoriy comparisons and paleoceanographic applications.

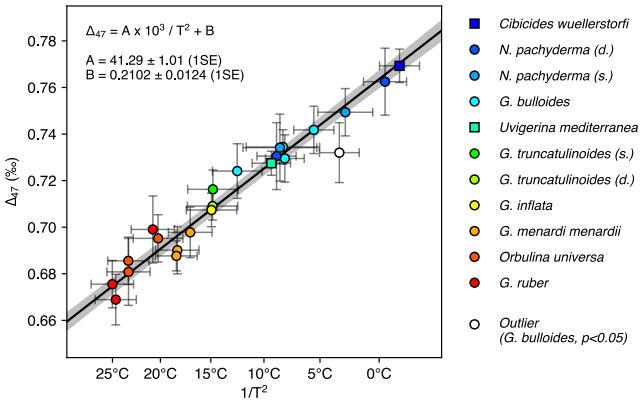

Figure 1 : Relationship between Δ_{47} and calcification temperature between –2 and 25 °C. These observations confirm the absence of significant species-specific biases or salinity effects, suggesting that Δ_{47} values in planktonic and benthic foraminifera are exclusively determined by temperature.

Datations croisées ($^{230}Th/^{234}U$ et ^{14}C) de voiles de calcite pour la chronologie de l'art pariétal

Valladas H, Pons-Branchu E., Dumoulin JP, Quiles A., Medina-Alcaide MA ; Sanchidrain JL. (2017) U/Th and C-14 cross dating of parietal calcite deposits: application to Nerja cave (Andalusia, Spain) and future perspectives. Radiocarbon 59 (6). 1955-1967

Shao Q., Pons-Branchu E., Zhu QP., Wei Wang W, Valladas H, Fontugne.M. (2017). High precision U/Th dating of the rock paintings at Mt. Huashan, Guangxi, southern China. Quaternary research, 88 (1) 1-13

Sanchidrián JL, Valladas H, Medina - Alcaide MA., Pons-Branchu E., Quiles A (2017) New perspectives for 14C dating of parietal markings using $CaCO_3$ thin layers: an example in Nerja cave (Spain). Journal of Archaeological Science reports 12. pp 74-80

Pons-Branchu E., Bourrillon R., Conkey M., Fontugne M., Fritz C., Gárate D., Quiles A., Rivero O, Sauvet G., Tosello G., Valladas H., White R. (2014). U-series dating of carbonate formations overlying Paleolithic art: interest and limitations. Bulletin de la Société préhistorique française, Tome 111, numéro 2, avril-juin 2014, p. 211-224

Jusqu'à ces dernières années, la chronologie des œuvres pariétales préhistoriques reposait surtout sur la méthode du carbone 14 par spectrométrie de masse par accélérateur, permettant de dater directement les dessins réalisées avec du charbon de bois (Arnold *et al.*, 1987, Valladas *et al.*, 2001). Pour les représentations non réalisées avec du charbon (oxyde de fer, gravures …), nous nous sommes intéressés à la datation des voiles de calcite recouvrant ces œuvres, ou à celle de leur support, afin de déterminer des bornes chronologiques « *terminus ante ou post quem* » pour leur réalisation.

Le travail méthodologique mis en œuvre a montré la nécessité de réaliser des datations croisées en utilisant à la fois la méthode uranium-thorium (ou $^{230}Th/^{234}U$) et celle du ^{14}C sur ces dépôts carbonatés, afin de déterminer de possibles « ouvertures du système géochimique » ou au contraire pour valider les âges obtenus. Cette méthodologie a été appliquée à des œuvres de la grotte de Nerja dans le sud de l'Espagne, mais aussi à des œuvres des Montagnes du Huashan, dans le Sud de la Chine (voir figure 1).

A Nerja, nous avons déterminé que des marques rouges non figuratives sont plus anciennes que 25 000 ans et peuvent être associées avec une phase d'occupation ancienne connue de la grotte (entre 39,035 et 25,555 cal BP). La datation de voiles de calcites sur et sous les peintures des montagnes du Huashan a quant à elle permis de contraindre leur âge entre 1856 ± 16 and 1728 ± 41 ans BP, soit entre les années 25 à 220 de notre ère.

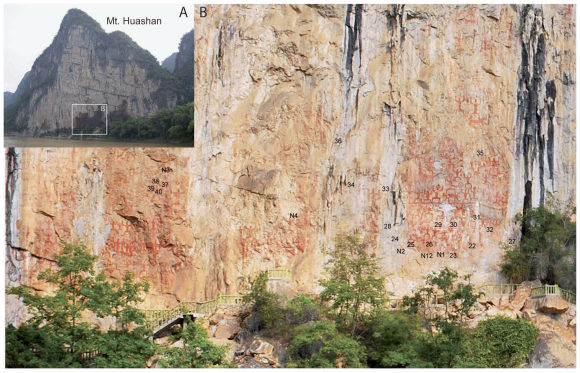

Fig. 1. (A) Mt. Huashan. (B) Part of the rock paintings; the numbers correspond to sample location.

Références

Arnold, M., E. Bard, P. Maurice & J.C. Duplessy. 1987. ^{14}C dating with the Gif-sur-Yvette Tandetron accelerator: status report. Nuclear Instruments and Methods in Physics Research B29: 120-123.

Valladas H., Clottes J., Geneste J-M., Garcia M. A., Arnold M., Cachier H., Tisnérat-Laborde N., "Evolution of prehistoric cave art". Nature 413, 4 October 2001, p. 479.

DATIM – DATation des Instruments de Musique

Vaiedelich S., Hatté C.

Projet Ile de France – Domaine d'Intérêt Majeur « Patrimoine et Matériaux)

DatIM ambitionne de lever les verrous scientifiques liés au positionnement chronologique de l'instrumentarium en ajoutant la datation ^{14}C à la palette d'approches classiquement utilisées. Au-delà de la poursuite de la construction d'une histoire de l'usage musical et des pratiques d'entretiens, de réparation ou de restaurations qui sont adressées à l'instrument de musique, elles consolideront l'émergence de concerts historiquement documentés, favorisant la valorisation des collections muséales ou privées. DatIM s'attachera à construire une chronologie autour de 3 corpus d'importance: 1- l'archet du XVIIème siècle et ses pratiques successives, 2- le clavecin et les questions de positionnement relatif dans le temps des éléments de caisse, de jeu et de piètements, 3- des luths emblématiques des XVI et XVII^{ème} siècle et l'authenticité de leur barrage.

DatIM combine les expertises de 4 entités, 2 acteurs publics et 2 acteurs privés, et l'émergence d'une nouvelle génération d'appareils de mesure du ^{14}C qui permet de travailler sur quelques 10µg de carbone (contre 1mg classiquement). Le croisement des expertises s'entend depuis la caractérisation in situ de l'échantillon, son prélèvement, la définition des contaminants potentiels et l'intégration de tous les indices chronologiques disponibles, relatifs et absolus, muséaux et physiques pour définir le cadre temporel de la vie des instruments. DatIM implique la muséologie, la caractérisation des matériaux, la chimie, la mesure physique et les statistiques bayesiennes. Au-delà des valorisations classiques sous forme d'articles ou de communications à destination des communautés ^{14}C, muséale et de facture instrumentale, DatIM s'implique également dans la communication vers les professionnels de la facture instrumentale et les experts liés à ces objet anciens ainsi que vers le grand public, notamment dans le cadre des actions sur Paris-Saclay.

ACCLIMATE (Elucidating Causes and Effects of Atlantic Circulation Changes through Model-Data integration) ERC project

Waelbroeck C., Roche D.M., Vazquez Riveiros N., Missiaen L., Lougheed B., Bouttes N., Quiquet A., Böhm E., Eynaud F., Mauclair L., Leroy L., Smialkowksi N., Moreira Martinez S., Rossignol L.

Vazquez Riveiros et al., *Geochemistry, Geophysics, Geosystems* 17, doi:10.1002/2015GC006234.
Burckel et al., *Climate of the Past* 12: 2061-1075, doi:10.5194/cp-12-2061-2016.
Quiquet et al., *Geosci. Model Dev.*, doi.org/10.5194/gmd-2017-116, in press.
Roche et al., *Geoscientific Model Development Discussion*, doi.org/10.5194/gmd-2017-251.
Missiaen et al., in revision in *Geochemistry, Geophysics, Geosystems.*
Vázquez Riveiros et al., submitted to *Nature Communications.*

The ACCLIMATE project consists in combining a set of consistently dated Atlantic deep-sea isotopic records with an isotopic proxy forward climate model through an innovative data assimilation scheme. The project objective is to define a model version able to reproduce the highly non linear behavior of the climate system observed over the last 40 ky in marine sediments and ice core records. Expected results include the first projections of future climate changes obtained with a model able to reproduce the highly nonlinear behavior of the climate system observed over the last 40 ky.

Methology: (1) 4-D reconstruction of the Atlantic ocean circulation: database of *consistently dated* Atlantic isotopic time series ($\delta^{18}O$, $\delta^{13}C$, Pa/Th, $\Delta^{14}C$) over the last 40 ky; (2) 4-D proxy forward modeling of the climate system: use of an *isotope-enabled model* in order to or strongly reduce the errors of interpretation of paleoclimatic records; (3) Model-data integration: apply a *data assimilation* procedure to produce states of the climate system that best explain the observations over the last 40 ky, while being consistent with the model physics.

The ACCLIMATE coring cruise took place in March 2016 in the South Atlantic on board R/V Marion Dufresne (see the website targeted at schools and the general public: http://www.sea.acclimateproject.eu/).

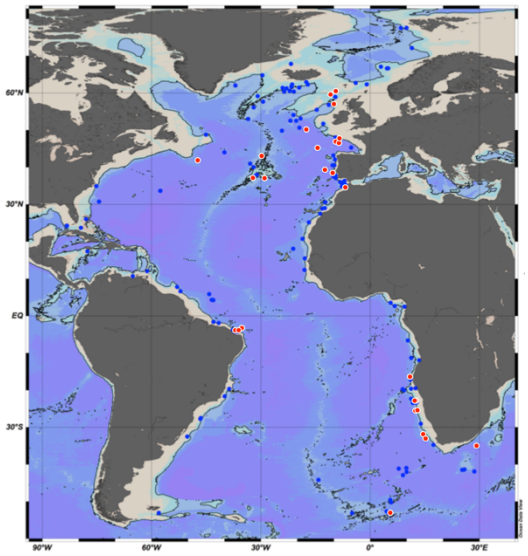

Fig. 1. ACCLIMATE data base spatial coverage: 166 cores with sedimentation rates > 5 cm/ky and sufficient dating information to be placed in a common chronological framework. blue dots: existing records, red dots: new records.

… prix et récompenses

Nature journal nominates its Top 10 people for 2018. **Valérie Masson-Delmotte**: a climatologist was a driving force behind the IPCC's stark report on global warming.

The journal *Nature* has named its Top 10 people who mattered in science in 2018. (article Nature)

In October, **Valérie Masson-Delmotte** and her colleagues presented the world with alarming news about its future. Within as little as a dozen years, Earth's average temperature could reach 1.5 °C above what it was in the mid-nineteenth century, triggering a wave of changes that would transform ecosystems and kill off most of the world's coral reefs, among many other impacts.

The warning came courtesy of a special report from the Intergovernmental Panel on Climate Change (IPCC), in which Masson-Delmotte played a primary part. A climatologist at the Laboratory for Sciences of Climate and Environment in Gif-sur-Yvette, France, and co-chair of the IPCC working group that assesses the physical science of climate change, Masson-Delmotte helped to gather the report's authors, coordinate their work and, ultimately, get the report approved by governments.

The IPCC normally takes the better part of a decade to produce its massive assessments, but the 1.5 °C report came together quickly, incorporating research published just weeks before the final draft was submitted for government review. "I'm really proud," Masson-Delmotte says. "We had a horribly stringent timeline, but I think we managed to build trust and ownership of the report by the authors."

The report makes clear that limiting warming to 1.5 °C would have huge benefits compared with allowing temperatures to surge to the 2 °C level. But keeping to 1.5 °C would require aggressive action to curb greenhouse-gas emissions. And even if nations could somehow achieve that, the world would look very different: entire ecosystems could be destroyed across more than 6% of the planet's terrestrial surface, and 70–90% of coral reefs would probably disappear.

"This report will be a hard one to ignore," says co-author Ove Hoegh-Guldberg, who is director of the Global Change Institute at the University of Queensland in St Lucia, Australia.

Diana Liverman, a geographer at the University of Arizona in Tucson, singles out Masson-Delmotte's work to improve diversity and representation in the IPCC. Women made up just 22% of the author team on the last assessment, completed in 2014; in this report, they comprised an unprecedented 40%. Masson-Delmotte also worked to elevate the role of early-career scientists and researchers from the global south. And for the next full climate assessment, due out in 2021, she has introduced procedures to promote engagement by all authors — including an online participation tool for scientists who are uncomfortable speaking up during meetings.

In an attempt to break down scientific silos, researchers from various disciplines worked together on every chapter. The result, Masson-Delmotte says, was an analysis that focused less on emissions scenarios and more on social, technological and governmental policies that could foster change — without exacerbating poverty and inequality around the world.

Masson-Delmotte spent ten days talking about the report and the wider IPCC process with delegates at the United Nations climate summit in late 2018. Now, she and the other co-chairs are pushing forward with two more reports — one on terrestrial biomes, the other on oceans and polar regions, slated for release in August and September 2019, respectively.

Similar to the IPCC itself — participation in which is a voluntary affair — Masson-Delmotte says that she is stretched to the limit. Her own research has been relegated to occasional nights, weekends and train rides, and she doesn't see as much of her two daughters and husband as she used to. "It's frustrating," she says. "But at the same time, it's awfully stimulating."